



UNIVERSITY OF
LIVERPOOL

**Synthesis of molecules containing Stiff Stilbene,
Dichlorocyclopropane and Anthracene-Maleimide
Diels-Alder Adduct for polymer mechanochemistry
investigations**

Thesis submitted in accordance with the requirements of
the University of Liverpool for the degree of
Doctor in Philosophy

by

Davide Gastaldello

Supervisor: Dr. Roman Boulatov

December 2018

Contents

Abbreviations.....	iii
Abstract.....	v
CHAPTER I. Polymer Mechanochemistry.....	1
Abstract	2
Introduction.....	2
Mechanophores : design and properties.....	3
Mechanophores undergoing electrocyclic ring opening.....	5
Mechanophores undergoing isomerization.....	10
Mechanophores undergoing reverse Diels-Alder.....	12
Mechanophores undergoing homolytic cleavage.....	13
Mechanophores undergoing cycloreversion.....	15
Techniques used in Polymer Mechanochemistry.....	16
Ultrasonic Irradiation.....	19
Atomic Force Spectrometer (AFM) – Single Molecule Force Spectroscopy (SMFS).....	20
Objectives of this thesis.....	26
References.....	29
CHAPTER II. Molecular force gate for stress-responsive polymers.....	31
Abstract	32
Introduction.....	32
Result and discussion.....	38
Molecular design.....	38
Synthesis of the “linker” molecule.....	39
Synthesis of dichlorocyclopropane.....	41
Assembling the macrocycles.....	43
Attempt to create a linker with shorter “arms”	46
Polymerization.....	47
Conclusions and future work.....	49
Experimental section.....	51
References.....	58

CHAPTER III. Synthesis of force probes containing Stiff-Stilbene.....	60
Abstract.....	61
Introduction.....	61
Result and discussion.....	63
Molecular design.....	63
Isolation of polymers via preparative GPC.....	67
Conclusions and future work.....	71
Experimental section.....	74
References.....	86
CHAPTER IV. Synthesis of topologically complex polymers with an H-shape.....	87
Abstract.....	88
Introduction.....	88
Result and discussion.....	92
Molecular design.....	92
Connecting the core to polystyrene chains.....	95
Conclusions and future work.....	97
Experimental section.....	101
References.....	110
CHAPTER V. General Conclusions and Perspectives	111
References.....	117

Abbreviations

AFM	atomic force spectroscopy
APT	adenosine triphosphate
ATP	attached proton test
BCB	Benzocyclobutene
BCO	Bycliclooctane
CRP	controlled radical polymerisation
D	Doublet
DA	controlled radical polymerisation
DBC	Dibromocyclopropane
DCC	Dichlorocyclopropane
DCM	dichloromethane
ddt	double double triplet
DFT	density functional theory
DHC	Dihalocyclopropane
DMAP	dimethylamminopyridine
DMF	Dimethylformamide
DMp	Distribution of peak molecular weight
Dt	Doublet of triplets
EDC	1-Ethyl-3-(3-dimethylaminopropyl)carbodiimide
eq	equivalent
EtOAc	ethyl acetate
gDBC	gem-dibromocyclopropane
gDCC	gem-dichlorocyclopropane
gDFC	gem-difluorocyclopropane
gDHC	gem-dihalocyclopropane
GPC	gel permeation chromatography
Hex	hexane
Hz	Hertz
LC	liquid chromatography
MPLC	medium pressure liquid chromatography

Mp	Peak molecular weight
NMR	nuclear magnetic resonance
prepGPC	preparative gel permeation chromatography
ROMP	ring opening metathesis polymerization
Rt	room temperature
SEC	size exclusion chromatography
SMFS	single molecule force spectroscopy
SS	Stiff Stilbene
t	triplet
tBuOK	potassium t-butoxide
t_{1/2}	half-life
T	temperature
TBAI	tetrabutylammonium iodide
THF	tetrahydrofuran
TLC	thin layer chromatography

Abstract

The projects described in the following chapters are all designed to understand how polymer architecture determines the distribution of stresses and the distribution of strains. Chapter I is a literature review which provides the background and the previous work on polymer mechanochemistry. From Chapter II, I describe my work on the synthesis of mechanophores and polymers, starting from a single polymer chain with various geometries, forces applied, loading scenarios. We wanted to start this investigation with something as simple as possible, *i.e.* a linear polymer, since its behavior under force has still many unresolved issues and once exploited there will be many potential applications in material design and engineering. Afterwards, we'll study the behavior of a more complex polymers (made by two different chains) and the last challenge will be the investigation on an H-shaped polymer (which has the closest structure to the polymers widely used in industry). What is really going to make an industrial impact is to understand how polymer topology structure affects the distribution.

Most materials industrially used are crosslinked, the topologically complex polymers we designed in the last chapter are models of those crosslinked materials used in industry. This is because a crosslinked moiety has at least three polymer chains coming from one point, but often has more complex geometries. The purpose of designing this series of increasingly more complex moieties is to understand how strains imposed externally distribute in macromolecular chains and how the distribution is determined by the molecular topology of the chain from a simple ideal model up to moieties which represent the widely used polymer materials which are chemically crosslinked. The exploration of the behavior under force of a series of increasingly more complex polymers (given that chapter I focuses on a single polymer chains, chapter II focuses on two polymer chains, while the final chapter focuses on four polymer chains) coherently links the three projects and addresses the broad question: How are stresses distributed along a polymeric material subjected to force?

CHAPTER I: Polymer Mechanochemistry

Abstract

A topic of particular interest in polymer science is the design of polymeric materials that exploit mechanochemical phenomena to respond to mechanical loads in ways that are more useful than catastrophic failure. While interesting prototypes of such stress-responsive materials have been reported^{1,2,3}, their incorporation in commercial products has been hampered by the lack of a general strategy to independently vary the chemistry triggered by the load and the threshold force at which this reactivity occurs. This task has been implemented by creating macrocycles that integrate two reactive sites, one that produces the desired chemistry and the other that controls the force at which this chemistry is triggered. Another challenge in polymer mechanochemistry is to understand the modifications of polymer chains under force. In order to do this, it's useful to have an easily detectable probe inside the polymer chain to follow qualitatively and quantitatively the behaviour of such polymer under force. Therefore, mechanoresponsive moieties has been synthesized and incorporated in linear polymers (Stiff-Stilbene-Polystyrenes) and topologically complex polymers (Anthracene-Maleimide Diels-Alder Adduct-Polystyrenes arranged in a "Star" and "H" shape).

Introduction

Polymer mechanochemistry plays an important role in understanding how polymeric materials respond to mechanical loads. Unfortunately, the complex mechanisms of such responses are still poorly understood. Polymer mechanochemistry is an important research topic because it plays an important role in our everyday lives. Polymers are subject to mechanical stress throughout their lifecycles, from production to recycling. A variety of phenomena triggered by mechanical force affect the generation, growth, and propagation of microcracks which are responsible for catastrophic failure of many polymeric materials, such as tires and impact-resistant materials (*e.g.* bulletproof vests).

The ability to understand the different mechanisms of mechanochemical phenomena could afford the discovery and improvement of new materials and processes. These include: self-healing materials (due to a structure capable of crosslinking or by undergoing a similar reaction triggered by force rather than simply causing material failure), polymer photo actuation (*i.e.* the direct conversion of light into motion to power autonomous nanomechanical devices, the control of information flow in optical computing, or improvement of mirrors or photovoltaic cells in solar capture schemes). Further application of mechanochemical phenomena could be the development of efficient systems to capture of waste mechanical energy and the development of tools to study polymer dynamics at sub-nanometer scales⁴. Polymer mechanochemistry may also be important in enhanced oil recovery, some other industrial application such as jet injection (*e.g.* during inkjet printing of organic electronics), polymer melt processing, high-performance lubrication and turbulent drag reduction⁵.

A common strategy of obtaining mechanochemically active polymers is to incorporate force-sensitive reactive sites in otherwise inert polymer chains and matrices. This method could improve our understanding of the mechanochemistry of entangled polymer chains because it provides experimental tools which quantify how and how fast mechanical loads propagate through amorphous polymer matrices to reactive sites. Moreover, it could allow the range of local forces and their distributions between the reactive site (mechanophore) and the polymer chain to be quantified.

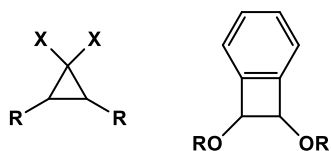
Mechanophores : design and properties

A mechanophore is a molecule designed in a specific way which allows it to respond to mechanical force in a predictable and useful manner. When it's incorporated in a polymer chain, the polymer acts as an actuator to transmit macroscopic force to the target. Another fundamental component in mechanophores design is their position in the polymer chain. The mechanophore should be incorporated into the middle of

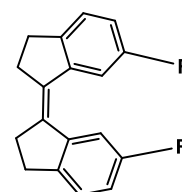
the chain with its active bond along the chain contour since the maximum tension force is at the middle point of the chain contour.

Several mechanochemically active molecules that undergo various reactions have been designed and used in different applications. They can be grouped according to the type of reaction experienced under force: isomerization, electrocyclic ring opening, reverse Diels-Alder, homolytic cleavage, dative bond scission and cycloreversion (**Figure 1**).

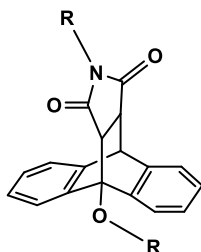
1)Electrocyclic ring opening



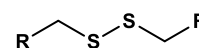
2)Isomerization



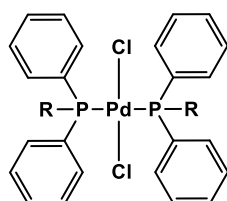
3)Reverse Diels-Alder



4)Homolytic cleavage



5)Dative bond scission



6)Cycloreversion

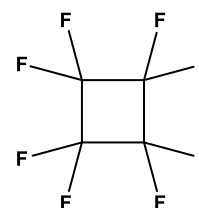


Figure 1: Examples of mechanophores with different mechanochemical behaviour.

Mechanophores undergoing electrocyclic ring opening

Electrocyclic ring opening is the reaction displayed by the largest portion of mechanophores when they experience force. Several uses and conditions have been investigated with a variety of different molecules. For example, polymers containing a non-scissile moiety such as bicyclo[4.2.0]octane were studied in sonicated solutions and the mechanism of the triggered ring opening reaction was proposed based on the stereochemistry of the products yielded. It has been shown that the reaction is mechanically driven (using a test polymer small enough to avoid mechanical activation, in contrast to thermal reactions whose rates are MW-independent)⁶. The reaction was later exploited to prepare self-healing materials by combining it with ethyl thioglycolate and a catalyst. Substituted cyclobutene has two possible products generated after the ring opening reaction (details shown in **Figure 2,a**). In the aforementioned study⁶, cycloreversion of cyclobutane was hypothesized as a non-concerted two-step process via a diradical intermediate affording a preferred “pro-EZ” conformer as product (**Figure 2,b**).

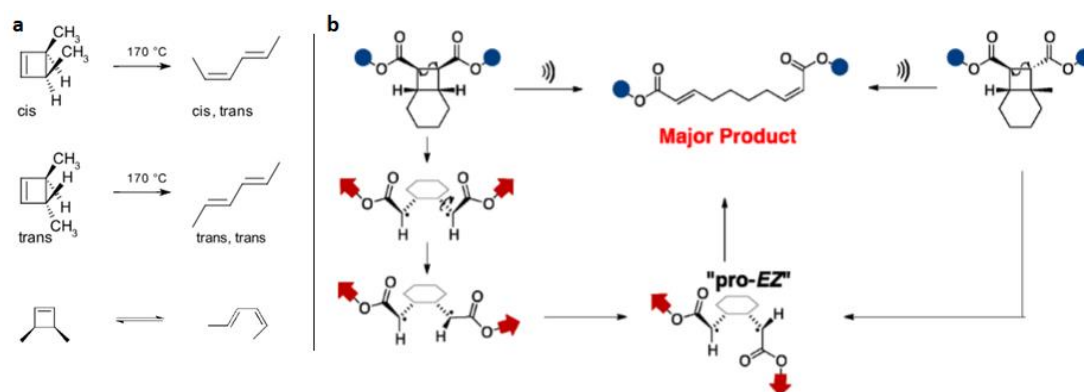


Figure 2: Ring opening reaction of a substituted cyclobutene. Due to its mechanochemical properties, cyclobutene can undergo the same reactions without heating, just with force applied (therefore is considered a mechanophore). Adapted from ref. ⁶. Copyright 2012 American Chemical Society.

However, it is possible to obtain different outcomes merely by using structural manipulation of the starting mechanophore (increasing substitution hinders diradical rotation resulting in increased retention of stereochemistry), since mechanical BCO activation is influenced by the structure.

Another important use of mechanophores is to explore the possibility of achieving certain reactions with force which could be otherwise forbidden. Craig demonstrated⁷ how three forbidden reactions could occur when they've been triggered by mechanical load (using SMFS to observe this behavior). In the case of cis-benzocyclobutene pulled in a disrotatory way, the ring-opening reaction not only occurs (despite being forbidden by Woodward-Hoffmann's rules) but it is faster and requires less force than the conrotatory pulling with trans-BCB (allowed) – therefore cis-BCB displayed greater mechanochemical reactivity (as shown in **Figure 3**).

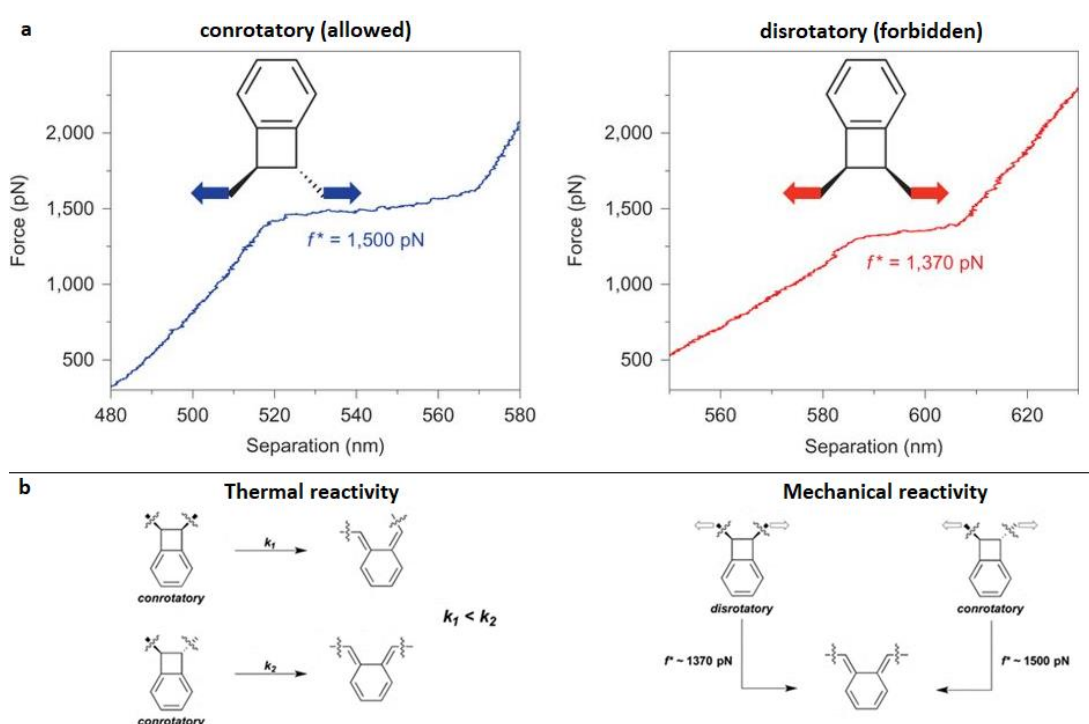


Figure 3: a) In blue, the arrows indicating an allowed pulling direction (conrotatory) and in red the forbidden pulling direction (disrotatory). The data were acquired with SMFS using benzocyclobutane (BCB) molecules as samples. b) Difference between the thermal and mechanochemical reactivity of cyclobutene. Adapted from ref. ⁸. Copyright 2015 Nature Chemistry.

When gDFC underwent ring opening reactions of both cis and trans isomers under mechanical forced, and the mechanism formed 1,3 diradicaloid transition state which could be trapped and could subsequently react with nitroxides or oxygen (mechanism shown in **Figure 4**). gDCC had the same behavior of gDFC but had a more complex ring opening mechanism given that chloride migration occurred (the conrotatory reaction here involves the largest measured force to a covalent chemical mechanism other than hemolytic bond scission).

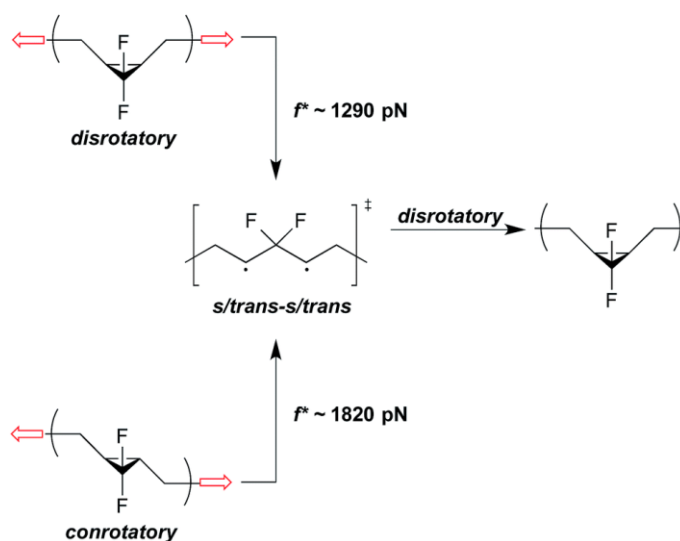


Figure 4: The difference of force required for the conrotatory vs the disrotatory ring opening reaction in dihalocyclopropane is crucial to understand mechanisms in this thermal and mechanochemical reaction. Reprinted from ref. ⁹. Copyright 2015 Chemical Science.

gem-Dihalocyclopropane (gDCC) has also been used to demonstrate a remote lever arm effect when it is incorporated in polymers¹⁰. In fact, gDCC ring opening is sensitive to the stereochemistry of an α -alkene substituent on the ring. gDCC was incorporated in a copolymer made by E-alkene, Z-alkene substituted gDCC and epoxide (this is mechanically inactive in the force range of interest, but it increases the attachment force between the tip of the instrument - atom force microscope - and the sample polymer). Changing the ratio of the three polymer components elicited a different response in SMFS measurements, indicating that compared to the Z isomer, the E isomer of the α -alkene acts as a lever which provides a greater mechanical advantage for an applied force.

The force magnitude and the distribution of stressed monomers along polymers chains using a gDHC functionalized polybutadiene have also been demonstrated¹¹. Instead of SMFS experiments, this objective has been achieved using H-NMR to observe the polymer behavior under force, since it is quantitative, and the chemical shifts of the resonances are sensitive to the localized chemical environment, allowing the characterization of the microstructure of the polymer. The ring opening

has been shown to be mechanically induced rather than being pressure induced in several experiments using different compression times. This showed that the ratio of activated monomers was the same, therefore the phenomenon is related only to the initial mechanical load. Moreover, it has also been demonstrated⁸ that the reaction outcome is different when the reaction is mechanically rather than thermally induced: the former yields both dihaloalkene isomers (with typical blocky repeating signals in H-NMR), the latter is selective towards cis-anti-dihaloisomers with subsequent HBr elimination (with random repeating signals in H-NMR). The comparison of NMR analysis of mechanical and thermal ring opening reaction of gDCC is shown in **Figure 5**.

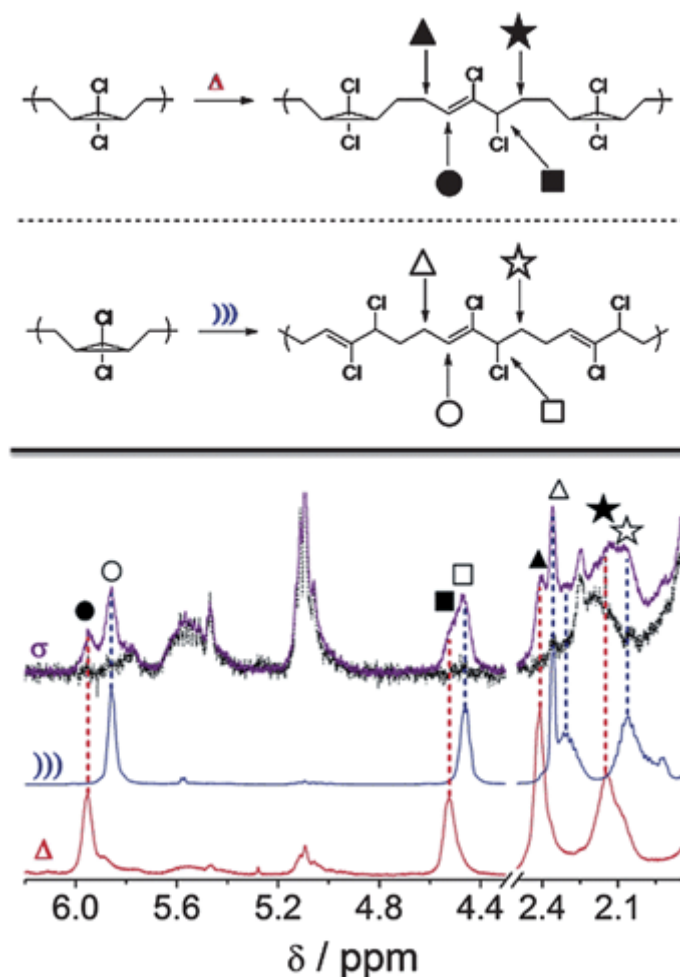


Figure 5: ¹H NMR chemical shifts from sonochemically []]]] and thermally [Δ] activated gDCC polymer indicate the presence of distinct microstructural environments along the polymer. Compressive [σ] gDCC activation leads NMR signals which are consistent with a mixture of the two chemical environments. Reprinted from ref. ¹². Copyright 2009 American Chemical Society.

Another interesting finding was that the size of the mechanically active domain

inside the polymer is smaller than the typical average entanglement spacing (10 monomers). In case of gem-dihalocyclopropanated polybutadiene it was around 4 monomers, that's because entanglement spacing aren't monodisperse and the shortest chain segment is the most likely to become overstressed. Another interpretation of this small domain size is that the local mechanophore provides stress relief extending polymer contour length, or the forces are independent by dynamics of shear flow but are different right at the entanglement point rather than between entanglements.

Since it has been demonstrated that forces tend to accumulate at the center of a polymer chain, Craig and coworkers¹³ synthesized a ABA copolymer creating the B block rich in mechanophore content (gDCC): ROMP was used because backbone rings cannot be easily introduced by the traditional polymerization of vinyl monomers. Furthermore, controlled radical polymerization was used to extend the chain yielding a high MW, this was required to experience sufficient shear forces along the polymer backbone. With this ABA copolymer they noticed a 55% ring opening, higher than the 35% obtained previously with polybutadiene-gDCC. Therefore, showing that the central block of the polymer experienced more force yielding a higher fraction of activated mechanophores.

Moreover, a polymer containing gDCC underwent several hundreds of ring-opening reactions when coupled with ultrasound-generated elongational shear flows. These ring-opening reactions were much faster than a single polymer chain scission. By incorporating both cis and trans gDCC in a polybutadiene copolymer, NMR analysis estimated that the probabilities for ring opening reactions were nearly the same for both isomers, although under stress-free conditions the cis isomers reacted 20 times faster than the trans (because of the symmetry forbidden conrotatory ring opening). In conclusion, it was possible to trigger multiple chemical response during a single short strain event in a polymer containing gDCC as mechanophore.

Mechanophores undergoing isomerization

In Dr Boulatov's previous work, it has been demonstrated that the same force-rate correlation governs the reactivity of dibromocyclopropane in stretched polymers and in strained small molecules¹⁴. Stretching a polymer can significantly change the reactivity of its monomers. These changes contribute to the response of polymeric materials to external loads and the behavior of polymers in shear flows, therefore understanding such phenomena at the molecular level with the goal of designing new types of photactuating, stress-responsive and other energy-transducing materials require a challenging extrapolation of the kinetics of a localized reaction in a stretched polymer from that of a suitable small-molecule reactant. Strain-induced reactivity of monomers in stretched polymers is typically quantified as the correlation between the reaction rate and the force needed to maintain the polymer in the stretched geometry¹¹. For a few localized reactions, such rate-force correlations can be measured in single-molecule force experiments.

At present these rate-force correlations can neither be calculated, nor extrapolated from the reactivity of an isolated monomer, considerably complicating both the atomistic interpretation of single-molecule force experiments and the identification of monomers for stress-responsive polymers. The experimental force-extension curves of dibromocyclopropanated butadienes were accurately reproduced using the data from measurements of force-rate correlations in a series of increasingly strained macrocycles (shown in **Figure 6**). The measured force-extension curve represents thousands of ring-opening reactions (unlike most single-molecule force measurements, such curves reflect ensemble-averaged reactivity of the cyclopropane moiety in stretched polymers).

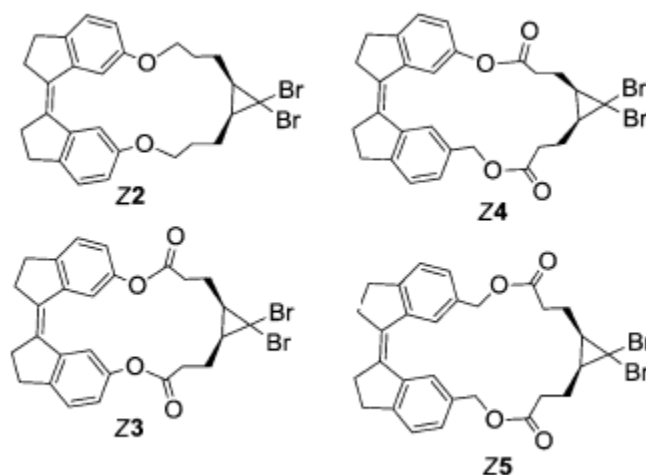


Figure 6: Macrocycles incorporated in a polymer to prove the correlation of certain force properties between a single monomer and the whole polymer. Reprinted from ref. ¹⁴. Copyright 2012 American Chemical Society.

In contrast, the minimal model of chemomechanical kinetics fails to reproduce the force-extension curves. Investigating the force-dependent ring-opening of dibromocyclopropane has the potential to yield novel types of stress-responsive polymers of unprecedented toughness.

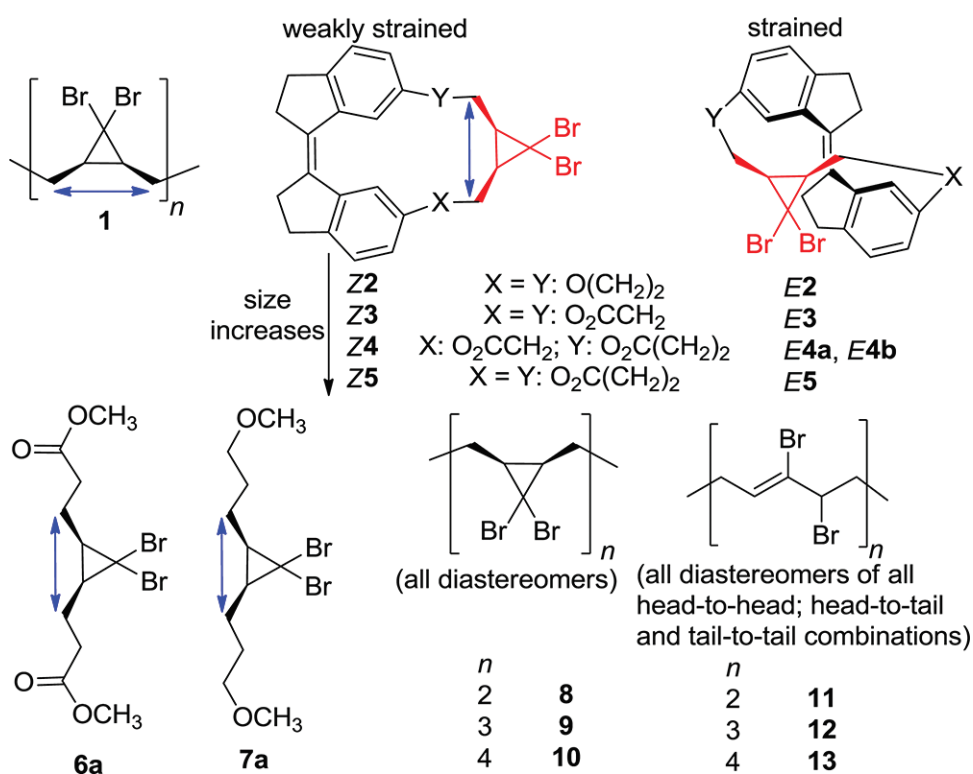


Figure 7¹⁴: Series of macrocycles with increasing internal strain. Reprinted from ref. ¹⁴. Copyright 2012 American Chemical Society.

Our group showed that the behavior of a polymer can be demonstrated merely by knowing: the kinetic stability of an isolated monomer as a function of the restoring force of one of its local coordinates, and the ratio of the local restoring force that one monomer experiences due to the force applied at the end of its polymer (a series of macrocycles with increasingly internal strain were used for this purpose, showed in **Figure 7**). With this, it will be possible to provide useful links between the atomistic model and the material, in order to further explain and describe the chemical reactivity of material under stress. Moreover, the behavior of a polymer with more than 10^8 molecular degrees of freedom could be exploited simply by knowing the properties of a single monomer.

Mechanophores undergoing reverse Diels-Alder

Anthracene-Maleimide DA adducts were used to create self-healing polymers: this phenomenon can be achieved with mechanochemical conditions rather than thermal. Diels-Alder (DA) cycloaddition is a convenient route for the formation of carbon-carbon bonds via a reaction under specific conditions that match the requirements of a “click” reaction. Diels-Alder cycloadditions are thermoreversible reactions and this feature has been exploited in the preparation of self-healing polymers carrying functionalities, either as the polymer chain-end or in the repeating units.

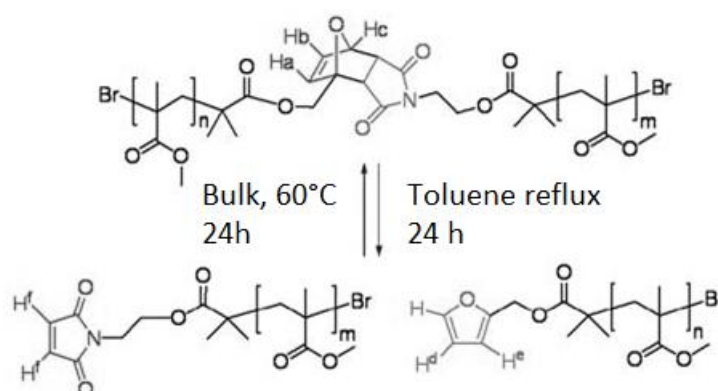


Figure 8: Mechanophore used by Syrrret and coworkers to prepare self-healing polymers. Reprinted from ref. ¹⁵. Copyright 2010 Polymer Chemistry.

The reverse DA reaction does not involve free radicals, therefore many side reactions that might regenerate the DA adduct are avoided. Diels–Alder moieties were first incorporated into polymers by Stevens and Jenkins, later, Saegusa and co-workers developed a thermally “mendable” polymeric DA network¹⁶. A Diels–Alder cross-linked polymer synthesized for the specific use of self-healing was prepared by Wudl et al. in 2003, using furan- and maleimide-based monomers cross-linking along the polymer backbone¹⁷. Syrrret and co-workers showed¹⁵ in their work that fractured polymer materials, heated to 120°C, exhibited 83% recovery of the polymer’s original strength (polymer shown in **Figure 8**). This fracture and repair cycle could also be repeated, making this the first real DA polymeric system displaying a self-healing behavior. The self-healing property of polymers is applicable to composite materials and large cross-linked networks. Advances in controlled radical polymerisation (CRP) allow for the synthesis of functional polymers with excellent control over molecular weight, molecular weight distribution, architecture and incorporation of functionality.

Mechanophores undergoing homolytic cleavage

Photochemistry of aliphatic disulfides is an important reaction due to its role in: the atmospheric processes, photoinitiation of polymerization reactions, synthetic chemistry, biochemistry and biophysics. The C-S bond homolysis controls photochemistry of organic disulfides at wavelengths <250 nm. At longer wavelengths, only the scission of the S-S bond is considered fundamental (except for tert-Bu and benzylic disulfides where C-S homolysis can be detected down to 300 nm irradiation wavelengths).

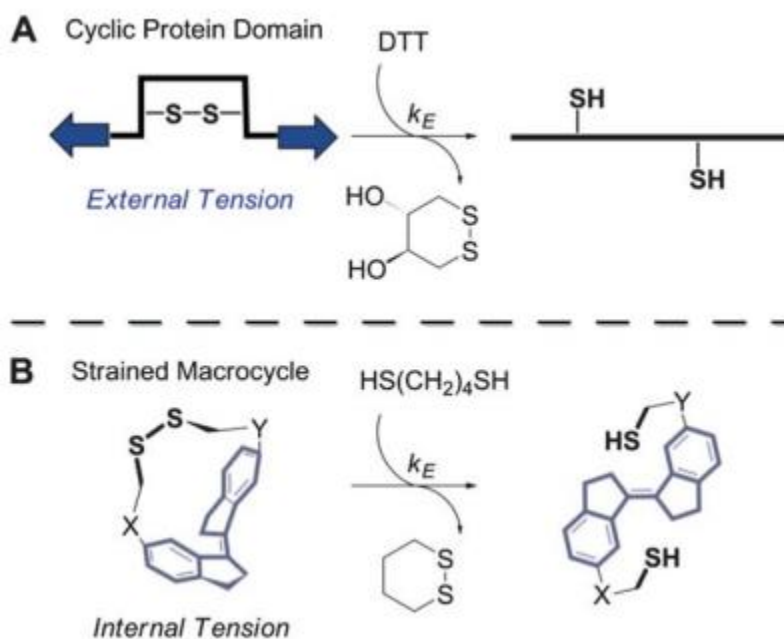


Figure 9: Difference between the S-S scission in a biological system (A) and when it's part of a mechanochemical moiety (connected with a Stiff-Stilbene in part B). Reprinted from ref. ¹⁸. Copyright 2009 Angewandte Chemistry International Edition.

Our research group previously synthesized a series of macrocycles (all including Stiff-Stilbene moieties) with the purpose of showing that stretching the disulfide moiety up to the restoring force of 350 pN along the S-S bond negligibly accelerates its reduction by thiols (shown in **Figure 19**)¹⁸. The measured rates of thiol/ disulfide exchange in the increasingly strained E macrocycles were within a factor of two of those in strain-free Z analogues, with the activation enthalpies differing only by 1 kcal/mol. This value is considerably smaller than the C-C bond electrocyclic dissociation present in a series of similar molecules. Using these mechanochemical moieties to quantify the strain in their E isomers could give insight into the mechanism of acceleration of disulfide bond reduction caused by protein stretching or also provide understanding of the factors causing the changes in reactivity of compressed/stretched molecules. The kinetics of S-S/thiol exchange were measured as a function of the restoring force of the disulfide moiety under tensile strain. In the past, the reactivity of disulfide moiety was broadly studied in dithiacyclopropane and dithiacyclobutane but was not studied in molecules displaying tensile strains. In fact, the aliphatic disulfides are strain free and therefore this factor doesn't play a role in the kinetics of this disulfide-thiol exchange reaction.

The data collected suggested that the force applied on the S-S moiety up to 350 pN of force on the disulfur bond did not accelerate the reduction to SH species. This revealed that stretching a molecule doesn't necessarily speed up fragmentation, as seen in macroscopic and daily experiences. The length of the scissile bond is not a suitable variable, moreover the dissociation rate of a covalent bond under tensile strain is proportional to the product of the restoring force and there is no real difference in the scissile bond length between the ground and transition state. It has also been shown that the kinetically important structural changes in a reacting molecule can be captured using a single internuclear distance and its choice could be guided by the molecular mechanism of the reaction.

Mechanophores undergoing cycloreversion

Perfluorocyclobutane polymers undergo chain scission upon mechanical force, but the process can be reversed by heat (150 °C) simulating the same polymerization conditions (reactions shown in **Figure 10**). Craig and coworkers demonstrated¹⁹ how the thermal-induced chain scission outcome is different from the mechanical-induced. The first mechanism yielded hexafluorocyclobutene and phenol – impossible to remend; the second afforded trifluorovinyl ether groups that could react via cross-linking reactions thanks to the stepwise mechanism of mechanical scission, which proceed via a diradical intermediate reactive to intermolecular addition reactions.

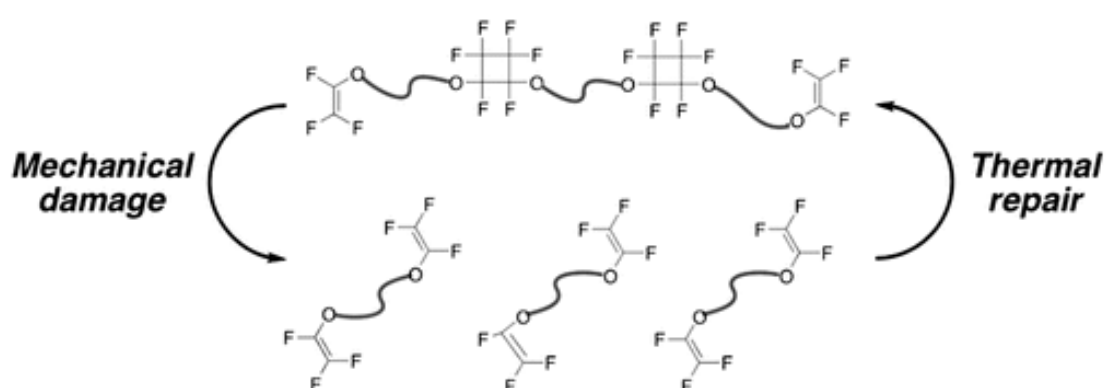


Figure 10: Perfluorocyclobutane used for cycloreversion reactions investigation by Craig. Reprinted from ref. ¹⁹. Copyright 2011 American Chemical Society.

Craig conducted this study by observing changes in polymer molecular weight by characterizing the products with F-NMR. This confirmed the mechanical nature of polymer degradation, since in the thermal process, degradation is independent of molecular weight (here degrades faster at higher MW). Moreover, when using a very small polymer there were no evidence of chain scission, given that the polymer is too small to experience significant mechanical force.

Techniques used in Polymer Mechanochemistry

To understand the response of materials to mechanical loads, it is necessary to develop experimental techniques to prove and test the theoretical predictions. Kinetic and mechanistic studies of chemical reactions in large materials remain outside the capabilities of modern science. More simple systems to test force-based models of reaction kinetics include shear-flow and single-molecule force methods, in which individual macromolecules are strained by macroscopic or microscopic tools, and molecular force probes in which molecular design is used to control the restoring force²⁰.

The most important methods are shear-flow (which has been used the longest), followed by single-molecule force methods, the development of which was improved by micromanipulation techniques, such as laser tweezers and atomic force microscope. Manipulating restoring forces of small reactants by molecular design and synthesis was considered the easiest way to allow force-dependent measurements of reactivity, rather than conducting such analysis on entire polymers. However, the improvement and development of this strategy was inhibited by the lack of suitable molecular architectures. In fact, it was challenging to modify the restoring forces of moieties with different reactivity in sufficiently small increments and over a sufficiently wide range to reveal broad trends.

There was an attempt to explain the reactivity of strained molecules (like cyclopropane) within the force formalism, though it was unsuccessful since such

molecules were too small to have degrees of freedom that could be approximated by force. Due to the progress in computational chemistry and analytical techniques throughout the literature, it was possible to design and synthesize molecules with a size which allow an explanation of their reactivity within the force formalism.

Shear-flow methods

The majority of shear-flow experiments are run in one of three configurations: 1) elongational flow; 2) transient flow and 3) acoustic fields (“elongational and transient flow” models are illustrated in **Figure 11**). In elongational flow a solution of a polymer is rapidly passed through a flow cell with an inlet at 90° to a pair of mutually-opposing outflow orifices. The geometry creates a stagnation point where some macromolecules are trapped and at some point, they break. In transient flow, a flowing solution encounters a sudden contraction. Kinetic and mechanistic studies of reactions in shear flows are still difficult to exploit because of both the limited observables and poorly understood control parameters^{21,22,23}. Acoustic fields are often generated when a polymer in solution is exposed to ultrasonic waves. The mechanism of how the solvent controls the macromolecular strain is still not well understood and appears to be distinct in the laminar and turbulent regimes. Shear flows with ultrasonic waves will be described in the next section “Ultrasonic Irradiation”.

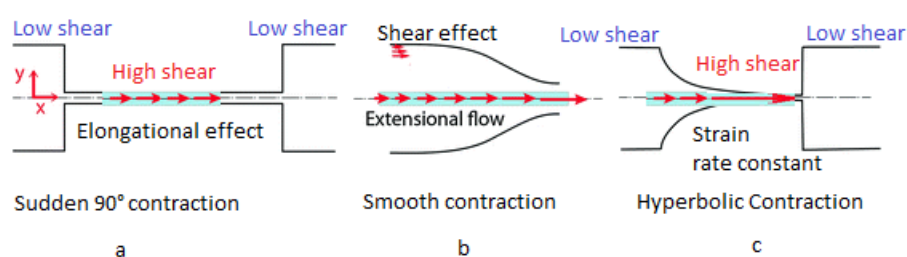


Figure 11: a) the polymer in solution encounter a 90° inlet in elongational flows. b) and c) are both examples of transient flow scenarios. Adapted from ref. ²⁴. Copyright 2014 Springer International Publishing Switzerland.

Most shear-flow experiments simply give information regarding changes in molecular weight, chemical composition of the polymer and molecular weight distribution. Obtaining a precise product speciation is difficult with this technique, since, in most experiments, only a tiny fraction of the polymer changes its chemical

composition. Estimates of strain are sometimes possible under conditions that do not result in chemical reactions. Experimental variables that are known to affect the observables include temperature, viscosity, concentration and molecular weight, with the obvious contribution of the intensity and length of the shear - generating perturbation. These variables are tightly coupled, but unfortunately there is no possibility to have a complete quantitative outcome from shear-flow analysis. Therefore, is not possible quantify the restoring force of macromolecules in shear-flow experiments.

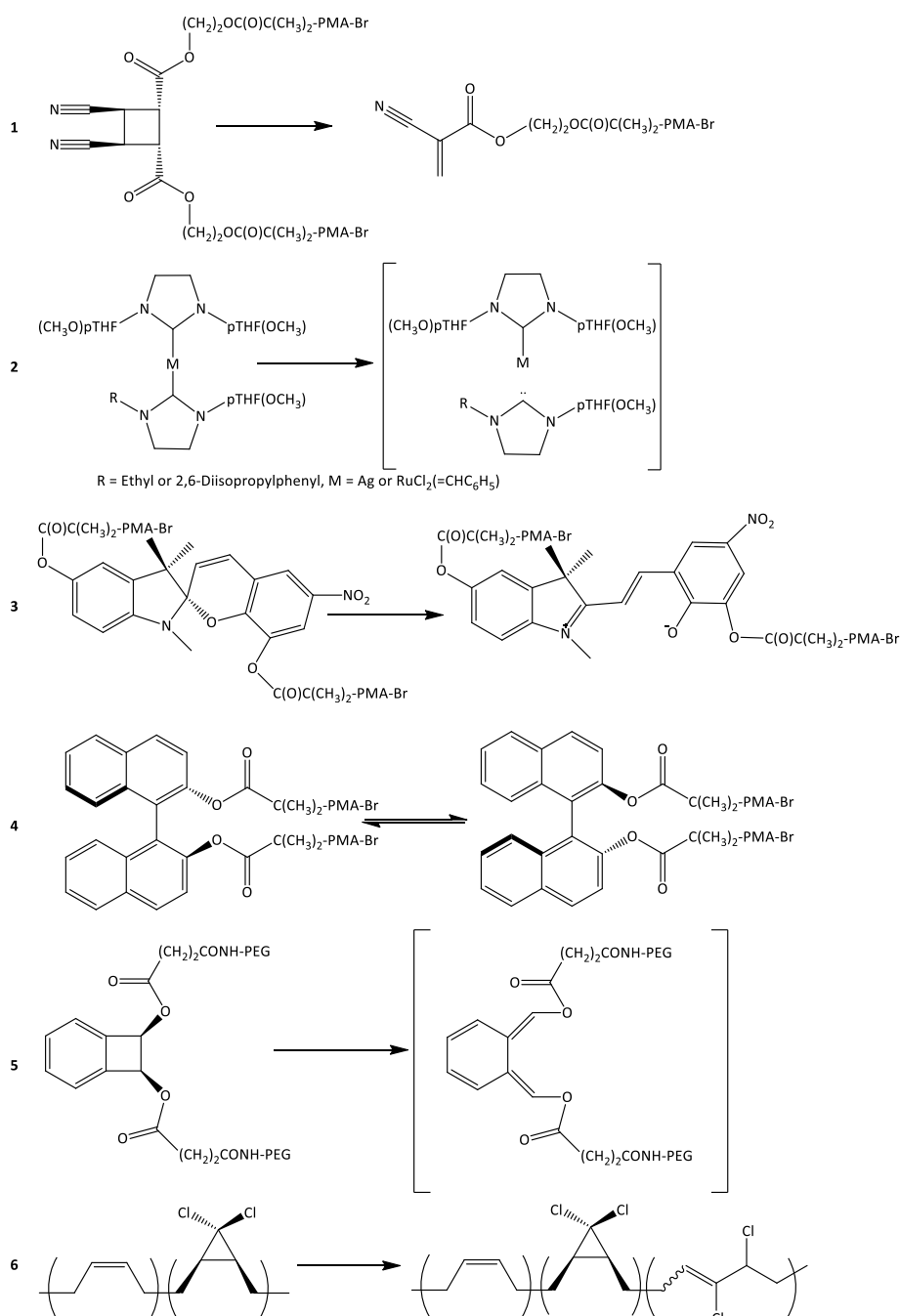


Figure 12^{25,26}: Some of the reactions that are accelerated in shear flow induced by acoustic field.

A variety of unimolecular isomerizations and dissociations have been shown²⁷ to be accelerated in polymers in shear flows (shown in **Figure 12**). The most important reactions were 1) cycloreversion of dicarboxydicyanocyclobutane; 2) dissociation of Ag and Ru complexes; 3) isomerization of a spiropyrane and a binaphthyl; 4) symmetry forbidden electrocyclic isomerization of cis-dialkoxycyclobutabenzene; 5) isomerization of cis- and trans-dihalocyclopropanes into allylic halides. The expected products were detected with an isotope-labelled or fluorogenic reagent (cases 1 and 4), by UV-vis or CD (case 3), by catalytic signal amplification (case 2) or by direct analysis of reaction mixtures by ¹H and ¹³C-NMR spectroscopy (case 5).

Ultrasonic Irradiation

Sonication (ultrasonic irradiation) is a widely used technique in polymer mechanochemistry for studying mechanophores. This is mainly due to the high strain rates it can produce, the relatively cheap cost of the instrument (compared with an atomic force microscope) and the user-friendly interface of the apparatus. The main use of sonication instruments aims to simulate the behaviour of a polymer chain under force. The ultrasonic degradation of polymers occurs during the nucleation, propagation and collapse of bubbles due to the action of acoustic cavitation in solution under ultrasonic irradiation, commonly called sonication.

If we apply a high energy acoustic field to a solution, the local pressure changes. When the ultrasonic pressure amplitude goes above the average pressure in the liquid, it causes a negative pressure. This negative pressure could overcome the cohesive forces of the fluid causing cavitation and therefore dissolved gases escape into cavities. Bubble collapse generates very high fluid strain rate (*i.e.* how much the flow rate varies spatially) near the bubble-solution interface. Because the strain rate decreases rapidly away from the bubble, nearby polymer chains become stretched, as the chain segments closer to the bubble move more quickly towards the site of collapse than segments away from it (as shown in **Figure 13**). It is important that during sonication, the chains do not interact directly with the ultrasonic energy. So,

polymer chain scission is therefore due to bubble collapse, which is an integral part of acoustic cavitation.

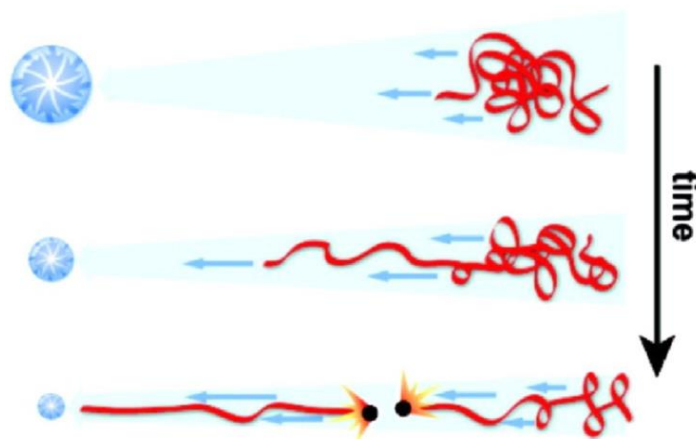


Figure 13: A representation of how acoustic cavitation in dilute polymer solutions stretches the polymer, with subsequent fragmentation at approximately the midpoint. The blue arrows represent the direction of the resulting fluid flows due to bubble collapse, with size proportional to their magnitudes. Adapted from ref. ²⁸. Copyright 2009 American Chemical Society.

Atomic Force Spectrometer (AFM) – Single Molecule Force Spectroscopy (SMFS)

AFM was created as a tool for the imaging of surfaces with high resolution. Due to the high resolution of force sensing, AFM can also be used to detect inter- and intramolecular interactions in systems immobilized on the surface of the instrument. The principle of SMFS is to manipulate a macromolecule that bridges an AFM tip and a substrate (the solid support). During the manipulation of the molecule bridge, a cantilever deflection-piezopath curve is recorded and later converted into a force-molecule extension curve. The molecular bridge can be created in many ways, which are classified into two different types: physisorption and chemisorption. With physisorption, the molecules are first adsorbed onto the substrate and then the tip captures one or more molecules from the substrate with the application of a compressive force. Chemisorption involves the binding of the molecule to the surfaces with a covalent bond. The sample we want to analyze will be modified by connecting with an unreactive moiety (containing oxygen for example) to create an oxygen bridge onto the instrument, without affecting the measurement. In both

chemo- and physisorption, the interaction between the tip and the target molecule must be stronger than the force required to trigger the mechanochemical reaction. Furthermore, the force resolution of a SMFS is about 10 piconewtons (pN) and this suits a variety of inter- and intramolecular interactions analysis.

Unlike sonication, SMF experiments suggest that reducing the average lifetime of *trans*-DHC to ~100 ms requires force 200-500 pN higher than that of the *cis* analogue, although the mechanistic basis of this difference remains unknown despite mechanochemical isomerization of DHCs being the most extensively studied reaction by SMFS. As mentioned in the above, SMFS operates by stretching isolated polymer chains using an AFM. A macromolecule is attached (usually chemically) to a glass slide at one terminus and to the tip of an AFM at the other terminus (**Figure 14**). The slide is slowly moved away from the stationary AFM tip, stretching the polymer. Bending of the AFM tip by the stretched macromolecule is measured to estimate the “restoring” force of the polymer. The data is recorded as a force-extension correlation.

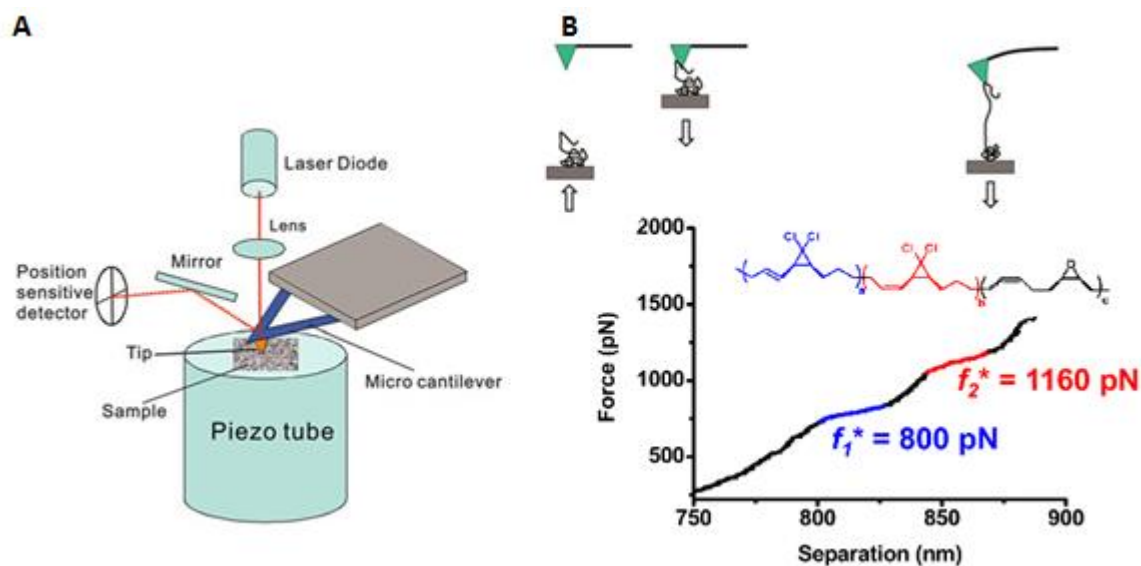
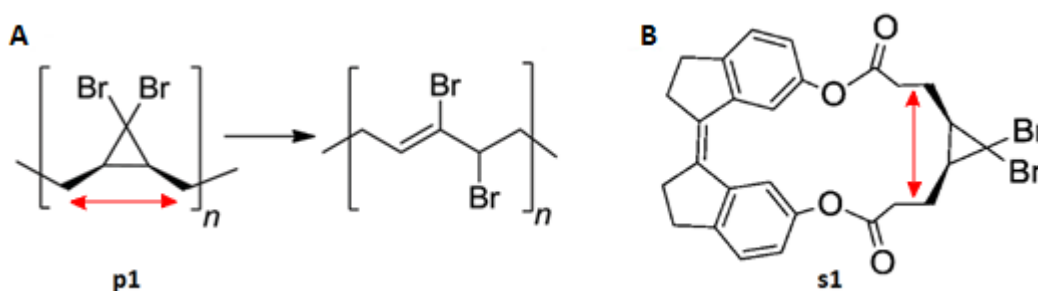


Figure 14: A) Schematics of AFM-based SMFS. B) Schematics of pulling a single polymer chain and the corresponding force curve obtained by SMFS; is shown the representative force curves of poly-DHCs obtained by SMFS at a retraction velocity of 300 nm/s. The blue and red regions of the plateaus are determined by inspection and provided to guide the eye only. Adapted from ref. ²⁹. Copyright 2015 Springer International Publishing Switzerland.

When the polymer chain is stretched to a force at which the half-life of reactive sites in the chain is reduced to ~100 ms, the sites react. If the product of this reaction has

a contour length longer than the reactant, the measured “extension” of the polymer chain increases without concomitant increase in the restoring force, *i.e.*, a plateau is observed on the force-extension curve (**Figure 14**, B). While the capacity to stretch isolated polymer chains and induce them to react at a certain extension is clearly fascinating, even the best designed SMF experiments yield data that is far more ambiguous than is useful or acknowledged by most practitioners. The most important issues are: the limited amount of information on the actual composition of the chain that is being stretched (as it’s picked up randomly from a mixture of chains), the lack of characterization of the product of the reaction and considerable uncertainties about the force responsible for the observed reaction.

Consequently, interpretations of SMF experiments often rely on quantum-chemical computations. The problem is that such computations can rarely, if ever, be performed at an *ab initio* level, and therefore must be benchmarked against a variety of experiments (other than the SMF experiment that they are designed to explain). Our group has developed a method⁴ that allows force-rate correlations to be studied over a far broader range of forces (and hence life-times) than is possible with SMFS or sonication. This method is based on quantifying the rate of mechanochemical induced reaction as a function of the restoring force generated in a single strained moiety, as illustrated below on an example of *cis*-dibromocyclopropane, cDBC (**Scheme 1**, A).



Scheme 1: A) gDBC polymer (**p1**) isomerization under load; B) one of the macrocycles containing gDBC used to demonstrate the relation between the behaviour under load of a polymer and one of its isolated monomer. Reprinted from ref. ¹⁴. Copyright 2012 American Chemical Society.

For example, to predict the micromechanical behaviour of dibromocyclopropanated polybutadiene (**p1**, **Scheme 1** A), which is dominated by mechanochemical

isomerization of the cyclopropane core, the group synthesized and measured kinetics of cyclopropane isomerization in a series of macrocycles, illustrated by **s1** (Scheme 1, B). To relate kinetics measured in macrocycles to that in the polymer, we quantified the strain imposed on the cyclopropane moiety in the macrocycles as a restoring force of an internuclear distance common to both molecular architectures (red arrow) using density functional theory (DFT) calculations. We argue that these calculations provide values of the force that are no worse than those estimated from SMF experiments because the calculations accurately reproduced a closely related (but experimentally measurable) quantity – the activation free energies of cyclopropane isomerization across the whole series of macrocycles.

The results of this approach are shown in **Figure 15**, which compares the measured and predicted micromechanical behaviour of polymer **p1** on example of a single force-extension curve at a particular pulling rate (3 $\mu\text{m/s}$). The agreement is remarkable given that predictions require us to extrapolate force-reactivity correlations (derived from macrocycles similar to **s1**) over 11 orders of magnitude of the rate constant, and a length scale of over 100 nm. Because force-reactivity correlation of a single monomer can be readily calculated, molecular design of reactive sites with complex mechanochemical behaviour (*e.g.*, allostery) is greatly simplified.

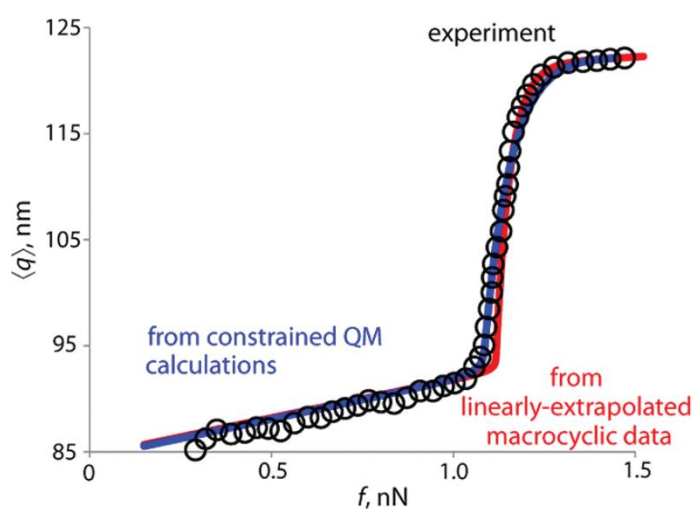


Figure 15 Measured (black o) and predicted (blue and red lines) micromechanical behaviour force-extension curves for **p1**. Reprinted from ref. ¹⁴. Copyright 2012 American Chemical Society.

All these experiments define parameters that control mechanochemical kinetics of DHC isomerization: 1) force-free activation free energy; 2) geometry of attachment (*cis* vs. *trans*); 3) polymer structure: the backbone lever-arm effect facilitates mechanophores activation (by incorporating gDHC both in polybutadiene (PBD) and polynorbornene (PNB), we can observe a lower activation force in PNB rather than PBD (900pN vs 1330pN). To understand the principles of a lever-arm effect, we could observe SMFS studies of the mechanically assisted ring opening of gDHC mechanophores: it has demonstrated that a PNB backbone acts as a lever that accelerates the rates of reactions relative to a poly(butadiene) backbone. This effect could be explained considering the internal molecular strain as a means of coupling a restoring force to a chemical reaction, as described by Dr. Boulatov. However, none of these are suitable to tune the force at which a DHC moiety will isomerize over a sufficiently wide range to be of practical utility.

Besides SMFS, NMR is another useful technique to monitor mechanochemical reactions, *e.g.* the distribution of stressed monomers along polymers chains (studying this behaviour on a gDHC functionalized polybutadiene⁷). Craig's group mostly used ¹H-NMR to determine the product generated when DHC-containing polymer is sonicated or a material is subjected to load, since NMR technique is quantitative and the chemical shifts of the resonances are sensitive to the localized chemical environment allowing characterizing the microstructure of the polymer.

Moreover, Craig and co-workers performed both compression and tension experiments of a series of polymers made of DBC³⁰(shown in **Figure 16**). The result showed a ratio of ring-opening reactions almost identical in all measurements (performed with different compression/tension times), indicating that this reaction is not time-independent under stress, but that the activation occurred during the initial load. It has highlighted that the reaction outcome is different when the reaction is mechanically rather than thermally induced. The mechanical reaction

yields both *trans*- and *cis*-anti-dihaloisomers (with typical blocky repeating signals in $^1\text{H-NMR}$, see **Figure 16**).

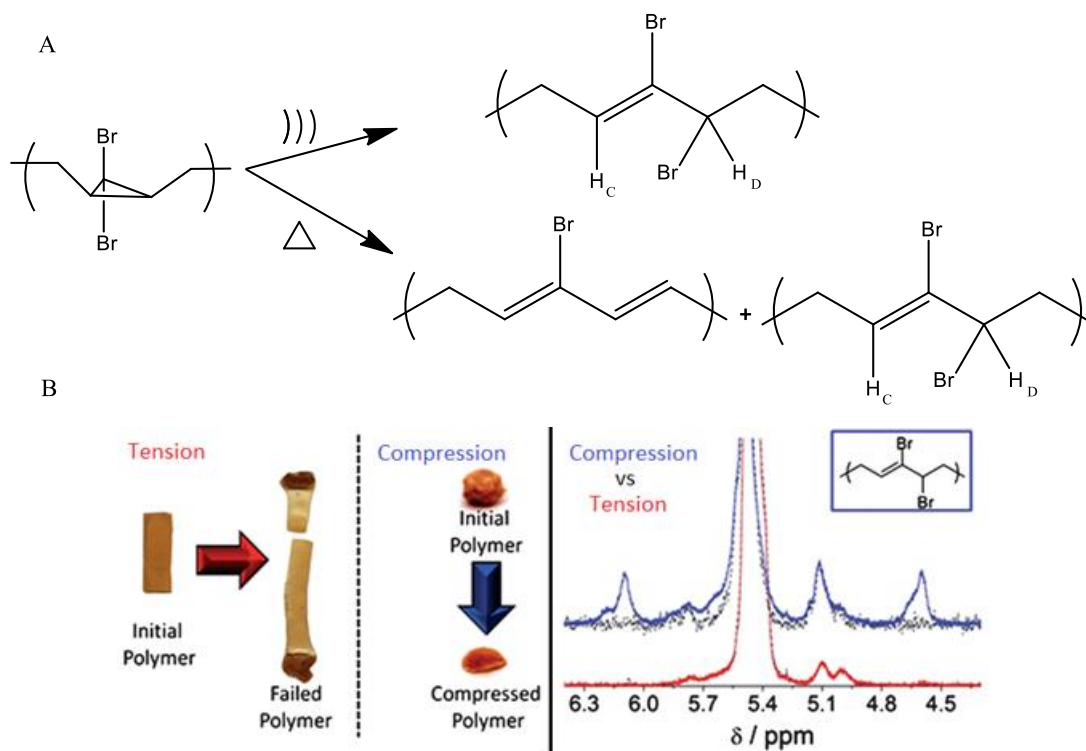


Figure 16: A) Outcomes of DBC after mechanical and thermal stress. B) Tension which cause polymer failure does not cause gDBC ring opening (bottom spectrum) when applied on a gDBC cast film (left) while compression (right) turns gDBC into the 2,3-dibromoalkene. Reprinted from ref.³⁰. Copyright 2011 Material Chemistry.

The thermal reaction (caused by heating the gDBC polymer for 17 hours at 165 °C in methyl benzoate, under N_2) is selective towards *cis*-anti-dihaloisomers and causes HBr elimination (with random repeating signals in $^1\text{H-NMR}$). There are no traces of any “cyclopropyl-allyl” rearrangement product after pyrolysis, but most likely evidence that dehydrobromination occurs in concert with ring opening, since 1,2-dibromo-3-methyl-2-butene is afforded as a sole product.⁸ The $^1\text{H-NMR}$ analysis obtained after pulsed ultrasound applied at the polymer solutions, showed no evidence for HBr elimination products of either the gDBC or gBCC polymer³⁰. Whereas thermolysis of the gBCC polymer resulted in the selective ring opening of the *cis*-anti- bromochloro isomer, both isomers were observed to ring open during compressive activation.⁷ The lack of isomeric selectivity during both sonochemical and compressive activation of gBCC polymer supports a dominant mechanical contribution to gDHC ring opening by compressive stress.

Objectives of this thesis

The next 3 chapters will each describe one project. Based on the literature and on previous work completed by our group, each chapter expands on several objectives fundamental for the development and understanding of polymer mechanochemistry. There are still gaps in the literature regarding the behavior of a variety of polymers geometry under stress. In order to exploit some of these unsolved questions (how the forces are distributed, where the polymer chains is most likely to break with various polymer geometries and topologies, how can we prevent a material failure), I synthesized a variety of molecules containing mechanophores with an unique design and specific properties. While conducting physical measurements on these molecules (trying to reproduce the same force and stress they would experience in daily life materials) we aim to promote “self-healing” and crosslinking reactions rather than material failure. We start from a simple linear polymer (with allosteric mechanochemical properties) then move onto a more complex moiety with two polymer chains (Stiff-Silbene-polystyrenes) and finally a topologically complex multi-arms polymer (H-shaped) which is really similar to the materials widely used in industry, because of this, daily mechanical loads and stresses will be used in a constructive and useful way.

Despite extensive previous research on mechanophores undergoing electrocyclic reactions, there are no previous records of using two mechanophore simultaneously in a monomer with the purpose of controlling the force required to trigger their ring opening reaction, and therefore the cleavage of the polymer material in which the monomer is included. Due to the large and useful amount of information available on dihalocyclopropane reactivity and chemistry, it was the perfect candidate to be coupled up with cyclobutane to create a molecule which can acts as a molecular gate. Force applied to a polymer (made by many repeating units of the macrocycle containing the active mechanophores) would trigger the ring opening reaction and break the macrocycle. Due to its allosteric nature, this would only happen after the “sacrificial molecule” (cyclobutane) undergoes ring-opening reaction. Therefore, the

first chapter will describe gated mechanochemistry, where the goal is to synthesize a molecule capable of controlling the intensity of force required to break it. In the molecular design another key aspect was to create reactive sites on the macrocycle where it could be possible to polymerize the monomer and obtain a polymer chain with a MW suitable for SMFS experiment. Moreover, the final polymer must include a neutral moiety with high affinity with the AFM present on the instrument. However, this must not compromise the measurements and therefore a copolymer containing epoxide mixed with a polymer of the macrocycle I synthesized could be the perfect substrate. This achievement could be helpful in designing materials to prevent an unexpected catastrophic failure.

Another important aspect in designing long lasting materials is to know where the force is distributed along the polymer chain under load. An extended polymer chain has the maximum tension force at the middle point of the chain contour. Therefore, when we incorporate the mechanophore into the middle of the chain with its active bond along the chain contour it's possible to follow the mechanochemical reaction triggered after force is applied. What is not properly understood is the force distribution among the whole polymer chain. When force is applied on a polymer chain, it is useful to know in what order and where the breaking points will occur. If we incorporate a mechanophore in the polymer, which can isomerize under force, will the isomerization reaction happen before the cleavage of the polymer chain connected to it? Our goal is to create a suitable polymer substrate with a known behavior to track and map the force at different points of the polymer chain. The second chapter will show how commercial polystyrene connected to a Stiff-Stilbene molecule breaks under sonication: we can follow the fragmentation pattern by incorporating a mechanophore in the polymer chain which has a known behavior. My contribution to the overall project was to synthesize the substrates suitable for physical measurements. Due to its properties, Stiff-Stilbene was chosen to be the best candidate for such investigation. The biggest challenge of this synthesis was the connection of the mechanophore to two commercial polystyrene chains, especially

given the isolation of pure product from unreacted polymer chains and/or side reactions bi-products.

Once a mechanism and a scission pattern of two polystyrene chains connected to a Stiff-Stilbene subjected to ultrasonic waves is formulated, a more complex unsolved matter could be: How the force will be displaced on a molecule where the mechanophore is connected to four polymer chains? To answer this question, the optimal candidate to study is an Anthracene-Maleimide (AntrMal) molecule synthesized via a Diels-Alder (DA) reaction instead of using Stiff-Stilbene as a mechanophore. Due to its structure, we can attach at least four polystyrene chains on the ends of this molecule. AntrMal has been used previously in literature to create self-healing material (due to the reverse Diels-Alder reaction triggered by force which creates reactive sites that can react with other sites on the chain). In the third chapter we aim to find an explanation of a very complex polymer fragmentation after sonication. My contribution to the overall project was the synthesis of substrates suitable for physical measurements. We choose to synthesize a polymer containing Anthracene-Maleimide DA adduct due to its shape since there is the possibility to create a "star" or "H-shaped" polymer. It will then be possible to ascertain where the polymer experiences the highest amount of force, and how many points will break under load.

References

- ¹ Larsen, M.B.; Boydston, A.J. *J. Am. Chem. Soc.* **2014**, 136,1276
- ² Seidel, C.A.; Kühnemuth, R. *Nat. Nanotechnol.* **2014**, 9,164–165
- ³ James, S.L.; Adams, C.J.; Bolm, C.; Braga, D.; Collier, P.; Friščić, T.; Grepioni, F.; Harris, K.D.; Hyett, G.; Jones, W.; Krebs, A. *Chem. Soc. Rev.* **2012**, 41(1),413–447
- ⁴ Ribas-Arino, J.; Marx, D. *Chem. Rev.* **2012**, 112,5412–5487
- ⁵ Kim, O.; Little, R.; Patterson, R.; Ting, R. *Nature* **1974**, 250,408–410
- ⁶ Kean, Z.S.; Ramirez, A.L.B.; Yan, Y.F.; Craig, S.L. *J. Am. Chem. Soc.* **2012**, 134,12939–12942
- ⁷ Kean, Z.S.; Niu, Z.; Hewage, G.B.; Rheingold, A.L.; Craig, S.L. *J. Am. Chem. Soc.* **2013**, 135,13598–13604
- ⁸ Wang, J.; Kouznetsova, T.B.; Niu, Z.; Ong, M.T.; Klukovich, H.M.; Rheingold, A.L.; Martinez, T.J.; Craig, S.L. *Nat. Chem.* **2015**, 7.4, 323.
- ⁹ Brown, Cameron L.; Craig, S.L. *Chem. Sci.* **2015**, 6.4,2158-2165.
- ¹⁰ Klukovich, H.M.; Kouznetsova, T.B.; Kean, Z.S.; Lenhardt, J.M.; Craig, S.L. *Nat. chem.* **2013**, 5.2,110.
- ¹¹ Black, A.L.; Lenhardt, J.M.; Craig, S.L. *J. Mater. Chem.* **2011**, 21,1655–1663
- ¹² Lenhardt, J.M.; Black, A.L.; Craig, S.L. *J. Am. Chem. Soc.* **2009**, 131,10818–10819
- ¹³ Black, A.L.; Orlicki, J.A.; Craig, S.L. *J. Mater. Chem.* **2011**,21,8460.
- ¹⁴ Akbulatov, S.; Tian, Y.; Boulatov, R. *J. Am. Chem. Soc.* **2012**,134,7620–7623
- ¹⁵ Syrett, J. A.; Mantovani, G.; Barton, W. R.; Price, D.; Haddleton, D. M. *Polym. Chem.* **2010**, 1.1 , 102-106.
- ¹⁶ Chujo, Y.; Sada, K. ; Saegusa, T. *Macromolecules* **1990**, 23, 2636–2641
- ¹⁷ Chen, X.; Wudl, F.; Mal, A. K.; Shen, H.; Nutt, S. R. *Macromolecules* **2003**, 36.6, 1802-1807.
- ¹⁸ Kucharski, T. J.; Huang, Z.; Yang, Q. Z.; Tian, Y.; Rubin, N. C.; Concepcion, C. D.; Boulatov, R. *Angew. Chem., Int. Ed.* **2009**, 48.38, 7040-7043.
- ¹⁹ Klukovich, H.M.; Kean, Z.S.; Iacono, S.T.; Craig, S.L. *J. Am. Chem. Soc.* **2011**, 133,17882
- ²⁰ Huang, Z.; Boulatov, R. *Pure Appl. Chem.* **2010**. 82.4, 931-951.

- ²¹ Müller-Fischer, N.; Tobler, P.; Dressler, M.; Fischer, P.; Windhab, E.J. *Exp. Fluids* **2008**,45, 917–926
- ²² Liu, X.; Zhang, C.; Yu, W.; Deng, Z.; Chen, Y. *Sci. Bull.* **2016**,61,811–824.
- ²³ Mulligan, M.K.; Rothstein, J.P. *Phys. Fluids* **2011**,23, 022004
- ²⁴ Faustino, V.; Pinho, D.; Yaginuma, T.; Calhelha, R.C.; Kim, G.M.; Arana, S.; Ferreira, I.C.; Oliveira, M.S.; Lima, R. *Springer* **2014**, 151-163.
- ²⁵ Davis, D. A.; Hamilton, A.; Yang, J.; Cremer, L. D.; Gough, D. V.; Potisek, S. L.; Ong, M. T.; Braun, P. V.; Martínez, T. J.; White, S. R.; Moore, J. S.; Sottos, N. R. *Nature* **2009**, 459, 68.
- ²⁶ Huang, Z.; Boulatov, R. *Pure Appl. Chem.* **2010**, 82.4 ,931-951.
- ²⁷ Piermattei, A.; Karthikeyan, S.; Sijbesma, R. P. *Nature Chem.* **2009**, 1, 133.
- ²⁸ Caruso, M. M.; Davis, D. A.; Shen, Q.; Odom, S. A.; Sottos, N. R.; White, S. R.; Moore, J. S. *Chem. Rev.* **2009**, 109.11, 5755-5798.
- ²⁹ Cheng, B.; Shuxun, C. *Polymer Mechanochemistry. Springer*, **2015**, 97-134
- ³⁰ Lenhardt, J.M.; Black, A.L.; Beiermann, B.A.; Steinberg, B.D.; Rahman, F.; Samborski, T.; Elsagr, J.; Moore, J.S.; Sottos, N.R.; Craig, S.L. *J. Mater. Chem.* **2011**, 21,8454–8459

CHAPTER II. Molecular force gate for stress-responsive polymers.

Abstract

In order to prevent a sudden material failure, it would be useful to control the force at which polymeric materials break under a mechanical stress or load. This could be done by designing a polymer material which includes a sacrificial moiety which will avoid a catastrophic failure under a certain force threshold. A fundamentally new approach to separate these two parameters has been tested by creating mechanoresponsive moieties that integrate two reactive sites, one that produces the desired chemistry and the other that controls the force at which this chemistry is triggered. We call this allosteric mechanochemistry. The objective of this chapter is to create a macrocycle with homoallosteric properties and another one with heteroallosteric properties. Both macrocycles contain mechanophores (a DCC + a cyclobutane for the heteroallosteric moiety and two DCC for the homoallosteric moiety) connected by linkers with terminal vinyl arms. The vinyl groups will be needed to polymerize the macrocycles into a linear single chain: this is the beginning of our investigation on the distribution of stresses along a polymer chain under force. The force will be applied on the polymer chain by an AFM instrument and the analysis will be performed with SMFS.

Introduction

One of the goals of mechanochemical research is to capture loads and stress applied to polymers and materials to drive useful chemistry or processes (such as polymer photoactuation). Another objective is to design and obtain nanomechanical devices and self-healing materials. It is possible that exploiting allosteric mechanochemistry may solve some of the current deficiencies of such mechanoresponsive materials. We are studying allosteric molecular constructs containing two or more mechanophores (stress-responsive moieties) arranged in parallel, where one reactive site is designed to control the reactivity of the other(s) even when all sites are identical.

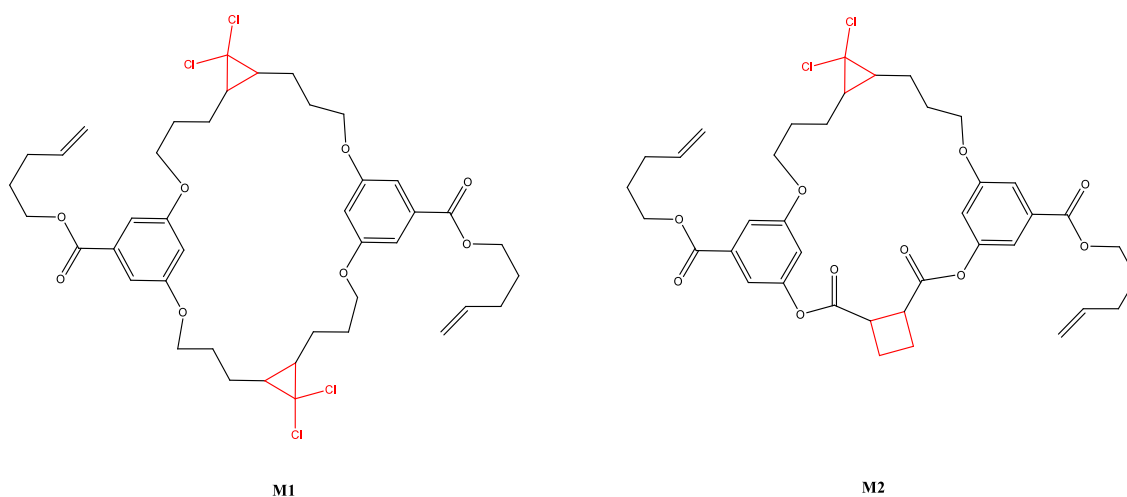


Figure 1: Target molecules containing mechanophores (highlighted in red). **M1** is designed to demonstrate homoallosteric mechanochemistry, **M2** - heteroallosteric mechanochemistry.

Another interesting question regarding the synthesis of these macrocycles is: How do the stresses distribute along the polymer chain under load once polymerized? In previous work, several experiments and scenarios have been used in order to understand the displacement of force on a linear polymer chain. Perkin, Chu and coworkers used fluorescently labelled DNA molecules to observe the stretching of individual polymers in a spatially homogeneous velocity gradient¹. They determined the probability distribution of molecular extension as a function of time and strain rate. Furthermore, they described the steady-state extension with a model consisting of two beads connected by a spring representing the entropic elasticity of a worm-like chain, but the same system wasn't applicable to the average dynamics.

Other extensive studies on linear polymer chains under load monitored by SMFS were performed by Craig and co-workers: they applied force to polybutadiene functionalized with mechanophores (dihalocyclopropanes) which caused isomerization^{2,3}. They concluded that the rearrangement of DHCs represented a potential mechanism for localized stress relief in polymers under load and they quantified the irreversible extension of the gDHCs at 1.2nN on the time scale of 10⁻² s. Moreover, they demonstrated that sonication of dihalocyclopropanated polybutadiene results in isomerization of multiple DHC units before a backbone C-C bond breaks. Mechanochemistry during sonication is characterized by low selectivity:

For example, in the absence of force *cis*-DCC isomerizes ~20 times faster than *trans*-DCC, whereas sonication of polymers containing approximately equal fractions of the two isomers randomly distributed along polymer chains suggest approximately equal probability of isomerization (shown in **Figure 2**). The origin of this suppressed selectivity remains unknown⁴.

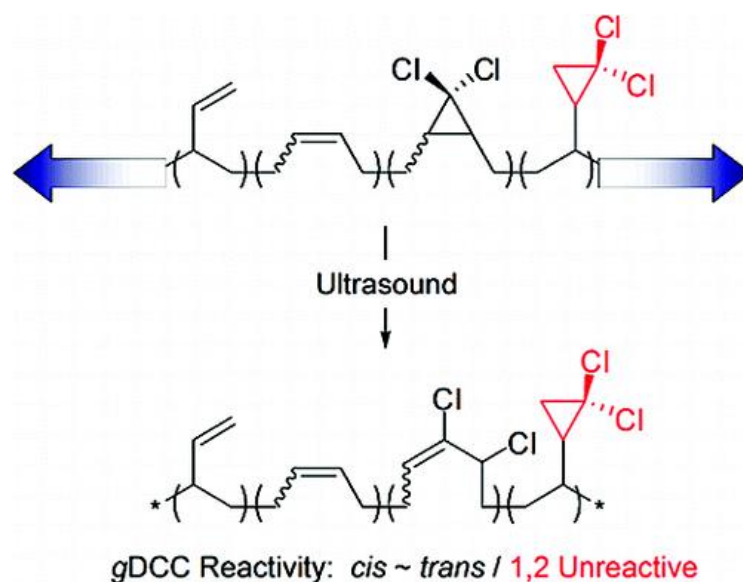


Figure 2: Even if the ring openings occur several hundred times more frequently than polymer chain scission, the *cis*-coupled gDCCs are slightly more likely to react than their *trans* isomers. Reprinted from ref. ⁵. Copyright 2009 American Chemical Society.

However, a clear qualitative and quantitative picture of the distribution of forces along a linear polymer chain under load still needs to be exploited, especially with mechanophores incorporated with an allosteric function. Therefore, a mechanophore with the greatest potential to yield practically useful stress-responsive materials is gem-dihalocyclopropane (**Figure 3**, B and C). Unfortunately, most DHCs do not survive loads larger than ~1 nN compared to ~2-3 nN at which noticeable fragmentation of polymer backbones is thought to occur⁵. Consequently, in practical applications, where loads corresponding to single-chain forces of ~1 nN and more can occur unexpectedly over a long time periods and at arbitrary parts of the stressed polymers, gDHCs will be consumed before or at parts other than those that require reinforcement to prevent catastrophic failure. In other words, gDHCs as currently demonstrated are unlikely to improve fatigue resistance of polymers under most practical conditions of use. The concept of allosteric mechanochemistry and molecular architectures will provide a general strategy of overcoming these

limitations. Allostery is the process⁶ by which macromolecules (*e.g.*, proteins) transmit the effect of binding at one site to another functional site separated by a distance longer than that over which electronic coupling is possible, allowing for regulation of activity (*e.g.* ATP hydrolysis). This effect is divided into homoallosteric (when the allosteric modulator is a substrate for a target enzyme), and heteroallosteric (when the modulator is not a substrate and it could be even an inhibitor instead). In our case, we are working with non-biological macromolecules, and the difference between homo- and heteroallostery depends on whether the two (or more) interacting functional sites are the same or not.

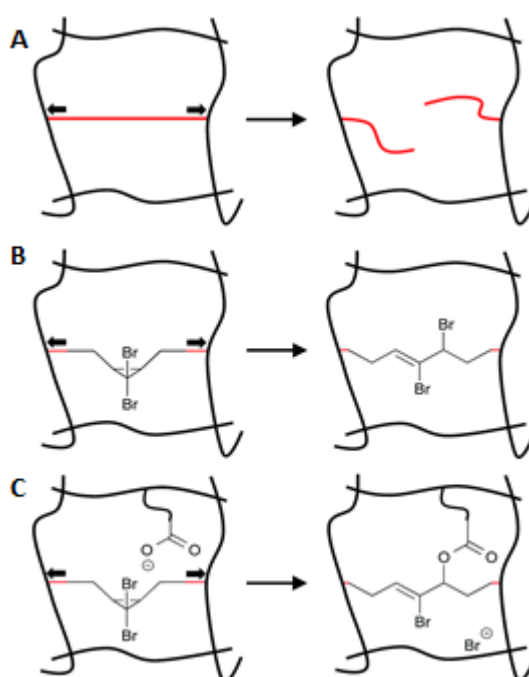
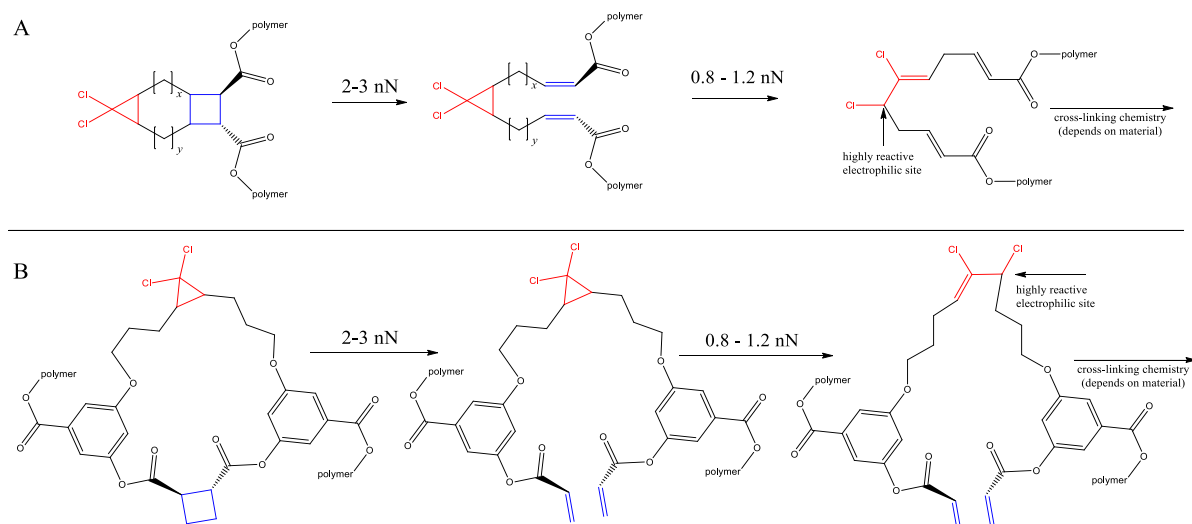


Figure 3: A) Stress in polymers localize along individual polymer subchains, resulting in chain scission that can lead to material failure. Mechanophores embedded into polymers can undergo a constructive, rather than a destructive response in these overstressed subchains. For example: B) gem-dibromocyclopropane will isomerize by undergoing fast ring opening in response to tensile forces of 1 nN or more, increasing local contour length that can provides local stress relief in overstressed chains; C) the 2,3-dibromoalkene products of the ring opening are cross-reactive toward mild nucleophiles such as carboxylates, and that reactivity has been exploited to generate in situ cross-linking and load-strengthening. Reprinted from ref. ⁷. Copyright 2015 Chemical Science.

Although the mechanochemical response of reactive sites can, under certain circumstances, be inferred from studying the behaviour of bulk polymers under load, this approach is highly inefficient and is at best qualitative. Instead, several strategies

designed to mimic loads imposed on individual polymer chains in bulk materials under more tractable conditions have been developed. Sonication of dilute polymer solutions is technically the simplest strategy, since it does not provide control or measure the force acting on polymer chains or the timescale over which the reaction takes place.⁸ Single-molecule force (SMF) spectroscopy allows a single polymer chain attached to an AFM tip to be stretched on a second's time scale.⁹ SMFS experiments allow relatively accurate estimates of the force at which a mechanochemical reaction occurs but can only measure reactions over a narrow range of timescales ($t_{1/2} \sim 10$ -100 ms). In addition to this, SMFS does not allow product characterization. A third method developed by our group used a series of increasingly strained macrocycles to extrapolate the mechanochemical reactivity of diverse functional groups.¹⁰ The range of forces in this method is the largest among any techniques of mechanochemical kinetics developed to date. All these methods have been used to study mechanochemistry of gDHCs.

Since the objective of this work is to demonstrate allosteric mechanochemistry and more broadly to follow the behaviour of a single linear polymer under load and the distribution of stresses along the chain, macrocycles suitable for allosteric mechanochemistry studies were designed using a combination of dihalocyclopropane and cyclobutane incorporated in the structure. Conceptually and synthetically, the simplest strategy to increase the maximum force a DHC moiety can withstand to ~ 2 nN is with a moiety shown in **Scheme 1, A**. Our collaborators and our group have now synthesized this moiety ($x=y=2$) and studied its mechanochemistry. In this molecule, the cyclopropane moiety experiences no force until the cyclobutane core dissociates ($t_{1/2} \sim 100$ ms at 2 nN). While suitable as a proof-of-the-principle demonstration of gated mechanochemistry, it's a fairly trivial illustration of the broad concept we are interested in (allosteric mechanochemistry) and offers no opportunity to adjust the threshold force.



Scheme 1: Effect of allosteric mechanochemistry on A) a polymer containing a macrocycle incorporating two mechanophores spaced by a short linker ($x=y=2$) synthesized by our collaborators; B) a polymer containing the target macrocycles of the project, with the same mechanophores (gDCC and cyclobutane) but with longer and different linkers, which allow more flexibility.

Consequently, my task has been to develop efficient syntheses of more general molecular architectures that are compatible with a broad range of reactive sites, and whose mechanochemistry could be controlled by homo- and heteroallosteric mechanism. It's possible to have control over these molecules by incorporating gDHC in a macrocycle containing a sacrificial moiety with higher isomerization threshold force (*i.e.* cyclobutane, which undergoes $[2 + 2]$ cycloreversion¹¹ at 2-3 nN). With this strategy, the cyclopropane will not experience force until the cyclobutane dissociates. Dr. Boulatov designed¹² specific macrocycles in order to demonstrate homo- and heteroallosteric mechanochemistry, using the following structure (shown in **Figure 4**): Two linkers, both connected to the mechanophores gDCC and cyclobutane and two terminal vinyl arms (necessary for copolymerization with epoxide¹³ via ring opening metathesis polymerization - ROMP).

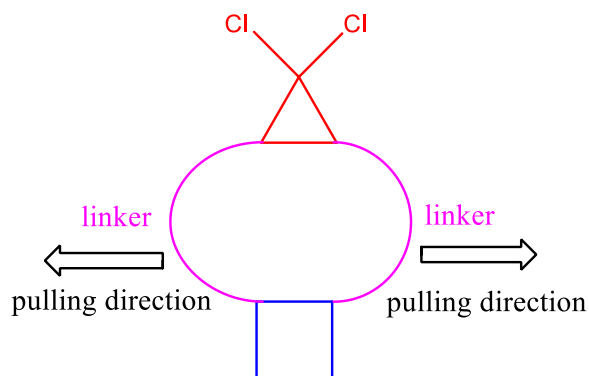


Figure 4: Model of a macrocycle designed to demonstrate heteroallosteric mechanochemistry.

The epoxide used for copolymerization is mechanically inactive in the force range of interest, but it would increase the attachment force between the tip of the instrument (atom force microscope) and the polymer to analyze. ROMP is used because backbone rings can't be easily introduced by the traditional polymerization of vinyl monomers.

Result and discussion

Molecular design

The first step in this project was designing the syntheses of macrocycles **M1-2 (Figure 1)**, each containing two (identical or distinct) mechanophores (red) connected by inert linkers. In **M1**, the two "coupled" mechanophores are identical, whereas in **M2**, they are different (cyclobutane and dichlorocyclopropane). Both macrocycles contain a pair of terminal $-\text{HC}=\text{CH}_2$ moieties for polymerization by ROMP. The syntheses are illustrated in **Scheme 2**.

Certain synthetic procedures were optimized on functionally similar but cheaper commercially available model compounds as shown in **Table 1**. Thus, resorcinol and 3-hydroxy-2-(hydroxymethyl)-2-methylpropanoic acid were used instead of dihydroxybenzoic carboxylic acid to optimize esterification (the second one was used to compare reactivity of phenolic groups and alcoholic groups toward esterification with carboxylic acid). 3,3-dimethylpentanedioic acid was used instead of gDCC dicarboxylic acid, cyclohexane-1,2-dicarboxylic acid instead of cyclobutane dicarboxylic acid.

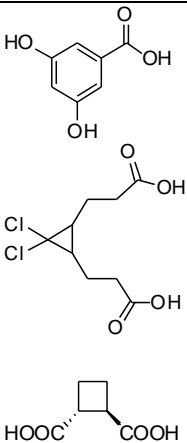
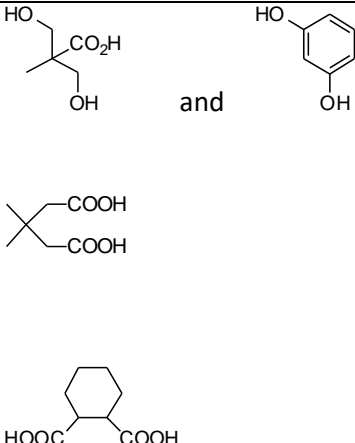
Original molecules	Model compounds used for optimizing conditions
	

Table 1: on the left, are shown the three building blocks of macrocycles **M1-M2**; on the right are stand-ins used for reactions optimization.

Synthesis of the “linker” molecule

The terminal vinyl arms of **M1-M2** were installed by esterifying the carboxylic acid of the dihydroxybenzoic acid with bromopentene using K_2CO_3 in DMF (**Table 2**). We chose pentene to ensure sufficient spacing of macrocyclic monomers in the polymer obtained by ROMP without increasing the flexibility of the polymer (Kuhn’s length) too much. Before using this strategy, other synthetic procedures were tried, unfortunately with negative results or other problems encountered. Steglich esterification using 1-Ethyl-3-(3-dimethylaminopropyl)carbodiimide (EDC) 4-Dimethylaminopyridine (DMAP) catalyzed was performed but the problem encountered in this case was the competitive esterification reaction between carboxylic acid with the phenolic groups on the same moiety. All the reaction conditions are shown in **Table 2**.

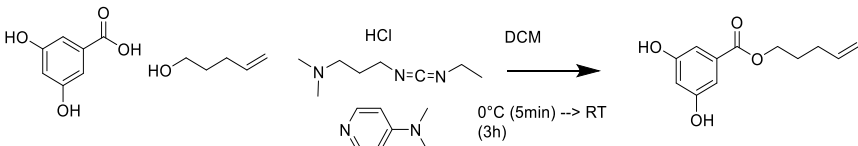
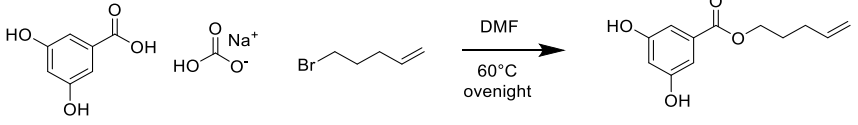
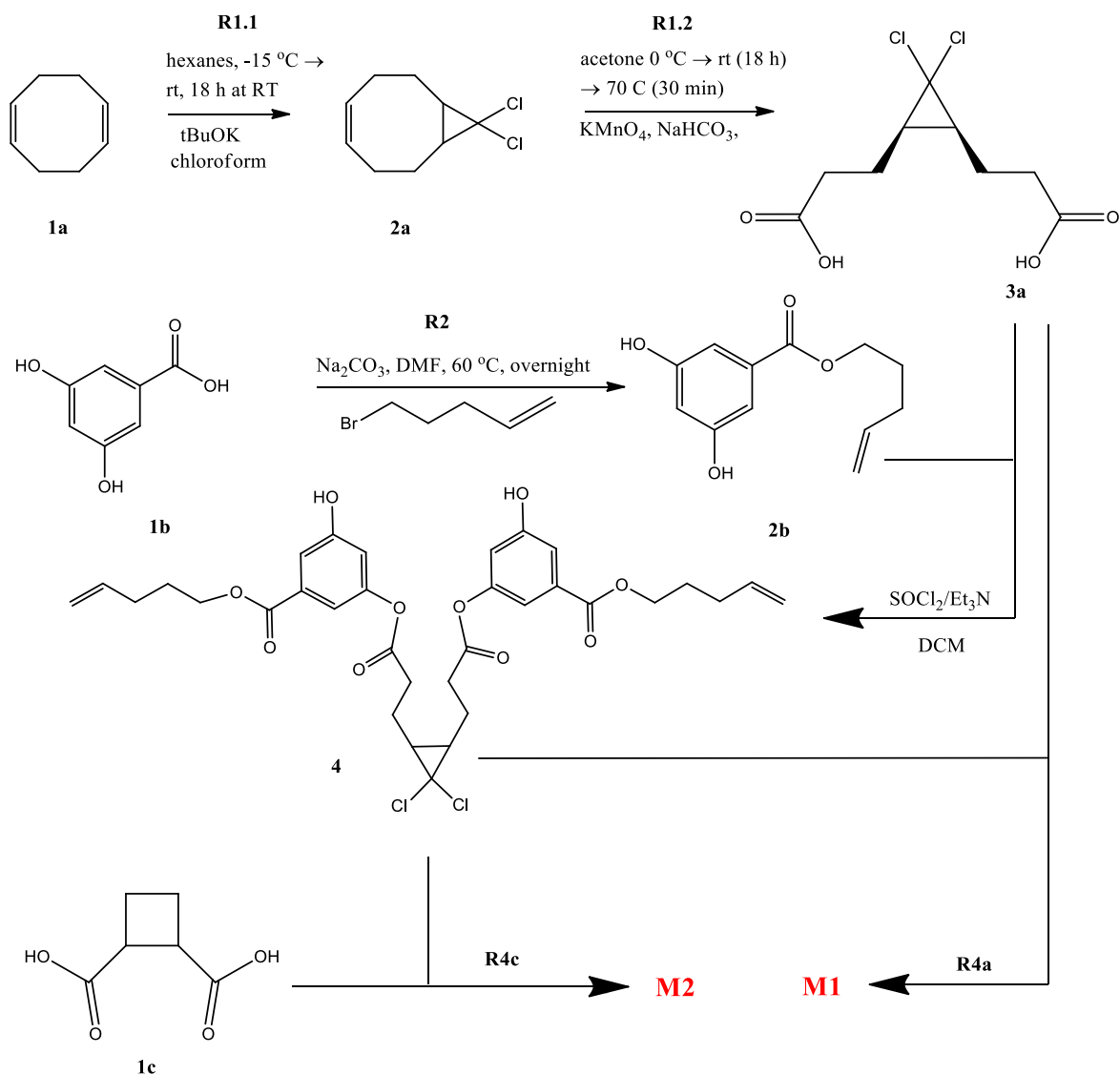
Reaction conditions	Reaction outcome
 <p>Reaction 1: 3,4,5-trihydroxybenzoic acid + allyl alcohol + N-ethyl-N-(4-dimethylaminopyridin-2-yl)propan-1-amine hydrochloride in DCM, 0°C (5min) → RT (3h) yields 3,4,5-trihydroxybenzoic acid allyl ester.</p>	<p>Abandoned due to side reaction</p>
 <p>Reaction 2: 3,4,5-trihydroxybenzoic acid + sodium acetate + allyl bromide in DMF, 60°C overnight yields 3,4,5-trihydroxybenzoic acid allyl ester.</p>	<p>Chosen and performed six times with an average yield of 88%</p>

Table 2: Method used to obtain the linker with terminal vinyl arm.



Scheme 2: Synthetic pathway for synthesis of macrocycles **M1** and **M2**.

Synthesis of dichlorocyclopropane

Cis-gDCC was synthesized in two steps from commercial cyclooctadiene¹⁴. First, a single C=C bond of cyclooctadiene was dichlorocyclopropanated using a strong base (tBuOK) in CHCl_3 (which generates highly reactive CCl_2 by first deprotonating CHCl_3 to yield CCl_3^- which rapidly and spontaneously expels Cl^-) in molar ratio of 1:1:1.15 for the diene, CHCl_3 and tBuOK.

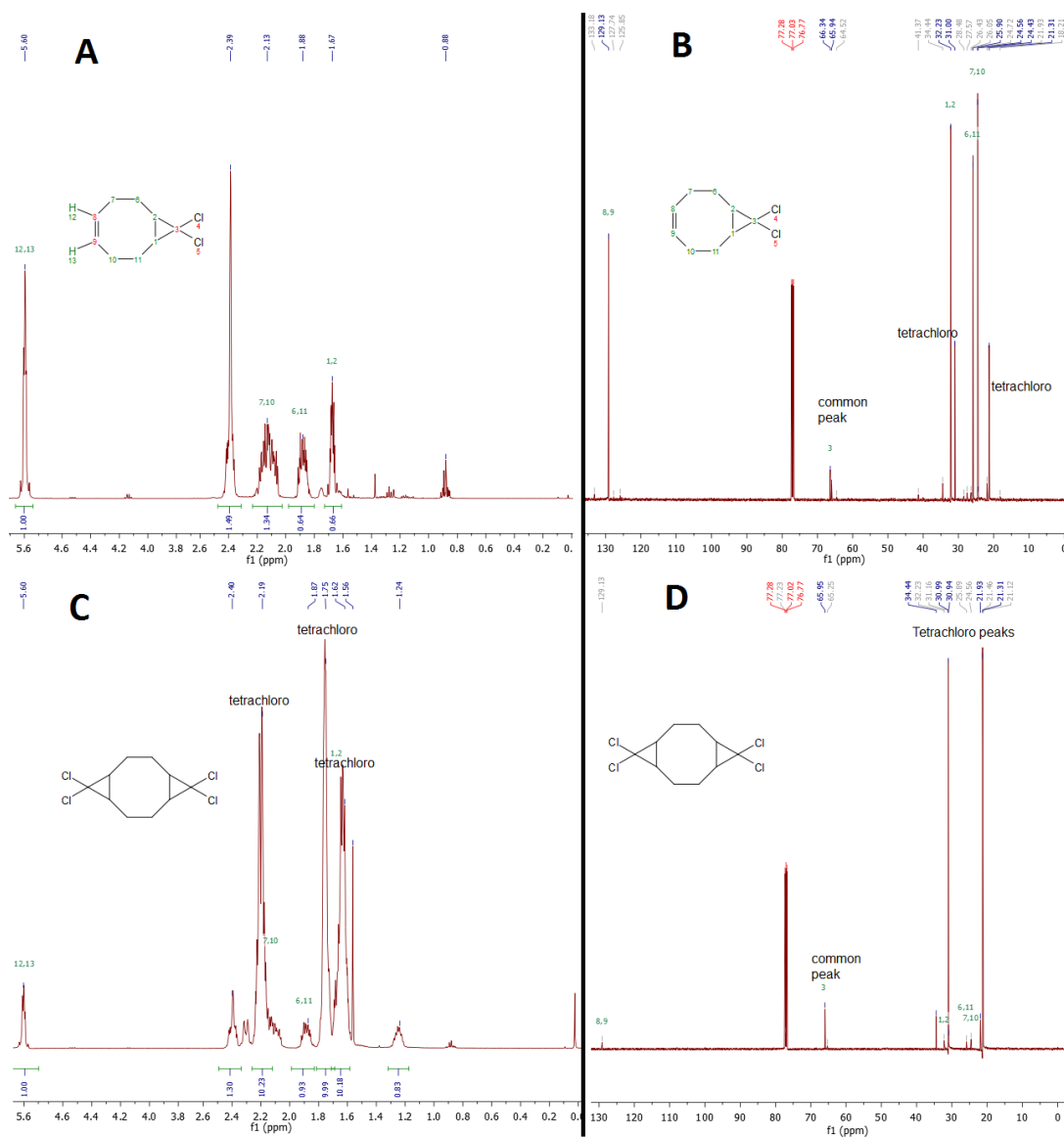


Figure 5: A) and B) are respectively ^1H -NMR and ^{13}C -NMR APT of (Z)-9,9-dichlorobicyclo[6.1.0]non-4-ene (the goal compound), C) and D) are respectively ^1H -NMR and ^{13}C -NMR APT of the white crystals. “Tetrachloro” marks shown on the NMR picture refer to **2a**, which is a side product, resulting from complete cyclopropanation on both double bonds of **1a**. Mother liquor and crystals were separated through a Buchner funnel; before proceeding with the next step another separation was required, since we could observe mixed signals of both compounds in all these NMR spectra.

This produced, after 12 h, a mixture of mono- and dicyclopropanated cyclooctadienes (respectively **2a** and **2as**), which, after the workup, resulted in white crystals of **2a** and colorless oil of **2as** as evidenced by ^1H NMR and ^{13}C APT spectra (**Figure 5**). Attempts to use 3-fold excess of the diene relative to tBuOK to ensure that only one of its C=C bond would cyclopropanate resulted in no reactions after 48 h.

The next step was an oxidation on the double bond of **2a** with a large excess of KMnO_4 , initially kept at 0°C due to its exothermicity, and later heated up to 70°C to

cleave the C=C bond. After this, the reaction mixture was acidified using 1M HCl solution and the goal compound was extracted with hot acetone (**3a**, **Scheme 3**). After medium-pressure LC purification, the overall yield of **3a** was 19%.

Assembling the macrocycles

Once **3a** and **2b** were successfully obtained, esterification was performed. In this case two different esterification methods were attempted: the first was successful with SOCl₂ converting the acid into an acyl chloride which easily reacts with the hydroxyl group on **2b**. At the same time, esterification was performed again with EDC/DMAP without any successful result (we observed presence of starting material unreacted even after 48 hours).

To esterify the starting material, two steps were necessary: the first step involved the addition of SOCl₂ in dry DCM with a drop of DMF as a catalyst¹⁵. After full conversion of the carboxylic acid, the excess of SOCl₂ was removed under vacuum and was evaporated with toluene. Then, the acyl chloride was added to a solution of **2b** dissolved in dry DCM containing 3 eq of Et₃N as a base to neutralize the HCl product (whose build-up could hydrolyze the esters). This reaction was performed using a 2:1 ratio of **2b** and **3a**, affording a pure product with 30% yield. We also used an excess of **2b** (6 eq to 1 eq of **3a**), to optimize the esterification on just one phenolic group: unfortunately, the yield in this case was very low (below 20%). Evidence of esterification are visible in ¹H-NMR spectrum (**Figure 6**): all the **3a** signals are present and the aromatic protons are different from the signals shown in the starting material, since there is no more symmetry in the molecule.

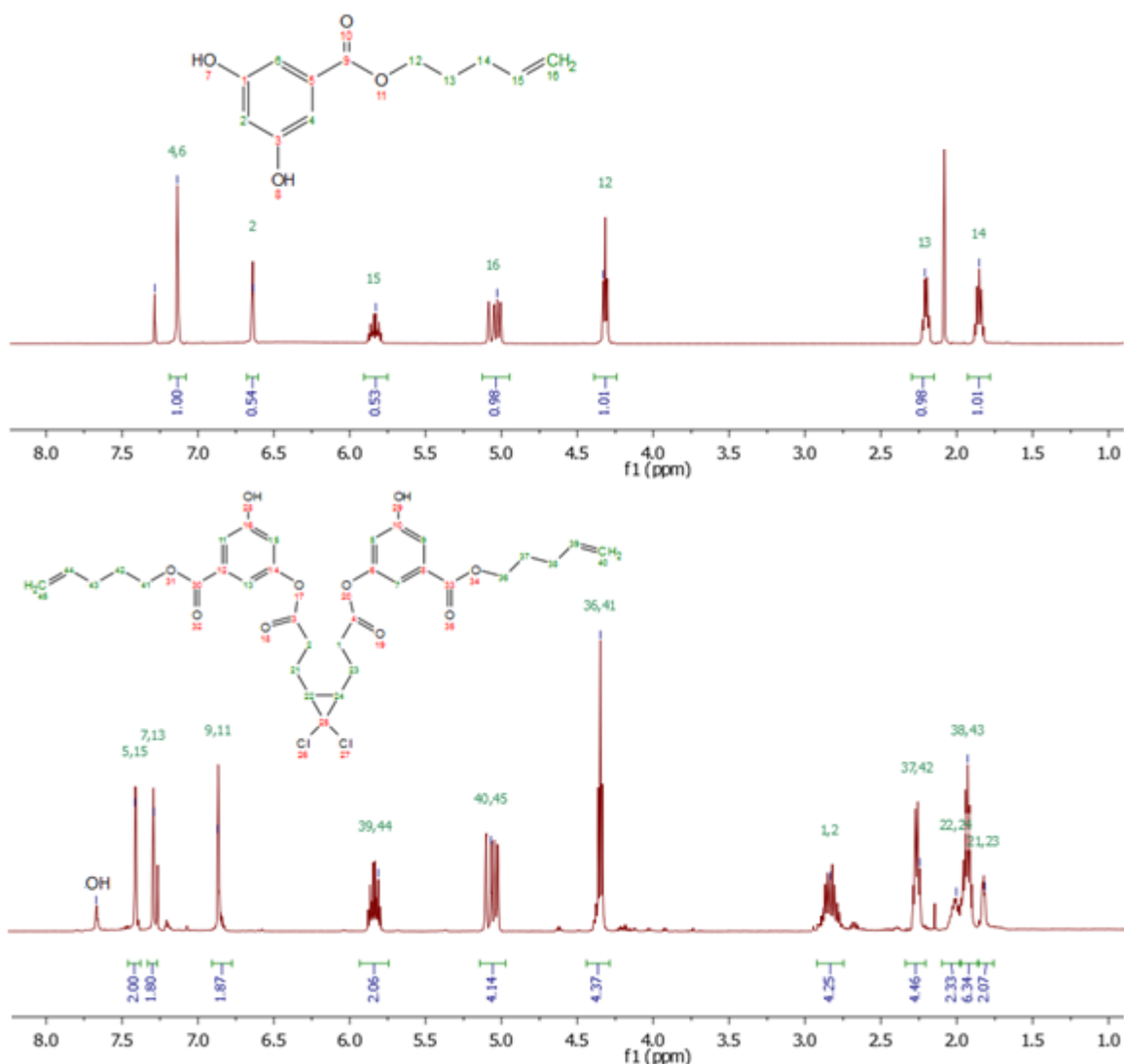


Figure 6: $^1\text{H-NMR}$ comparison of the **2b** (starting material-on the top) with the product after esterification with **3a**. It's easy to observe the changes in aromatic signals and the appearance of new signals belonging to **3a**.

The last step for macrocycles synthesis was esterification with another **3a** molecule to yield **M1** or with **1c** to yield **M2**. The same esterification method used before (**R3**) was performed for both macrocycles synthesis. To favor macrocyclization vs. oligomerization of the precursors, the reactions must be run at high dilution: initially it was run at 1 mM, in accordance with previous literature¹⁶.

The spectroscopic and chromatographic analysis of the reaction mixtures was contradictory. In both cases, the products obtained after medium-pressure LC isolation manifested a single molecular peak in mass spectrum corresponding to the desired macrocycles (see the Experimental section data) but their $^1\text{H-NMR}$ spectra (**Figure 7**) suggested the presence of multiple (but chemically similar) compounds.

The moieties on TLC show a long strike, potentially containing more than one spot, though this was difficult to distinguish. The interpretation of these contrasting data suggests the presence of either two stereoisomers of the target compounds. It was impossible to separate the mixture by medium-pressure LC. Despite the nature of the final compounds obtained, it could still be possible to try the copolymerization of these moieties with an inert molecule containing cyclopropane (necessary to connect the material to the AFM tip for the SMFS experiment).

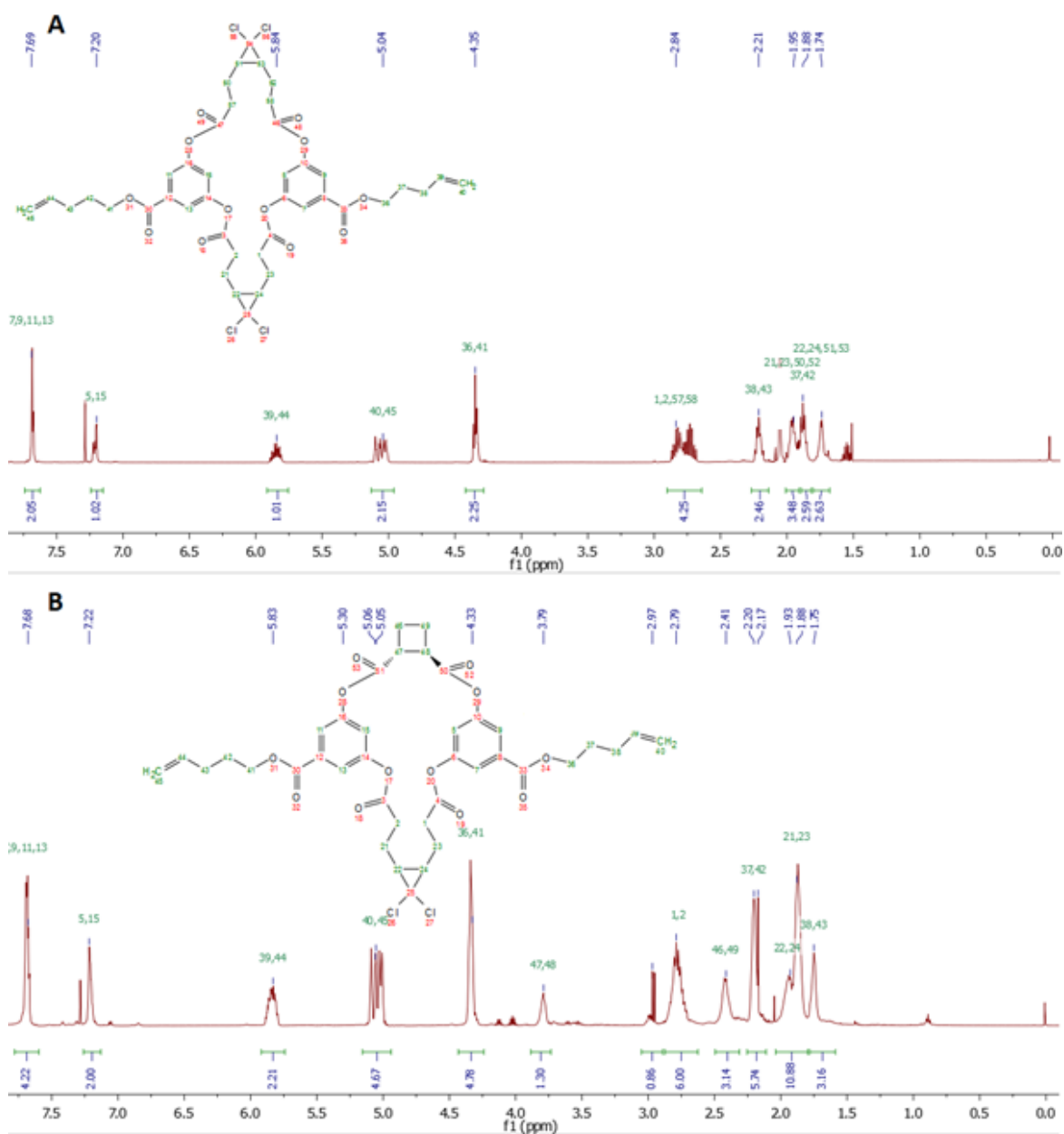
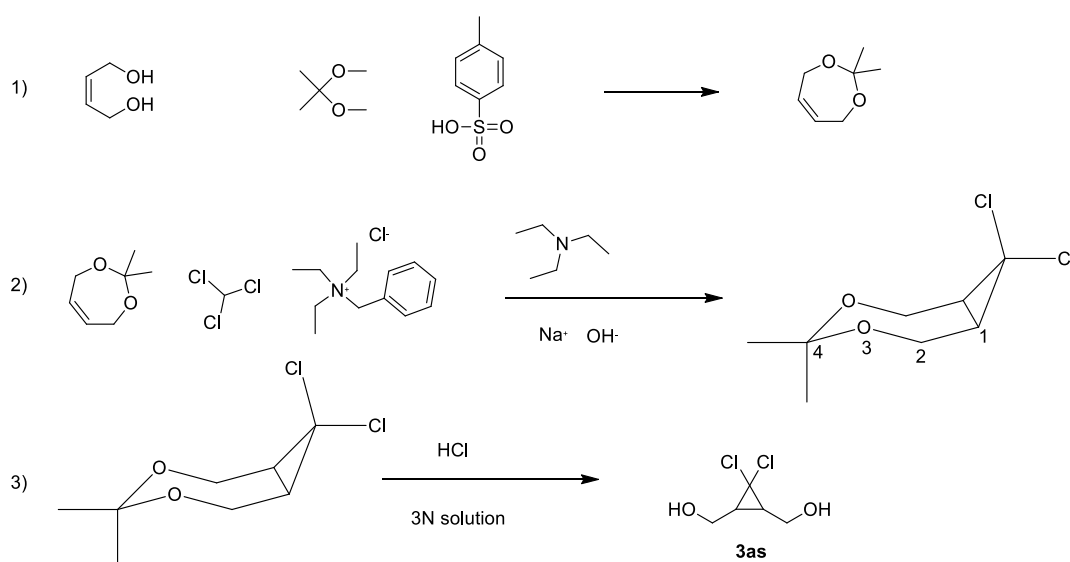


Figure 7: $^1\text{H-NMR}$ spectra of A) **M1** and B) **M2**. Wrong signals multiplicity indicates that both macrocycles are mixtures of products rather than single pure compounds.

Attempt to create a linker with shorter "arms"

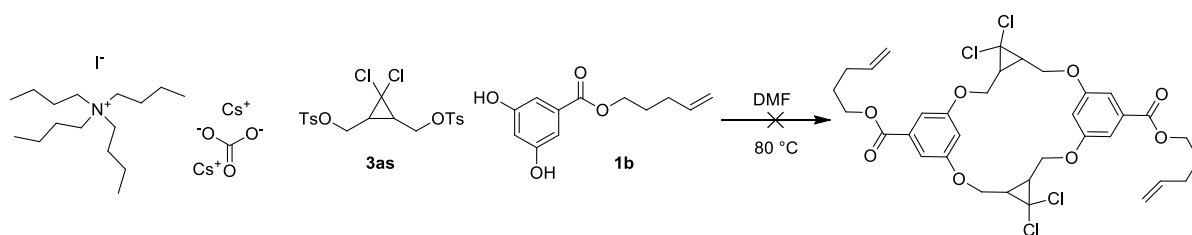
Monocyclopropanation with cyclohexadiene to obtain a *cis*-DCC derivative with shorter linkers was attempted. Unfortunately, this chemical is considerably more reactive than cyclooctadiene: even at a low temperature (-15 °C) the reaction was difficult to control due to its exothermicity and it was abandoned.

In the meantime, synthesis (**Scheme 3**) of gDCC was performed to obtain the cyclopropane with terminal alcoholic group (**Scheme 3, 3as**) as reported in the literature¹⁷. In this case the synthetic pathway was longer, with more expensive chemicals and the final yield lower (around 10%), so **R1.1** and **R1.2** was the preferred synthetic route. Moreover, the arms of the cyclopropane yielded would have been perhaps too short to connect smoothly two linkers molecules to them.



Scheme 3: Alternative pathway to obtain DCC as a diol, **3as**.

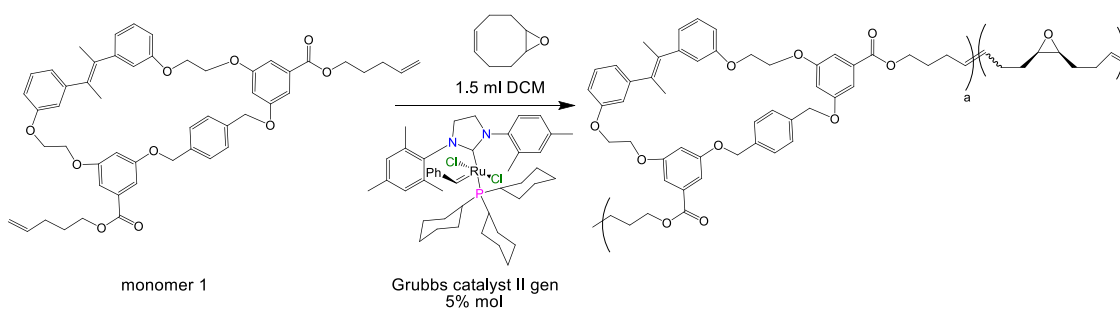
3as was converted into a tosylate and used to try a one pot macrocyclization¹¹ with **1b**, in molar ratio of 1:1:20 for Cs_2CO_3 and with a catalytic amount of TBAB (used as a phase transfer catalyst since the presence of Cs salt) in DMF (**Scheme 4**). Unfortunately, no reaction occurred after 48hours, TLC showed just unreacted starting material: interpretation of this failure could be the presence of moisture or the solvent used was not rigorously dry.



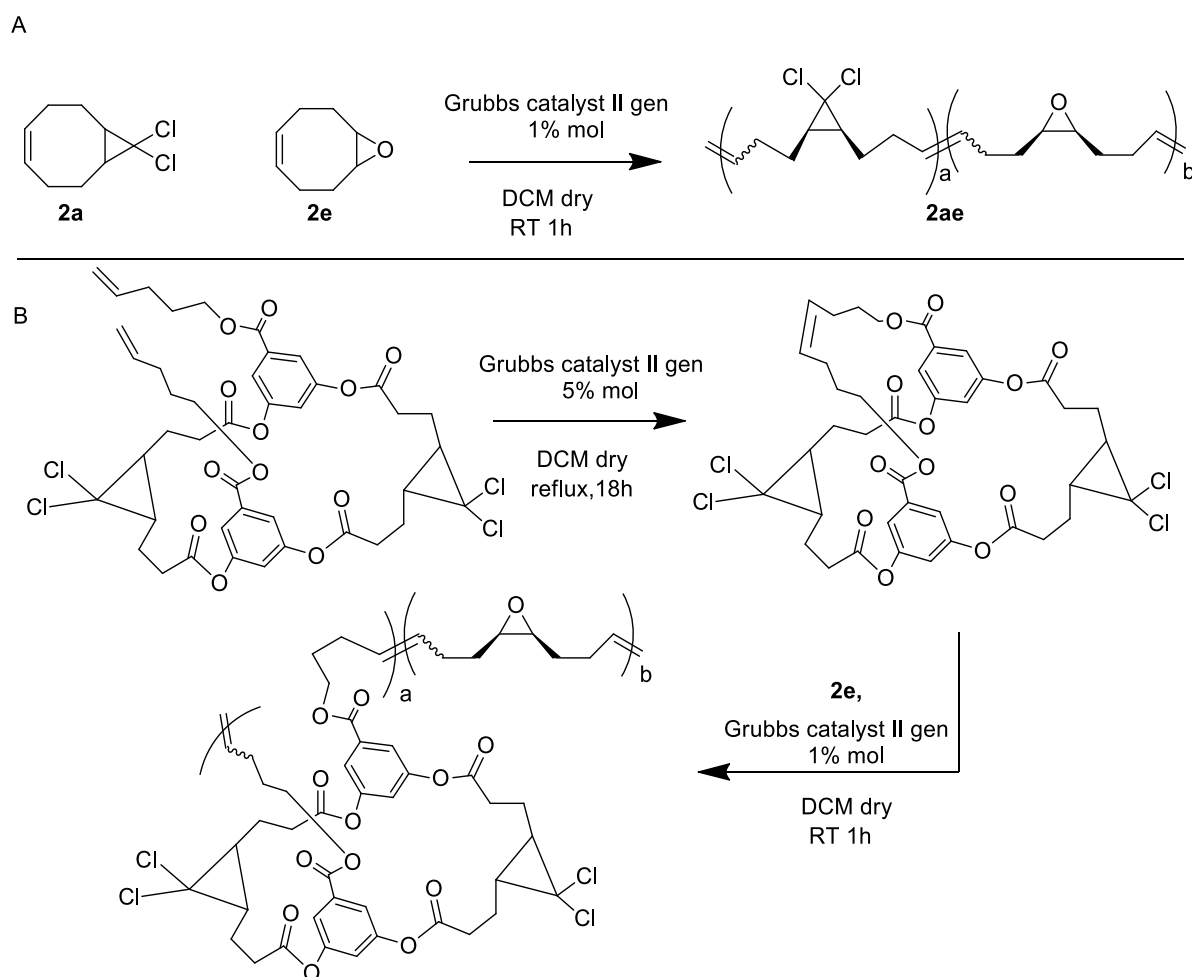
Scheme 4: One step macrocyclization attempt, unsuccessful.

Polymerization

To become familiar with polymerization technique, a reaction using Grubbs II gen catalyst, epoxide, (*Z*)-9-oxabicyclo[6.1.0]non-4-ene (**2e**) and **2a** (instead of the entire macrocycle) was performed (**Scheme 6, A**). Two sequential vinyl methatesis reactions on the macrocycles are required, because backbone rings can't be easily introduced by the traditional polymerization of vinyl monomers¹⁸. The first reaction is necessary to connect the terminal vinyl arms present on **2b**. Once the closed macrocycle is obtained, the next step is a copolymerization reaction with **2e** (**Scheme 6, B**). Another attempt of copolymerization to test the outcome of this reaction was performed using a similar moiety synthesized by a colleague (**Monomer 1, Scheme 6**).



Scheme 5: ROMP reaction between a molecule similar to the final macrocycle (monomer 1) and **2e**.



Scheme 6: A) ROMP reaction between **2a** and **2e**; B) two-steps preparation of a polymer containing **M1** and **2e**, suitable for SMFS measurements.

Despite several attempts, we were unable to obtain the final polymer with sufficient MW to be attached to the AFM tip. Due to the nature of the macrocycle (an oligomer potentially already closed) we also attempted to skip the first step (ring closure using 5% of Grubbs catalyst II gen) and directly performed the copolymerization with the epoxide molecule. The outcome of this copolymerization yielded material with MW always minor than ~3KDa, even under different conditions (we tried to change solvent, time, temperature, amount of catalyst). We concluded that the stereoisomers mixture or the oligomer **2e** may inhibit or poison the catalyst and the polymerization reaction was not able to yield the product with the desired size. Therefore, further manipulation on the ring closure reaction is required to allow the copolymerization, or other polymerization strategies may be used to obtain the final copolymers ready for SMFS experiments.

Conclusions and future work

In this project, I focused on the synthesis of strained macrocycles containing two mechanophores arranged in a way that they could control the force at which the macrocycle opens. Although the final products are mixtures of two stereoisomers or an oligomer, it would be useful to incorporate these moieties in a polymer chain so that their behaviour could be followed under force. This would support and develop the design and synthesis of mechanochemically active materials which could act as “molecular gate”. By creating a single monomer with these properties, the whole polymer will not break until the sacrificial moiety undergoes ring opening reaction. Knowing and controlling the force necessary to break a polymer material would be helpful in material design and development. The synthesis of macrocycles containing mechanophores would be easier when following the methods and conditions I have improved throughout the synthesis of the various moieties in this project. I demonstrated how the choice of a cyclooctadiene is more convenient than a cyclohexadiene in the preparation of the dihalocyclopropane (due to the longer arms generated after the ring opening reaction, which allow to connect it easier to other molecules avoiding a hindered moiety).

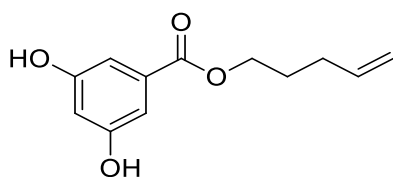
Moreover, the conversion of carboxylic acids into acyl chloride moieties has been shown to be an easy, effective, fast and economically advantageous way to assemble the various parts of the macrocycle via nucleophilic reactions. The macrocyclization reaction shouldn't be performed with less than 1mM concentration to avoid side products, even with very low concentration the product may result in a mixture of isomers or an oligomer. The moieties I've synthesized, once polymerized, would contribute to the understanding of how stresses are displaced along a single polymer chain. This is important because it would also help to explain the behaviour of more complex polymers (up to crosslinked materials) which are the most similar to the polymers widely used in industry.

The future direction for this project is to obtain polymers of M1 and M2 in order to perform SMFS measurements. Exploiting homoallosteric and heteroallosteric behaviour of the macrocycles M1 and M2 incorporated in a polymer could be useful

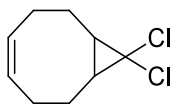
to design new and innovative materials and processes. Macrocyclization is a very challenging reaction because it requires a very low concentration and must be performed under rigorously anhydrous conditions. Despite this, the risk of side products such as oligomers or a single esterification rather than double esterification on both acid groups of the mechanophores are all plausible scenarios, since a strained molecule is trying to be afforded (not an energetically favorable reaction).

Experimental section

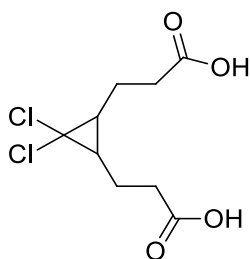
All reactions were performed under argon atmosphere using standard Schlenk techniques unless otherwise noted. All reagents were purchased from Sigma-Aldrich, Fisher Scientific or Fluorochem. DCM was purified using a solvent purification system. Flash chromatography was performed on Silicycle F60 (230-400 mesh) silica gel. Medium pressure liquid chromatography (MPLC) was performed on a Teledyne ISCO CombiFlash RF 200. ^1H and ^{13}C NMR spectra were referenced to the residual solvent peak (CDCl_3 δ = 7.26 (^1H) and 77.16 (^{13}C)) were collected on a Bruker 500MHz spectrometer. NMR spectra were analyzed using Mestrenova software. Mass spectra were run by operators using Micromass LCT Mass Spectrometer, using Ionization mode: ES^+ , Sample inlet: Syringe Pump, Sample run in MeOH, Sample Cone Voltage: 60 Volts.



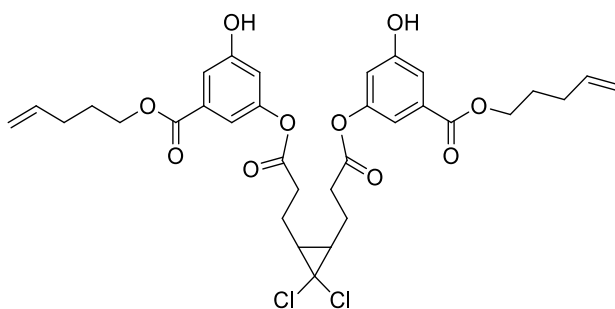
Synthesis of Pent-4-en-1-yl 3,5-dihydroxybenzoate, 2b¹⁹. A mixture of **1b** (3 g, 19.47 mmol) and NaHCO_3 (1.635 g, 19.47 mmol) is mixed in DMF forming a dispersion and stirred in a round-bottom flask. The reaction mixture seems not completely dissolved in DMF for the first minutes, but after this time there is no more left on the flask bottom. After other 5 minutes 5-bromopent-1-ene (2.306 ml, 19.47 mmol) is added to the solution. The reaction mixture was stirred at 60 °C overnight Water (15 mL) was added. Organic phase was separated. The water phase was extracted with hexane (2*15 mL). The solvent was removed under reduced pressure to yield crude product. Flash chromatography purification (SiO_2 , EtOAc:Hexane) afforded the product (3.645 g, 84%) as a pale yellow liquid which crystallize. ^1H NMR (500 MHz, CDCl_3) δ 7.58 (s, 2H), 7.12 (d, J = 2.3 Hz, 2H), 6.66 (t, J = 2.3 Hz, 1H), 5.78 (ddt, J = 16.9, 10.2, 6.6 Hz, 1H), 5.06 – 4.93 (m, 2H), 4.27 (t, J = 6.6 Hz, 2H), 2.19 – 2.09 (m, 2H), 1.86 – 1.75 (m, 2H). ^{13}C -NMR (125MHz, CDCl_3): δ = 27.65, 29.98, 65.07, 109.01, 115.41, 131.85, 137.24, 157.18, 167.45.



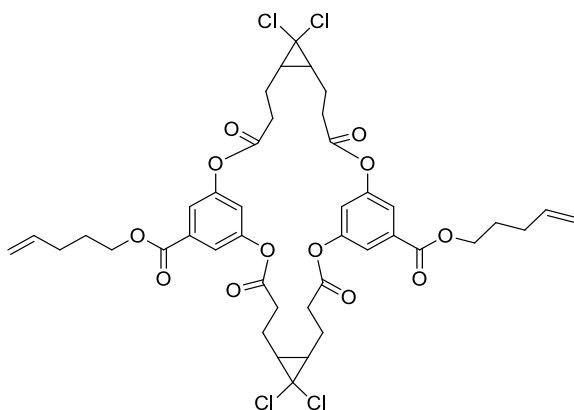
Synthesis of (Z)-9,9-dichlorobicyclo[6.1.0]non-4-ene, 2a²⁰. CHCl₃ (7.41 ml, 92 mmol) was added drop wise to a vigorously stirred dispersion of **1a** (11.34 ml, 92 mmol) and tBuOK (11.93 g, 106 mmol) in Hexane (150 ml) at -15 °C. The mixture was allowed to warm to rt and was stirred for 18 h. Water (15 mL) was added. Organic phase was separated. The water phase was extracted with hexane (2*15 mL). The solvent was removed under reduced pressure to yield crude product. Flash chromatography purification (SiO₂, EtOAc:Hexane) afforded the product (2.541 g, 76%) as a colorless liquid. ¹H-NMR (CDCl₃, 500 MHz): δ 1.77 (m, 4H), 2.07 (m, 2H), 2.19 (m, 2H), 2.36 (m, 2H), 5.56 (m, 2H). ¹³C-NMR (CDCl₃, 125 MHz): δ 25.8, 26.8, 33.0, 39.2, 129.0



Synthesis of 3,3'-(3,3-dichlorocyclopropane-1,2-diyl)dipropionic acid, 3a²¹. KMnO₄ (9.23 g, 58.4 mmol) was added in small portions to a stirred mixture of **2a** (5.45 g, 19.5 mmol) and NaHCO₃ (1.64 g, 19.5 mmol) in acetone (50 mL) at rt. The resulting mixture was stirred for 2 days. Excess permanganate was destroyed by the addition of MeOH and the reaction mixture was evaporated to dryness. The residue was treated with water (100 mL) and filtered to remove MnO₂. Water layer was acidified with 2N HCl to pH~2 and evaporated to dryness. The remainder was extracted with hot acetone (2*50 mL). The solvent was removed under reduced pressure to yield crude product. Flash chromatography purification (SiO₂, EtOAc:Hexane) afforded the product (4.41 g, 66%) as a colorless viscous oil. ¹H-NMR (CDCl₃, 500 MHz): δ 1.75 (m, 6H), 2.55 (m, 4H); ¹³C-NMR (CDCl₃, 125 MHz): δ 22.3, 32.3, 32.5, 34.8, 179.2



Synthesis of Di(pent-4-en-1-yl)5,5'-((3,3'-(3,3-dichlorocyclopropane-1,2-diyl))bis(propanoyl))bis(oxy))bis(3-hydroxybenzoate), 4. In a round bottomed flask under nitrogen is added **3a** (0.325 g, 1.274 mmol) in dry DCM. Then is added SOCl_2 (0.372 ml, 5.10 mmol). After that a drop of DMF is added to the reaction mixture. The reaction is stirred at rt for 3 hours, then the solvent is evaporated with rotavapor, and all the excess of SOCl_2 removed dissolving the residue in toluene and again under vacuum with rotavapor. The residue is dissolved in dry DCM and added dropwise over 5 minutes to a solution of **2b** (0.566 g, 2.55 mmol) in dry DCM charged with Et_3N (0.533 ml, 3.82 mmol) and stirred overnight at rt. Water (15 mL) was added. Organic phase was separated. The water phase was extracted with DCM (2*15 mL). The solvent was removed under reduced pressure to yield crude product. Flash chromatography purification (SiO_2 , EtOAc:Hexane) afforded the product as a yellow oil (0.198g, 23%). $^1\text{H-NMR}$ (500MHz, CDCl_3): δ = 7.48 – 7.40 (m, 2H), 7.35 – 7.29 (m, 2H), 6.92 – 6.79 (m, 2H), 5.83 (ddt, J = 16.9, 10.2, 6.6 Hz, 2H), 5.13 – 4.95 (m, 4H), 4.33 (q, J = 7.3, 6.5 Hz, 4H), 2.87 – 2.69 (m, 4H), 2.27 – 2.14 (m, 4H), 2.03 – 1.90 (m, 2H), 1.91 – 1.79 (m, 6H), 1.79 – 1.68 (m, 2H). $^{13}\text{C-NMR}$ (125MHz, CDCl_3): δ = 25.20, 27.76, 31.91, 33.01, 64.96, 113.90, 114.55, 115.51, 120.29, 132.38, 137.26, 151.20, 157.09, 165.90, 170.78, 171.31. HRMS [ESI] calculated for ($\text{C}_{42}\text{H}_{44}\text{Cl}_4\text{O}_{12}$ + Na): 686.0392 ; found: 686.03571.



Synthesis of Di(pent-4-en-1-yl)63,63,163,163-tetrachloro-3,9,13,19-tetraoxo-2,10,12,20-tetraoxa-1,11(1,3)-dibenzena-6,16(1,2)-

dicyclopropanacycloicosaphane-15,115-dicarboxylate, M1. In a round bottomed flask under nitrogen is added **3a** (0.4 g, 1.568 mmol) in dry DCM. Then is added SOCl_2 (0.458 ml, 6.27 mmol). After that a drop of DMF is added to the reaction mixture. The reaction is stirred at RT for 3hours, then the solvent is evaporated with rotavapor, and all the excess of SOCl_2 removed dissolving the residue in toluene and again under vacuum with rotavapor. The residue is dissolved in dry DCM and added dropwise over 5 minutes to a solution of **4** (1.040 g, 1.568 mmol) in CHCl_3 charged with Et_3N (0.656 ml, 4.70 mmol) and stirred overnight at rt Water (15 mL) was added. Organic phase was separated. The water phase was extracted with DCM (2*15 mL). The solvent was removed under reduced pressure to yield crude product. Flash chromatography purification (SiO_2 , EtOAc:Hexane) afforded the product as a yellow oil (0.673g, 49%). $^1\text{H-NMR}$ (CDCl_3 , 500 MHz): δ =1.76 (m, 4H), 1.88 (m, 8H), 1.96 (m, 4H), 2.23 (m, 4H), 2.78 (m, 8H), 4.35 (m, 4H), 5.04 (m, 4H), 5.85 (m, 2H), 7.21 (m, 2H), 7.70 (m, 4H). $^{13}\text{C-NMR}$ (125MHz, CDCl_3): δ =20.33, 20.83, 31.91, 33.01, 63.98, 113.90, 114.55, 115.51, 120.29, 132.38, 137.26, 150.83, 157.09, 165.90, 164.76, 170.44. HRMS [ESI] calculated for ($\text{C}_{42}\text{H}_{44}\text{Cl}_4\text{O}_{12} + \text{Na}$): 905.1455 ; found: 905.1439.

M1 MS Spectrum below

Multiple Mass Analysis: 3 mass(es) processed

Tolerance = 20.0 PPM / DBE: min = -30.0, max = 200.0

Isotope cluster parameters: Separation = 1.0 Abundance = 1.0%

Monoisotopic Mass, Odd and Even Electron Ions

1110 formula(e) evaluated with 3 results within limits (all results (up to 1000) for each mass)

Sample:- PM158 run in MeOH Cone = 50V

D. Gastaldello / RB

1191P 15 (0.844) AM (Cen,4, 80.00, Ar,5000.0,556.28,0.70,LS 30); Sm (SG, 10x4.00); Cm (4:33)

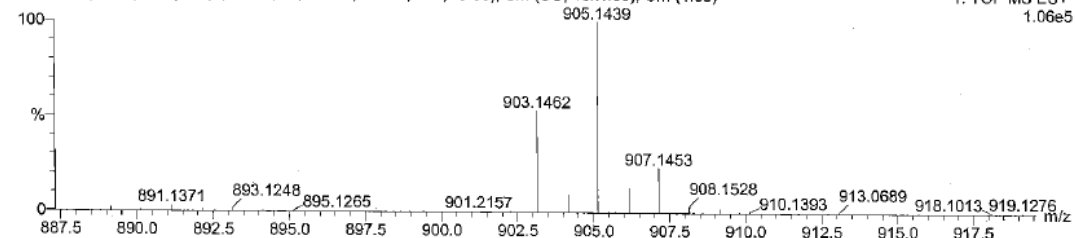
Operator: MM

LCT 05-Apr-2016 16:56:20

Chemistry Dept. Univ. of Liverpool

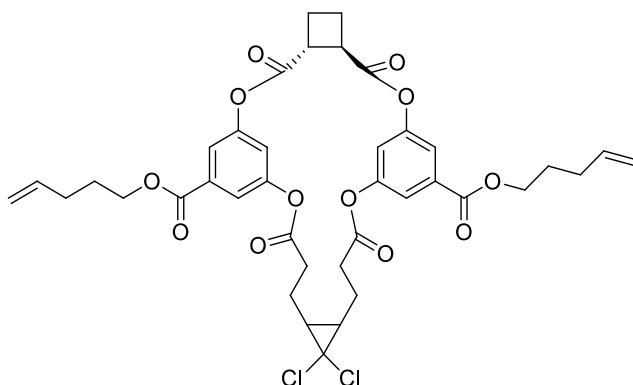
1: TOF MS ES+

1.06e5



Mass	RA	Calc. Mass	mDa	PPM	DBE	Score	Formula
903.1462	53.22	903.1485	-2.3	-2.5	18.5	1	C42 H44 O12 23Na 35Cl4
905.1439	100.00	905.1455	-1.6	-1.8	18.5	1	C42 H44 O12 23Na 35Cl3 37Cl
907.1453	23.37	907.1426	2.7	3.0	18.5	1	C42 H44 O12 23Na 35Cl2 37Cl2

Figure 8: HRMS report of M1.



Synthesis of Di(pent-4-en-1-yl) (41R,42R)-123,123-dichloro-3,5,9,15-tetraoxo-2,6,8,16-tetraoxa-1,7(1,3)-dibenzena-4(1,2)-cyclobutana-12(1,2)-

cyclopropanacyclohexadecaphane-15,75-dicarboxylate, M2. In a round bottomed

flask under nitrogen is added **1c** in dry DCM. Then is added SOCl₂ (0.176 ml, 2.411 mmol). After that a drop of DMF is added to the reaction mixture. The reaction is stirred at rt for 3hours, and then all the excess of SOCl₂ and solvent removed under vacuum affording a white powder. This product is dissolved in dry DCM and added dropwise over 5 minutes to a solution of **4** (0.4 g, 0.603 mmol) in DCM charged with Et₃N (0.252 ml, 1.808 mmol) and stirred overnight at rt. Water (15 mL) was added.

Organic phase was separated. The water phase was extracted with DCM (2*15 mL). The solvent was removed under reduced pressure to yield the crude product. Flash chromatography purification (SiO₂, EtOAc:Hexane) afforded the product as a yellow oil (0.148g, 32%). ¹H-NMR (CDCl₃, 500 MHz): δ=1.75 (m, 4H), 1.88 (m, 4H), 1.93 (m, 2H), 2.20 (m, 4H), 2.41 (m, 4H), 2.79 (m, 4H), 3.79 (m, 2H), 4.33 (m, 4H), 5.05 (m, 4H), 5.83 (m, 2H), 7.22 (m, 2H), 7.68 (m, 4H). ¹³C-NMR (125MHz, CDCl₃): δ=20.33, 22.03, 27.76, 30.05, 31.87, 32.88, 65.00, 115.48, 119.96, 120.09, 132.62, 137.29, 150.84, 164.74, 170.48, 170.96. HRMS [ESI] calculated for (C₃₉H₄₀Cl₂O₁₂ + Na + MeOH): 793.1795 ; found: 793.1782.

M2 MS Spectrum below

Multiple Mass Analysis: 2 mass(es) processed

Tolerance = 20.0 PPM / DBE: min = -30.0, max = 200.0

Isotope cluster parameters: Separation = 1.0 Abundance = 1.0%

Monoisotopic Mass, Odd and Even Electron Ions

371 formula(e) evaluated with 2 results within limits (all results (up to 1000) for each mass)

Sample: ParalMech-160 run in MeOH Cone = 50V

D. Gastaldello / RB

1256P 31 (1.724) AM (Cen,4, 80.00, Ar,5000.0,556.28,0.70,LS 1); Sm (SG, 10x4.00); Cm (5:34)

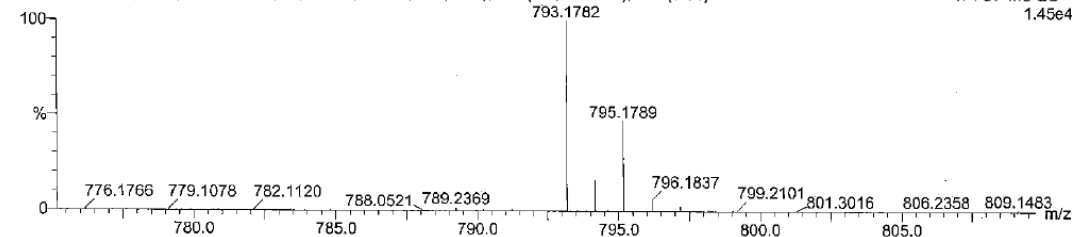
Operator: MM

LCT 26-Apr-2016 13:51:26

Chemistry Dept. Univ. of Liverpool

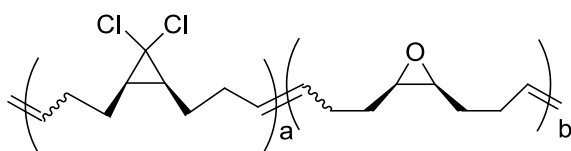
1: TOF MS ES+

1.45e4



Mass	RA	Calc. Mass	mDa	PPM	DBE	Score	Formula
793.1782	100.00	793.1795	-1.3	-1.6	18.5	1	C ₃₉ H ₄₀ O ₁₂ 23Na 35Cl ₂
795.1789	47.01	795.1765	2.4	3.0	18.5	1	C ₃₉ H ₄₀ O ₁₂ 23Na 35Cl 37Cl

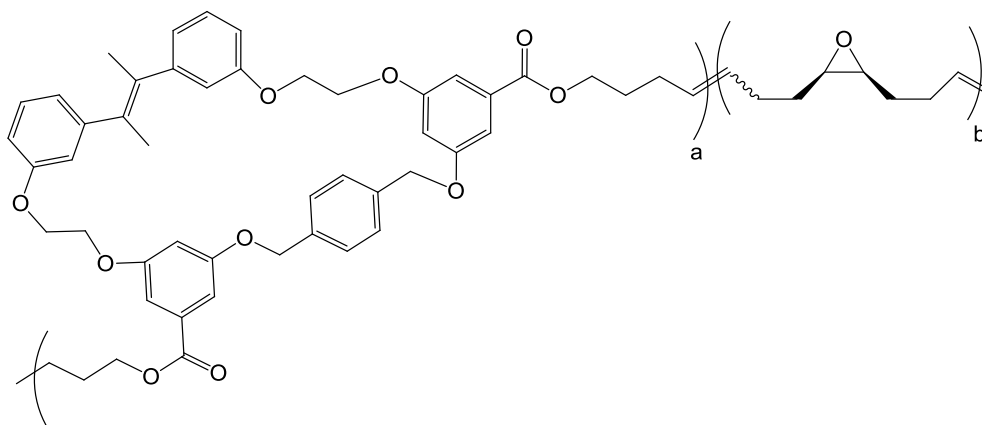
Figure 9: HRMS report of M2



Synthesis of model polymer, 2ae. **2a** (0.154 g, 0.805 mmol) and **2e** (0.099 ml, 0.805 mmol) were dissolved in 0.15 mL DCM and deoxygenated with N₂ for 10 minutes. 1.0 mg (1% mol) Grubbs II generation catalyst was dissolved in 1 mL DCM and

deoxygenated for 20 minutes. 0.1 mL of the Grubbs catalyst solution was transferred to the monomer solution via a syringe. The viscosity of the solution increased after 10 minutes and stirring ceased quickly. 0.3 mL of DCM was added to the solution to allow the stirring to continue and the reaction was allowed to proceed for another 1h. The reaction mixture was quenched with 1 mL of ethyl vinyl ether and stirred for 1h. The reaction was then precipitated in MeOH, redissolved in DCM and reprecipitated in MeOH and dried on a vacuum line. Procedure based on the procedure used in literature²².

Synthesis of model polymer no.2



Monomer 1 (0.120 g, 0.143 mmol) and (Z)-9-oxabicyclo[6.1.0]non-4-ene (0.099 ml, 0.805 mmol) were dissolved in 0.15 mL DCM and deoxygenated with N₂ for 10 minutes. (E)-benzylidene(1-(2,4-dimethylphenyl)-3-mesitylimidazolidin-2-yl)(tricyclohexylphosphoranyl)ruthenium(VI) chloride (0.005 g, 5.97 μmol) was dissolved in 1 mL DCM and deoxygenated for 20 minutes. 0.1 mL of the Grubbs catalyst solution was transferred to the monomer solution via a syringe. The viscosity of the solution increased after 10 minutes and stirring ceased quickly. 0.3 mL of DCM was added to the solution to allow the stirring to continue and the reaction was allowed to proceed for another 1h. The reaction mixture was quenched with 1 mL of ethyl vinyl ether and stirred for an hour. The reaction mixture was then precipitated in methanol, redissolved in DCM and reprecipitated in methanol and dried on a vacuum line.

References

- ¹ Perkins, T.T.; Smith, D.E.; Chu, S. *Science* **1997**, 276, 5321, 2016-2021.
- ² Wu, D.; Lenhardt, J. M.; Black, A. L.; Akhremitchev, B. B.; Craig, S. L. *J. Am. Chem. Soc.* **2010**, 132, 15936–15938.
- ³ Lenhardt, J. M.; Black, A. L.; Beiermann, B. A.; Steinberg, B. D.; Rahman, F.; Samborski, T.; Elsagr, J.; Moore, J. S.; Sottos, N. R.; Craig, S. L. *J. Mater. Chem.* **2011**, 21, 8454.
- ⁴ Klukovich, H.M.; Kouznetsova, T. B.; Kean, Z. S.; Lenhardt, J. M.; Craig, S. L. *Nat. Chem.* **2013**, 5, 110.
- ⁵ Lenhardt, J. M.; Black, A. L.; Craig, S. L. *J. Am. Chem. Soc.* **2009**, 131, 10818.
- ⁶ Preller, M.; Dietmar, J.M. *Structure* **2013**, 21.11, 1911-1922.
- ⁷ Brown, C. L.; Craig, S.L. *Chem. Sci.* **2015**, 6.4, 2158-2165.
- ⁸ Lauterborn, W.; Kurz, T. *Rep. Prog. Phys.* **2010**, 73, 106501
- ⁹ Wang, J.; Kouznetsova, T.B.; Niu, Z.; Ong, M.T.; Klukovich, H.M.; Rheingold, A.L.; Martinez, T.J.; Craig, S.L. *Nat. Chem.* **2015**, 7, 323–327
- ¹⁰ Akbulatov, S.; Tian, Y.; Boulatov, R. *J. Am. Chem. Soc.* **2012**, 134 (18), 7620-3.
- ¹¹ Kean, Z. S.; Niu, Z.; Hewage, G. B.; Rheingold, A. L.; Craig, S. L. *J. Am. Chem. Soc.* **2013**, 135 (36), 13598-604.
- ¹² Wang, J.; Kouznetsova, T. B.; Boulatov, R.; Craig, S. L. *Nat. Comm.* **2016**, 7, 13433.
- ¹³ Wang, J.; Kouznetsova, T. B.; Kean, Z. S.; Fan, L.; Mar, B. D.; Martinez, T. J.; Craig, S. L. *J. Am. Chem. Soc.* **2014**, 136 (43), 15162-5.
- ¹⁴ Pustovit, Y.M.; Ogojko, P.I.; Nazaretian, V.P.; Rozhenko, A.B. *J. Fluorine Chem.* **1994**, 69.3, 231-236.
- ¹⁵ Nishshanka, U.; Attygalle, A. B. *J. Mass Spectrom.* **2008**, 43 (11), 1502-1511.
- ¹⁶ Martí-Centelles, V.; Pandey, M. D.; Burguete, M. I.; Luis, S. V. *Chem. Rev.* **2015**, 115 (16), 8736-8834.
- ¹⁷ Al-Dulayymi, A.; Li, X.; Neuenschwander, M. *Helv. Chim. Acta* **2000**, 83.7, 1633-1644.
- ¹⁸ Wang, J.; Kouznetsova, T. B.; Niu, Z.; Ong, M. T.; Klukovich, H. M.; Rheingold, A. L.; Martinez, T. J.; Craig, S. L. *Nat. Chem.* **2015**, 7 (4), 323-7.

- ¹⁹ Brown, D. P.; Duong, H. Q. *J. Heterocyc. Chem.* **2008**, 45(2), 435-443
- ²⁰ Binger, P.; Büch, H.M. *Top. Curr. Chem.* **1987**, 77-151
- ²¹ Pustovit, Y. M.; Ogojko, P. I.; Nazaretian, V. P.; Rozhenko, A. B. *J. Fluorine Chem.* **1994**, 69.3,231-236.
- ²² Hodge, P.; Kamau, S. D. *Angew. Chem. Int. Ed.* **2003**, 42, 2412–2414

CHAPTER III. – Synthesis of force probes containing Stiff-Stilbene.

Abstract

Another plausible model to understand the force distribution in a polymer under force, is made by two polymer chains connected to each other by a mechanophore. This scenario is more challenging compared to the single linear polymer designed in Chapter II, therefore it could give more insights into polymer mechanochemistry understanding, once exploited. In order to quantify how the force varies along the chain of mechanochemically fragmenting macromolecule, I synthesized a series of polystyrenes with different MW containing a single a mechanically-labile group (Stiff-Silbene). We will derive the force distribution by integrating the measured rates of competition between simple C-C backbone bond scission and this mechanophore reaction with quantum-chemically calculated force-dependent activation free energies. The force will be applied with ultrasonic irradiation (sonication) on the polymers synthesized.

Introduction

During sonication of dilute polymer solutions, the process of acoustic cavitation results in multiple types of complex flow. Under certain shear elongational flows, polymer chains are stretched and experience enough force to undergo chain scission. The average distribution of force experienced by each chain is not currently known, apart from the fact that the chain midpoint experiences on average the greatest force¹. Most kinetic modelling of linear polymer chain scission begins with the assumption that fragmentation occurs within roughly the central 15% of the chain, the exact probability of fragmentation at each point given by a stoichiometric kernel (as shown in Madras work²). To further understand the response of each chain subjected to elongational flow, a mechanophore (a moiety containing mechanically-labile bonds) can be incorporated into the chain. Though such experiments comprise the standard technique used in the laboratory for studying mechanochemistry. Further knowledge of how force is distributed in a linear polymer chain during sonication will allow a more informed molecular design for future studies involving synthesis of mechanophore-containing polymers. For example, a polymer could be

synthesised where a pre-determined amount of mechanophore would activate upon sonication for a certain duration of time. Knowledge of how force is distributed will be useful in new areas of study such as the release of species which catalyse further reactions upon application of force, and gating of mechanochemical reactions.

Previous studies, in which the extent of mechanophore-activation has been determined, have focused on one of the two following polymeric designs³: (1) incorporation of a centrally-located scissile mechanophore, such as the Diels-Alder adduct of anthracene and maleimide in either linear or star-shaped polymer, (2) random copolymerisation of non-scissile mechanophores such as poly(*gem*-dichlorocyclopropane) (poly(gDCC)), or mechanically weaker bonds like peroxides throughout the length of the chain⁴. Both strategies rely on the selectivity of the mechanophore reaction in comparison to chain scission of the C-C covalent backbone bond scission. In this project, a mechanophore, stiff stilbene, will be incorporated into linear polystyrene chains (**Figure 20**), and the distribution of stiff stilbene within each sample will be determined. Upon experiencing sufficient force, Stiff Stilbene isomerises from the *cis*- to the *trans*-isomer, and the different extinction coefficients of each isomer above 300 nm wavelength will allow quantification of their relative amounts each fraction of polymer.

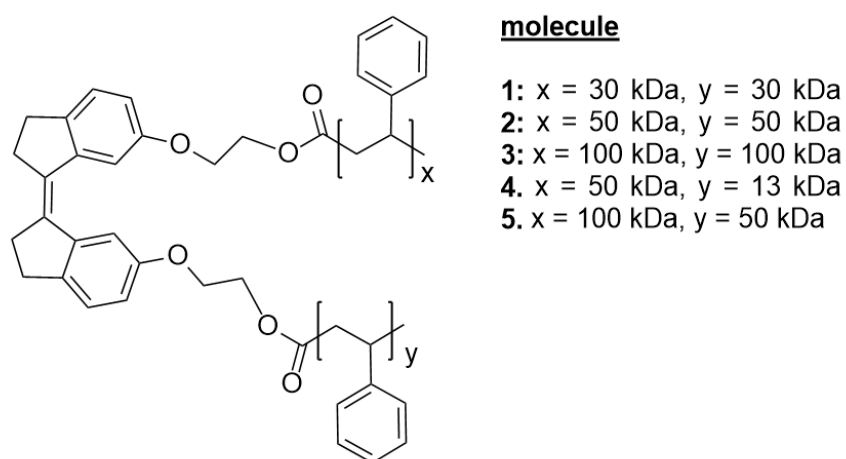


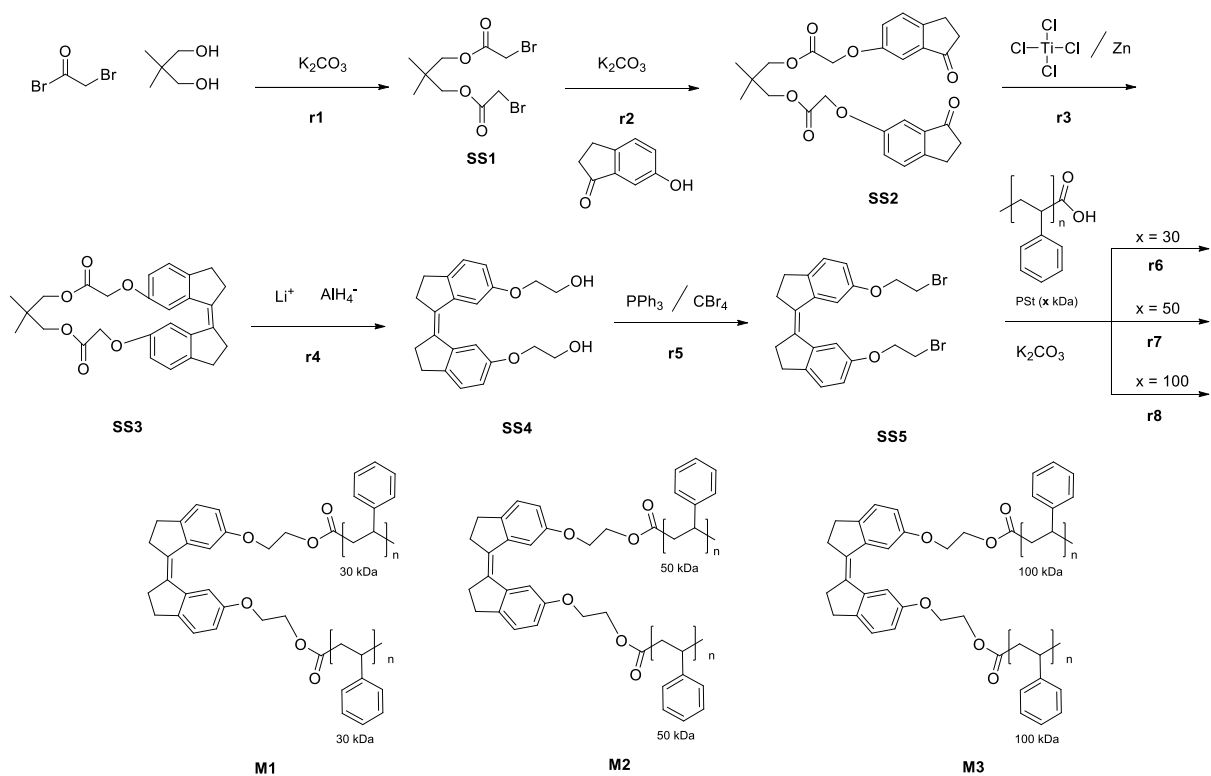
Figure 20: The stiff stilbene-containing polystyrene chains which were sonicated during this study. A kinetic scheme will be developed, allowing the number of chains of polymers containing *cis*- and *trans*-stiff stilbene in the dimer and product distribution to be determined at each sonication time, and compared with the experimental result. The

studies in which the initial reaction occurs at the mechanophore during sonication often use nuclear magnetic resonance (NMR) spectroscopy. The ratio of the mechanically-transformed group can be obtained, and from this, parameters such as the percentage activation of the initial mechanophore can be calculated. In the case of scissile mechanophores, it is possible to obtain the ratio of polymer chains which break at and away from the mechanophore.

Result and discussion

Molecular design

Stiff stilbene-based macrocycles were previously synthesized by Boulatov's group in order to investigate its alkaline hydrolysis as a function of restoring force, proving that it's insensitive to mechanical force, which coincides with MD simulations⁵. Moreover, we reported the reduction of organic disulfides that were also incorporated in Stiff Stilbene based macrocycles by phosphines in water to get new insight into the kinetics of mechanochemical reactions⁶. Stiff stilbene probe molecules **M1-3**, containing central stiff stilbene were synthesised in five steps with overall yield greater than 10% according to the literature (synthetic **Scheme 7**⁷).



Scheme 7: Synthesis of stiff stilbene probe and incorporation centrally into polystyrene chains of total mass 60 kDa (**M1**), 100 kDa (**M2**) and 200 kDa (**M3**).

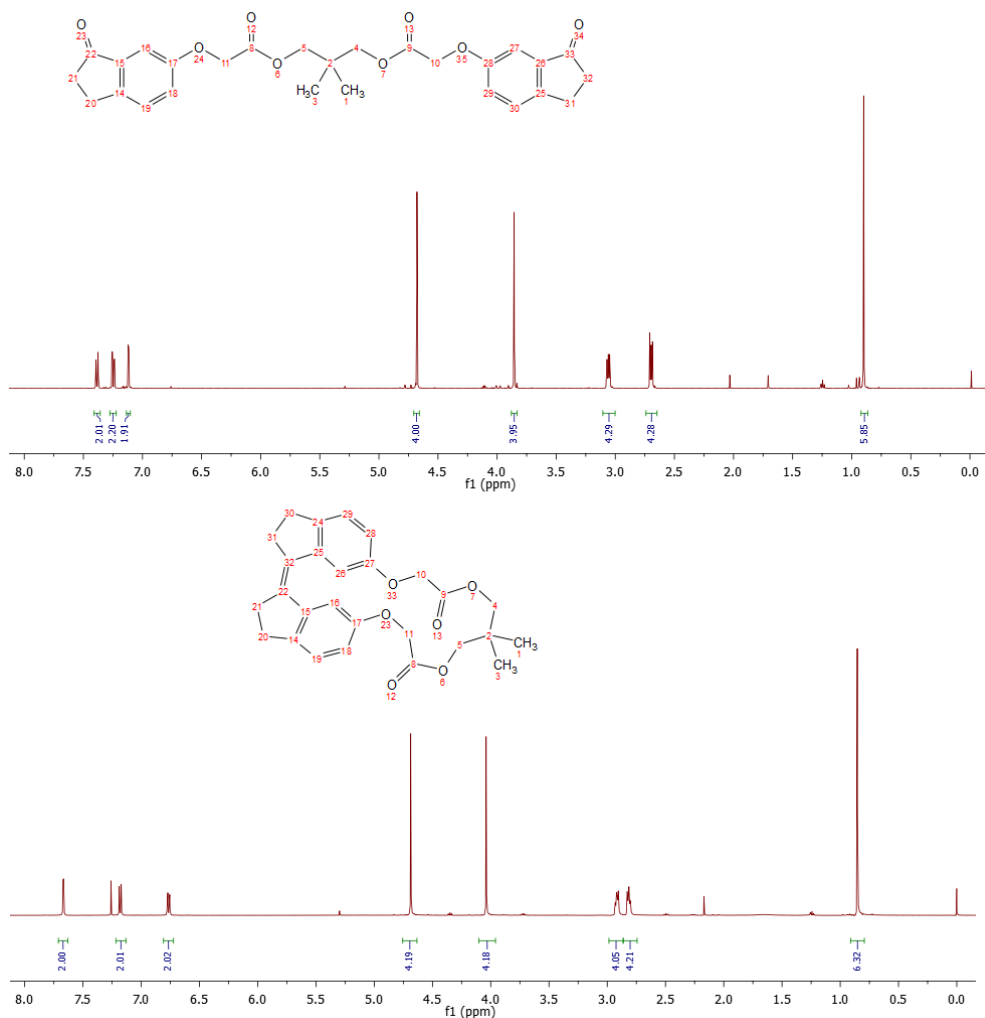


Figure 21: H-NMR comparison of starting material and isolated product after a successful McMurry coupling.

One of the key aspects of the synthetic route was the McMurry coupling (r3⁸). This was necessary to obtain the final product as Z-Stiff Stilbene. As described in previous work by Dr. Boulatov and our group⁹, it's fundamental to obtain a Z isomer in order to run this project. In fact, Stiff Stilbene has two stable and structurally distinct isomers that can be accessed via photoisomerization¹⁰. Instead of being attached to an AFM tip, the C₆ and C₆₀ atoms of Z-isomer of the stiff stilbene can be bridged with a linker where a functional group of interest could be incorporated to form a macrocycle. The relaxed Z-isomer is then converted to E-isomer with a large increase in the C₆...C₆₀ distance upon irradiation at 365 or 375 nm, generating a substantial restoring force within the molecule. Therefore, it's essential to pursue the correct synthetic route for Z-Stiff-Stilbene.

The work up of the reaction was challenging, and the isolation of the final product required extra care (due to the emulsion generated from the zinc powder and the solvent, several filtrations were performed to overwhelm this issue). The success of the reaction was confirmed by NMR (which display a shift in key signals compared to the starting material).

The last step of the synthetic scheme was necessary to attach the polystyrene chains to the Stiff-Stilbene core using a protocol routinely performed by our group: this being the reaction between the Br terminal group and the terminal carboxylic acid on the polystyrene with K_2CO_3 in dry DMF. For this reason, the terminal -OH groups on the Stiff Stilbene were converted into Br groups causing a noticeable shifting in the NMR (as shown in Figure 22).

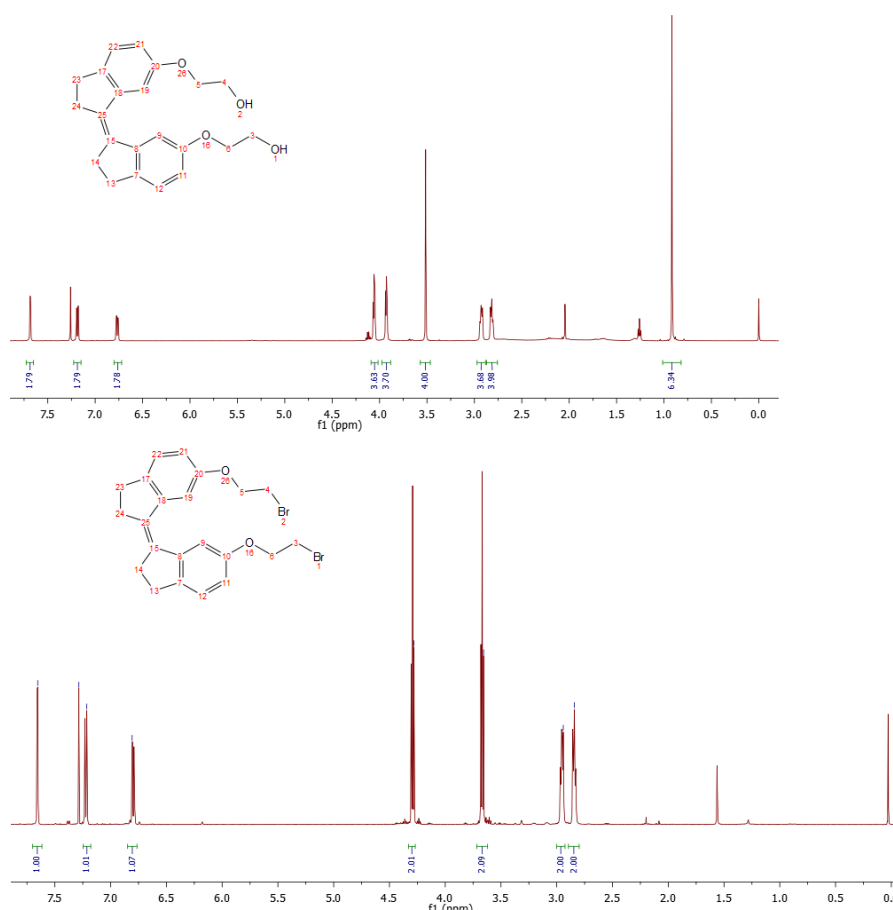
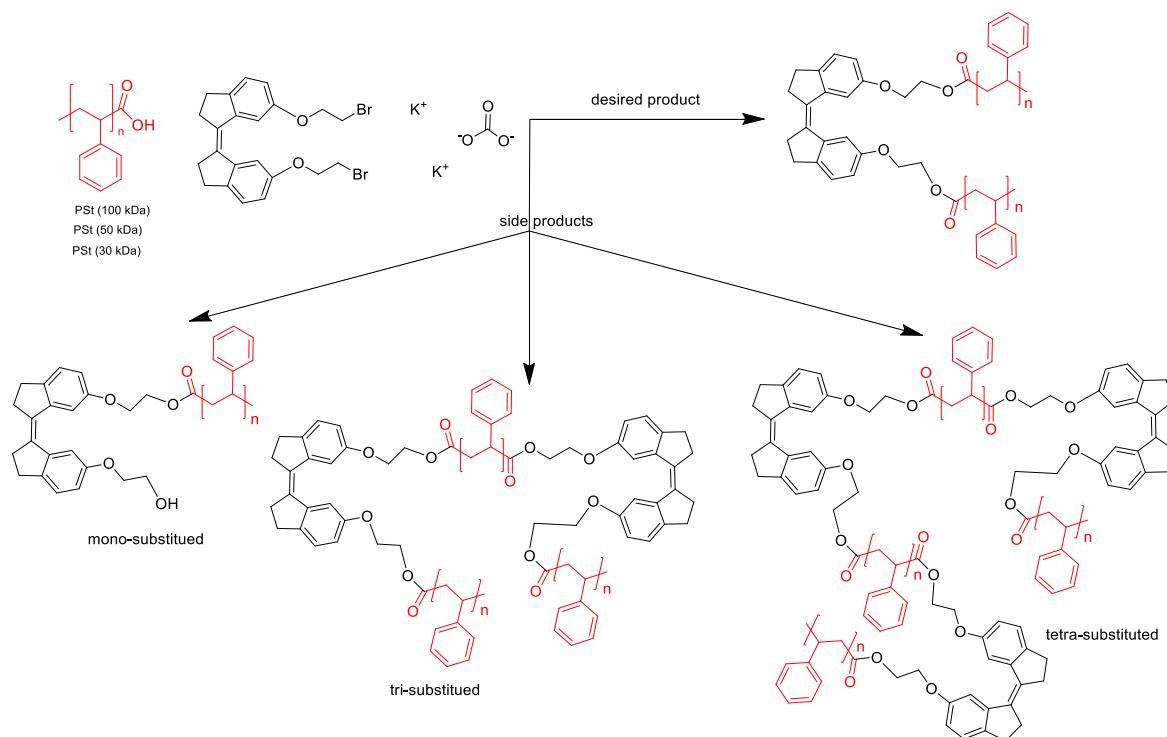


Figure 22: H-NMR comparison of starting material and isolated product after a successful conversion of OH terminal groups into Br groups.

Isolation of polymers via preparative GPC

The hardest task in this project was to isolate the goal compounds (Stiff-Stilbene core connected to polystyrene chains) from unreacted starting material and side products. Each reaction r6, r7 and r8 yielded a mixture of component which was hard to separate using prep-GPC. Using a concentration of 0.1mg/ml of reaction mixture dissolved in EtOAc the instrument was not able to separate all the components during the first run. As shown in **Figure 17**, almost every 2ml vial of solution eluted by the prepGPC after the first run was still a mixture of components (only vials 4,5,6,and 7 – labelled as Series4,5,6,7 – contained pure isolated product). Another prep GPC separation was therefore necessary in order to get more material, the vials 8-12 were combined and the procedure repeated.



Scheme 8: r6,r7,r8 scheme with side products explicated. The polystyrene chains are in red, the three subproducts identified after prep GPC were: a Stiff Stilbene connected to only one polystyrene chain, a system of two Stiff-Stilbene molecules linked with three polystyrene chains and a system of two Stiff-Stilbene molecules linked with four polystyrene chains.

Before starting the separation, a SEC run was made on the reaction mixture in order to have an approximate idea of how many peaks and species were present (**Figure 16**). Using a Matlab script created by Dr. Boulatov, it was then possible to analyze

the contents of each vial (precise mass of the polymer chain in Da, molecules of Stiff-Stilbene per chain at peak max, peak intensity at 260nm and many other data shown in **Figure 24**). Thanks to the calibration curve created to establish the size of the polymer chains analysed, it was possible to figure out the exact size in Dalton of the commercial polystyrene used (sold as 100 KDa but around 96 KDa).

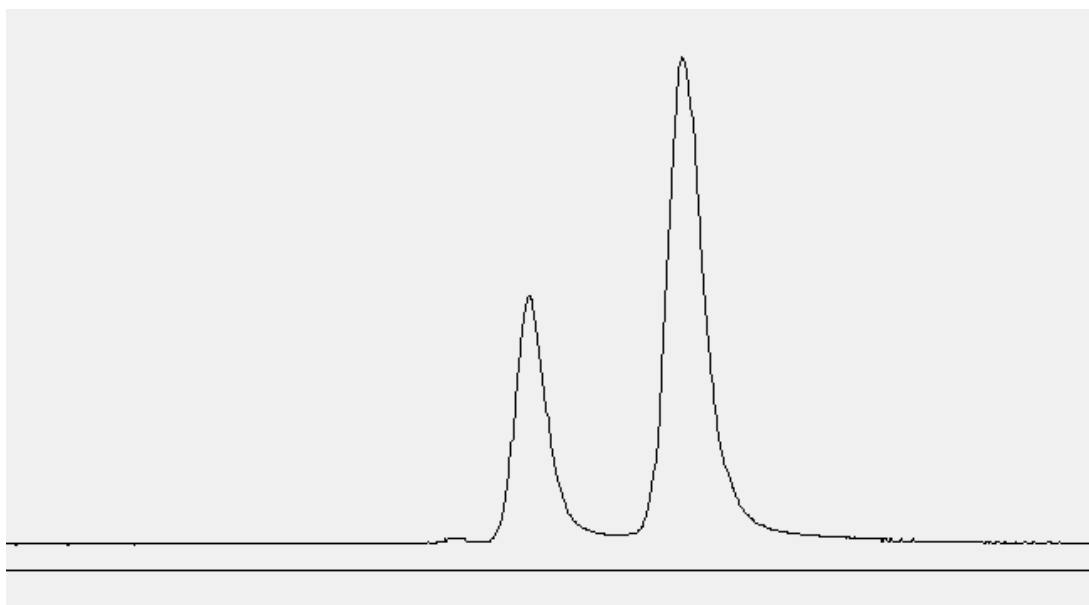


Figure 23: SEC of reaction mixture. The first peak contains the desired product, the second peak is unreacted starting polystyrene.

The reason why tri- and tetra- substituted Stiff Stilbene-polystyrene are side products is due to the inter-connection of Stiff-Stilbene molecule (which creates three or more reactive sites for the polystyrene), and also due to the nature of the starting material. In fact, some of the commercial polystyrene is not mono-carboxy terminated but it contains two carboxylic acid ending groups. The identification of such impurities with three or four polystyrene chains connected to the Stiff Stilbene was suggested by the size in KDa obtained after prepGPC.

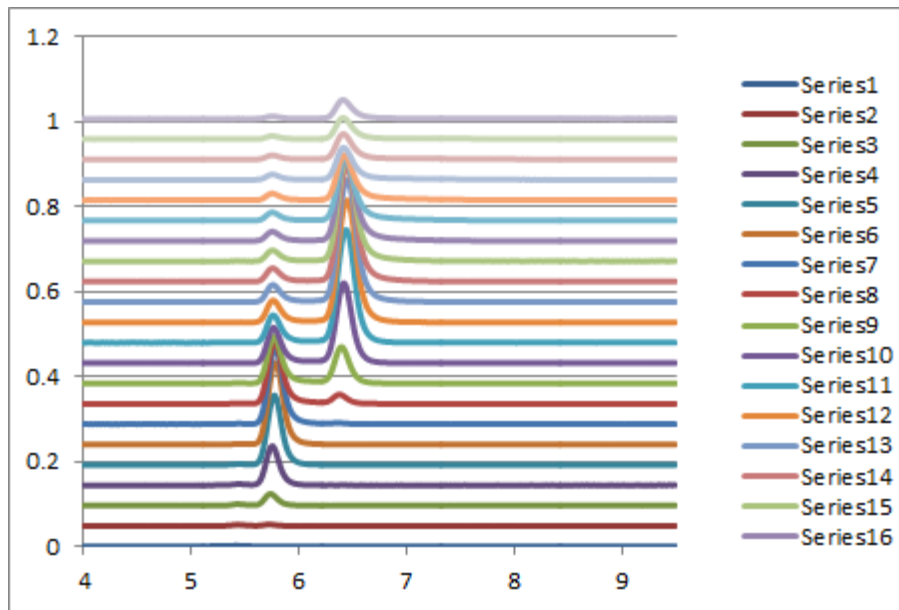


Figure 24: Chromatograms of each vial (labelled as “Series”) contents after the first separation with prep GPC. Vials 4-7 contain the isolated product, vials 8-12 will be combined and will undergo another prep GPC separation.

vial	4	5	5	6	6	7	7	8	9	10
peak rettime	5.401704	5.430036	5.720015	5.428369	5.735013	5.435035	5.750012	5.770011	5.78001	5.78001
peak intensity @260 nm	0.00157	0.003025	0.003575	0.003484	0.02755	0.002772	0.092173	0.163799	0.192547	0.178578
Amount Desired Peak			0.541621		0.887751		0.970803			
overlaps on left?	0	0	0	0	1	0	0	0	0	0
overlaps on right?	0	0	0	1	0	0	0	0	0	0
Mp (Da)	289400	279600	202700	280200	199500	277900	196500	192600	190600	190600
DMp	8500	8200	5900	8200	5800	8100	5800	5600	5600	5600
SS molec. per chain at peak max	0	0	0	0	0.910561	0	0.860993	0.84261	0.83427	0.842337
error	0	0	0	0	0.026584	0	0.025498	0.024586	0.024597	0.024833
E/Z ratio at peak max	0	0	0	0	1	0	1	1	1	1
error	0	0	0	0	0.00377	0	0.003398	0.00346	0.00347	0.00343

1st injection

vial	2	3	3	4	4	5	5	6	7	8
peak rettime	5.406704	5.420036	5.718348	5.433369	5.726681	5.428369	5.740013	5.756679	5.771677	5.773344
peak intensity @260 nm	0.00134	0.002739	0.00184	0.003374	0.016215	0.003077	0.066645	0.144912	0.187945	0.18065
Amount Desired Peak			0.401758		0.827744		0.955872			
overlaps on left?	0	0	0	0	0	0	0	0	0	0
overlaps on right?	0	0	0	0	0	0	0	0	0	0
Mp (Da)	287600	283000	203000	278500	201300	280200	198500	195200	192200	191900
DMp	8400	8300	5900	8100	5900	8200	5800	5700	5600	5600
SS molec. per chain at peak max	0	0	0	0	0.73064	0	0.872211	0.846924	0.844407	0.844359
error	0	0	0	0	0.021696	0	0.025585	0.024827	0.024696	0.024735
E/Z ratio at peak max	0	0	0	0	0.999999	0	1	1	1	1
error	0	0	0	0	0.006739	0	0.003653	0.003634	0.003577	0.003619

2nd injection

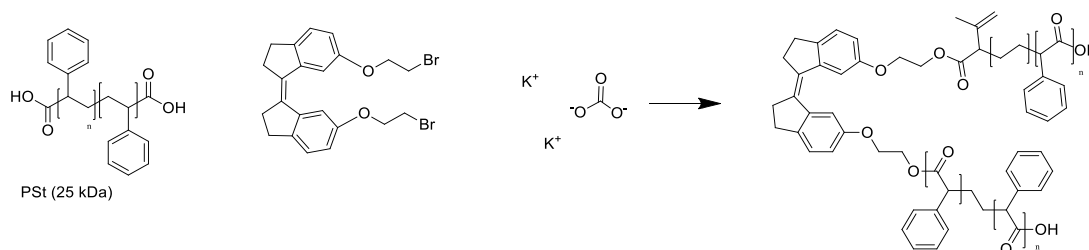
vial	2	3	3	4	4	5	5	6	7	8
peak rettime	5.430036	5.433369	5.716681	5.433369	5.728347	5.440035	5.745013	5.760012	5.773344	5.773344
peak intensity @260 nm	0.001323	0.002745	0.002485	0.00329	0.021096	0.00264	0.078834	0.153333	0.184226	0.170651
Amount Desired Peak			0.475162		0.865096		0.967599			
overlaps on left?	0	0	0	0	0	0	0	0	0	0
overlaps on right?	0	0	0	0	0	0	0	0	0	0
Mp (Da)	279600	278500	203400	278500	200900	276300	197500	194500	191900	191900
DMp	8200	8100	6000	8100	5900	8100	5800	5700	5600	5600
SS molec. per chain at peak max	0	0	0	0	0.99373	0	0.868985	0.858561	0.849762	0.855535
error	0	0	0	0	0.029307	0	0.02562	0.025254	0.024888	0.025052
E/Z ratio at peak max	0	0	0	0	0.999999	0	1	1	1	1
error	0	0	0	0	0.003819	0	0.003688	0.003563	0.003518	0.003427

3rd injection

Figure 25: Output from the Matlab script which shows a complete analysis of all the vials eluted after prepGPC. The vials highlighted in green are the ones containing the pure isolated desired product.

Due to the high amount of reaction mixture, each separation required more than one injection (the maximum amount tolerated by the instrument is 0.5ml injection with a 100mg/ml maximum concentration).

A control reaction using commercial polystyrene with two terminal carboxylic acid groups was run to confirm the hypothesis about the impurities. After SEC and prepGPC analyses, the size of the polymers suggested the formation of a species containing one or two Stiff Stilbene cores linked with one, two, three and four polystyrene chains.



Scheme 9: Control reaction using Stiff Stilbene and polystyrene dicarboxylic acid terminated

vial	6	6	7	7	8	8	8	9	9	9	10	11	11	12	12	
peak rettime	6.363301	6.608284	6.373301	6.619949	6.371634	6.629949	6.993256	6.371634	6.638281	7.011588	6.644948	7.026587	6.641614	7.039919	6.65328	7.048252
peak intensity @260 nm	0.004349	0.002361	0.004798	0.008898	0.003612	0.018569	0.001243	0.002074	0.023804	0.009037	0.020361	0.036631	0.012509	0.078166	0.007631	0.103693
overlaps on left?	0	1	0	1	0	1	1	0	1	1	0	1	0	1	0	1
overlaps on right?	1	0	1	0	1	1	0	1	1	0	1	0	1	0	1	0
Mp (Da)	110900	89600	109900	88700	110100	87900	64200	110100	87300	63200	86800	62400	87000	61700	86200	61200
Dmp	3200	2600	3200	2600	3200	2600	1900	3200	2500	1800	2500	1800	2500	1800	2500	1800
SS molec. per chain at peak max	1.673081	0	0.96665	0.774986	1.792586	1.043687	0	0	1.015877	0.59885	1.004836	0.53877	0.957301	0.535406	1.123315	0.551402
error	0.048697	0	0.100246	0.085174	0.052717	0.030973	0	0	0.029192	0.134241	0.029026	0.015599	0.027613	0.015667	0.032727	0.01626
E/Z ratio at peak max	0.999999	0	0.96555	0.976276	0.999999	1	0	0	1	0.98803	1	1	1	1	1	1
error	0.005373	0	0.096103	0.10341	0.006307	0.003386	0	0	0.003353	0.219687	0.003118	0.003517	0.003534	0.003201	0.003909	0.002989
vial	13	13	13	14	14	14	15	15	16	16	17	17	18	18	19	19
peak rettime	6.641614	7.051585	7.684872	6.65828	7.054918	7.70987	7.053251	7.733202	7.056584	7.751534	7.054918	7.761533	7.051585	7.764866	7.044919	7.764866
peak intensity @260 nm	0.004805	0.096973	0.009747	0.003266	0.0734	0.057542	0.048471	0.165654	0.031548	0.281326	0.021244	0.322556	0.015161	0.303169	0.011307	0.258729
overlaps on left?	0	0	1	0	0	1	0	0	0	0	0	0	0	0	0	0
overlaps on right?	0	1	0	0	1	0	0	0	0	0	0	0	0	0	0	0
Mp (Da)	87000	61000	34400	85800	60900	33600	60900	32900	60800	32300	60900	32000	61000	31900	61400	31900
Dmp	2500	1800	1000	2500	1800	1000	1800	1000	1800	900	1800	900	1800	900	1800	900
SS molec. per chain at peak max	1.083868	0.552583	0	0	0.557782	0.040984	0.565512	0.028567	0.568867	0.023078	0.614063	0.023609	0.55926	0.02312	0.59505	0.024578
error	0.031402	0.016349	0	0	0.016527	0.007068	0.01676	0.000944	0.016887	0.00073	0.018208	0.000749	0.016568	0.000737	0.017524	0.000773
E/Z ratio at peak max	0.999999	1	0	0	1	0.95769	1	0.993712	1	1	1	0.99368	1	0.993209	1	1
error	0.005202	0.003039	0	0	0.002957	0.162686	0.003066	0.018341	0.003062	0.021132	0.003359	0.020782	0.003702	0.02102	0.003967	0.019685

Figure 26: Output obtained after a prep-GPC purification done on the sample. In yellow is highlighted one of the key factors to prove a successful reaction, *i.e.* the presence of one Stiff-Stilbene molecule per two polymer chains (or in this case 0.5 molecules per 1 polystyrene chain). In green are highlighted the vials containing the species with the right Mp (expressed in Dalton) I wanted to isolate from the reaction mixture.

All the data processed by the Matlab script rely first on a calibration curve (polynomial) generated by Dr Boulatov. The analysis of polymer molecular weight distributions by conventional (GPC) requires a retention time and molecular weight calibration curve created from a set of standards. Polystyrene or polyolefin standards in trichlorobenzene (TCB) can be used for high temperature GPC of polyolefins in TCB.

The polystyrene narrow standards are used with appropriate Mark-Houwink parameters¹¹ to generate polyolefin equivalent molecular weights. For this project a calibration curve suitable for the analysis of polymers from ~ 10-300KDa was made. Beside the Mp and its distribution (DMp), other data were required to identify the right moieties synthesized for this project. As shown in **Figure 20**, the other parameters collected were: the peaks retention time, the peak intensity at 260nm (and this is crucial to identify the presence of Stiff-Stilbene species, acceptable normalized values for such parameter were around 0.1, much lower intensities meant a miniscule presence of valuable material mixed with a higher amount of unreacted starting material – commercial polystyrene). The “right and left overlaps” indicate whenever the peak is not isolated and clean but is overlapped with the signals of another moiety. In most cases I was able to combine fractions with high peak intensity. However, because the majority of fractions were still a mixture of components, I isolated the goal compounds completely with another prep GPC run.

The same procedures were used to isolated pure products from reactions r7 and r8. Reaction schemes and data after prepGPC for polymers containing 50KDa and 30 KDa commercial polystyrene are in the Experimental section.

Conclusions and future work

In conclusion, I successfully completed the synthesis of polymers attached to a mechanophore molecule (Stiff-Stilbene) placed at one end and commercial polystyrenes of various sizes. This will enable subsequent studies on the material which would lead to further understanding on how stresses are distributed on polymers with this (or a similar) structure. Moreover, this narrower scope allowed me to refine certain methods and to improve the synthesis of the final products which will be helpful for future work since it is possible to speed up this synthesis or even a synthesis with a similar structure. The pattern of side products generated during the polystyrene attachment to the Stiff-Stilbene and their retention times during the isolation of the goal product during prepGPC is helpful data when aiming to get the same products faster in future synthesis. Since all the data provided from

HPLC and prepGPC are describing the behavior of commercial polystyrene connected to a smaller molecule via nucleophilic substitution, the protocols and methods I describe may be helpful for general synthesis and purification of polystyrenes-based moieties.

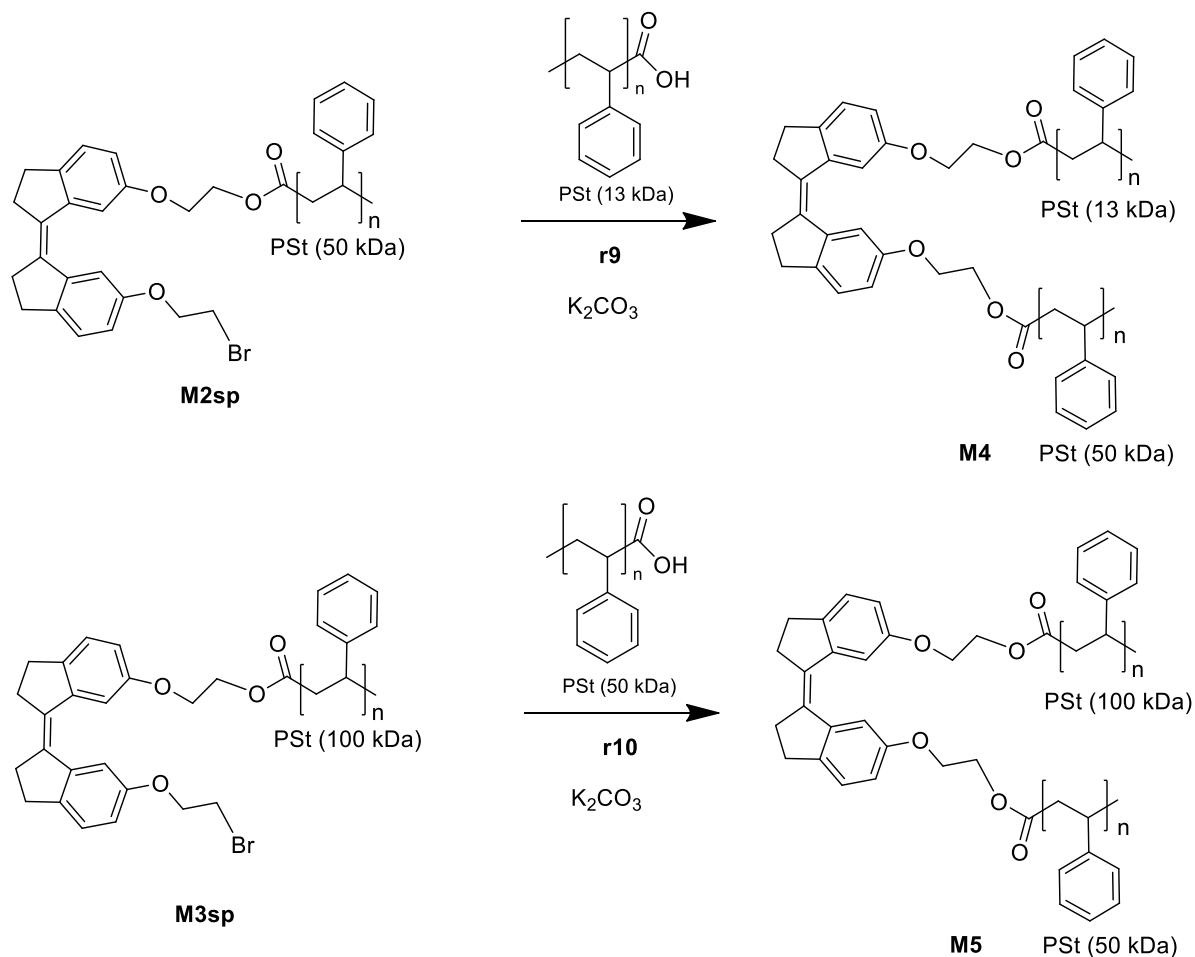
Future work will involve physical measurements run by my colleagues on the material I've synthesized. The final objective is to understand how the force will distribute and therefore how the polymer will break under stress. The fragments of a mechanochemically fragmented polymer chain may remain trapped in the elongational flow and become stretched enough to fragment themselves, leading to sequential chain scission. In this case, the bulk rate of generation of secondary fragmentation products will exceed the rate of primary fragmentation of the same fragment. To test this possibility, narrow polydispersity polystyrene standards will be sonicated to high conversion of starting material, to ensure a sizeable amount of secondary scission has occurred. The obtained SEC traces will be modelled assuming Gaussian distributions of initial polymer and primary and secondary scission products, to obtain bulk rate constants for both primary and secondary scission. In the literature, secondary scission is often neglected due to the difficult in resolving the primary product (that which has undergone scission only once) and chains which have been broken twice, or possibly even more, depending on sonication conditions, timescales, etc. If we consider only primary and secondary scission, the following first-order rate equations 6-8 give the expected balance of concentrations for each distribution (R = initial polymer, P = primary product, P' = secondary product):

$$(1) \quad [R]_t = [R]_0 e^{-k_1 t}$$

$$(2) \quad [P]_t = \frac{k_1}{k_2 - k_1} [R]_0 (e^{-k_1 t} - e^{-k_2 t})$$

$$(3) \quad [P']_t = \left(1 + \frac{k_1 e^{-k_2 t} - k_2 e^{-k_1 t}}{k_2 - k_1}\right) [R]_0 (1 - e^{-(k_1 + k_2)t})$$

Another interesting point of future research would be to perform the same analysis on a set of “off-centre” polymers, synthesizing a variety of Stiff-Silbene connected to two polystyrene chains with a different MW (as shown in the scheme below). This would be helpful in order to see whether the fragmentation pattern would change with a slightly more complex scenario.



Scheme 10: Further synthesis of molecules **M4-5**, which contain stiff stilbene probe off-centre with total masses of 63 kDa and 150 kDa, and stiff stilbene located roughly 20 and 33% of the way along the chain, respectively.

Experimental section

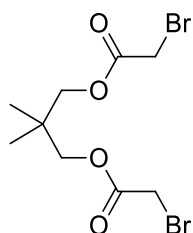
All reactions were performed under argon atmosphere using standard Schlenk techniques unless otherwise noted. All reagents were purchased from Sigma-Aldrich, Fisher Scientific or Fluorochem. DCM was purified using a solvent purification system. Flash chromatography was performed on Silicycle F60 (230-400 mesh) silica gel. Medium pressure liquid chromatography (MPLC) was performed on a Teledyne ISCO CombiFlash RF 200.

Mass spectra were run by operators using Micromass LCT Mass Spectrometer, using Ionization mode: ES^+ , Sample inlet: Syringe Pump, Sample run in MeOH, Sample Cone Voltage: 60 Volts. HPLC and GPC analyses were performed on a Shimadzu Prominence system with LC-20AT solvent delivery unit with integrated FCV-10AL VP quaternary gradient mixer, DGU-20A5 degasser, SPD-M20A photodiode array detector, CBM-20A system controller, SIL-20AHT autosampler with Rheodyne 7725i manual injector, CTO-20A column oven. J.T. Baker Silica Gel column (250 × 4.6 mm, particle size: 5 μm diameter) column was used for analytical HPLC ; Waters Prep Nova-Pak HR Silica column (19 x 300 mm, particle size: 6 μm diameter) was used for semi-preparatory HPLC; a set of three Agilent columns (PLgel 300 × 7.5 mm, 5 μm , 500 Å; PLgel 300 × 7.5 mm, 5 μm , 1,000 Å and PLgel 300 × 7.5 mm, 5 μm , 10,000Å) with a guard (PLgel 50 × 7.5 mm, 10 μm) was used for analytical GPC; a set of two Agilent columns (PLgel 300 × 25 mm, 10 μm , 1,000 Å and PLgel 300 × 25 mm, 10 μm , 10,000Å) with a guard (PLgel 25 × 25 mm, 10 μm) was used for preparatory GPC. Flow rate of THF for analytical GPC: 1 mL/min; for preparatory GPC: 5mL/min. Column heater temperature: 30 oC. SEC analyses were done on a Waters Acquity UPLC system with Acquity UPLC binary solvent manager, Acquity UPLC sample manager, Acquity UPLC column heater, Acquity UPLC PDA detector. A set of two Waters Acquity APC columns (APC XT 450, 150 × 4.6 mm) were used for SEC. Flow rate of THF: 0.6 mL/min. Column heater temperature: 30 oC. All polymers solutions were filtered through PTFE syringe filters (pore size: 0.45 μm) prior GPC/SEC analysis. The GPC and SEC columns were calibrated using narrow polystyrene standards obtained from Sigma-Aldrich and Scientific Polymers Inc.

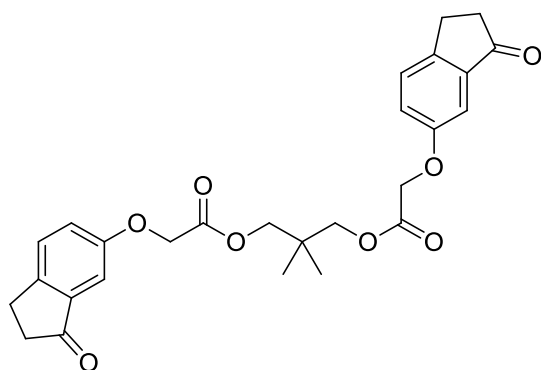
Ultrasound experiments were performed on a Vibra-Cell VCX 750 liquid processor from Sonics and Materials with an aluminum coupler for two solid probes (part # 630-0562) and two solid probes (tip diameter: 1/2" (13 mm); Length: 53/8" (136 mm); part #630-0219) with stainless steel collars. Three-neck Suslick cells were made by a School of Physical Sciences Workshop (University of Liverpool). The distance between the horn tip and the bottom of the Suslick cell was 10 mm.

High-resolution mass spectrometry (HRMS) was performed on a Micromass LCT TOF Mass Spectrometer at the University of Liverpool Mass Spectrometry Laboratory.

^1H and ^{13}C NMR spectra were referenced to the residual solvent peak (CDCl_3 δ = 7.26 (^1H) and 77.16 (^{13}C)) were collected on a Bruker 500MHz spectrometer. NMR spectra were analyzed using Mestrenova software.



Synthesis of 2,2-dimethylpropane-1,3-diyl bis(2-bromoacetate)⁵. 2-bromoacetyl bromide (4.01 ml, 46.1 mmol) was added dropwise to a stirred solution of 2,2-dimethylpropane-1,3-diol (2 g, 19.20 mmol) in DCM at room temperature. The reaction mixture was stirred for 30 min. potassium carbonate (13.27 g, 96 mmol) was added to the reaction mixture and stirring continued for another 10 min. The reaction mixture was poured onto water (100 mL); DCM layer was separated and aqueous layer was extracted with DCM (2 * 100 mL). combined organic layers were dried over MgSO_4 and evaporated. The product after evaporation was 5.89g, with a yield of 89%. ^1H -NMR (500MHz, CDCl_3): δ = 4.01 (s, 4H), 3.85 (s, 4H), 1.02 (s, 6H). ^{13}C NMR (126 MHz, DMSO) δ 167.6, 74.5, 34.4, 25.8, 22.3.



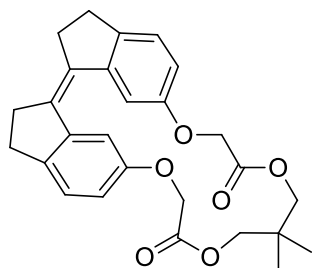
Synthesis of 2,2-dimethylpropane-1,3-diyl bis(2-((3-oxo-2,3-dihydro-1H-inden-5-yl)oxy)acetate)⁵.

2,2-dimethylpropane-1,3-diyl bis(2-bromoacetate) (3.50 g, 10.12 mmol) was added to a mixture of 6-hydroxy-2,3-dihydro-1H-inden-1-one (3 g, 20.25 mmol) and potassium carbonate (4.20 g, 30.4 mmol) in CH₃CN (100 mL). The reaction mixture was dropped to stir under N₂ overnight.

TLC (EtOAc : Hex= 1: 1; sample poured onto water and extracted with EtOAc) showed one product (R_f=0.3); no starting material (R_f=0.5) and minor impurities above and below the product.

The reaction mixture was evaporated; the residue was dispersed in EtOAc (150 mL) and washed with water (500 mL); aqueous layer was extracted with DCM (150 mL). Combined EtAOc and DCM fractions were dried over MgSO₄; evaporated.

The residue was purified on Combiflash (80 g gold SiO₂ column; 3rd use; 0-2CV: 0%EtOAc in DCM; 2-6 CV: 0->100%EtOAc in DCM gradient; 6-10CV: 100% EtOAc; the product came out after 4 CV in tube 6-11). TLC showed major product R_f=0.3; white solid; m= 3.8 g, 77% yield. ¹H-NMR (500MHz,CDCl₃): δ=7.40 (d, 2H, J = 8.4 Hz), 7.25 (dd, 2H, J = 8.4 Hz, 2.8 Hz), 7.13 (d, 2H, J = 2.8 Hz), 4.68 (s, 4H), 3.86 (s, 4H), 3.07 (t, 4H, J = 5.6 Hz), 2.70 (t, 4H, J = 5.6 Hz), 0.90 (s, 6H). ¹³C NMR (126 MHz, DMSO) δ 206.1, 169.5, 157.8, 149.8, 138.9, 119.6, 109.6, 74.7, 65.8, 36.4, 34.5, 25.8, 22.4.



Synthesis of Z(-1,2,11,12,20,21-hexaydro-11,11-dimethyl-3,5>17,19-Dietheno-10H-dicyclopenta[n,p] [1,4,8,11]tetraoxacyclonadeci-8,14*7H,15H-dione⁵.

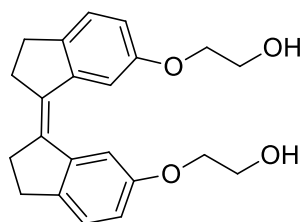
Titanium tetrachloride (4.36 ml, 39.5 mmol) was added dropwise to a stirred suspension of ZINC (5.17 g, 79 mmol) in dry THF (1000 mL). The resultant mixture was refluxed for 1.5 h (85 deg C in the oil bath). A solution of 2,2-dimethylpropane-1,3-diyl bis(2-((3-oxo-2,3-dihydro-1H-inden-5-yl)oxy)acetate) (3.8 g, 7.91 mmol) in dry THF (300 mL) was added dropwise to refluxing reaction mixture via a dropping funnel over a period of 3 h (1 drop/sec). After the addition of substrate was complete the mixture was refluxed for more 30 min. The mixture was cooled to room temperature and poured onto saturated ammonium chloride aq. solution (200 mL). THF layer was separated and aqueous layer was extracted with EtOAc. Combined organic fractions were dried over MgSO₄ and evaporated.

The residue was pushed through SiO₂ on CombiFlash (no column; SiO₂ in cartridge) with 0->100 % EtOAc in Hex. Collected ~40 tubes. Tubes 19-38 were combined and evaporated.

That resulted in some dark brown oil (~4 g); treated it with ether and decanted ether layer from produced solid. This (1.8 g) is pure product by TLC. After evaporation of ether fraction obtained black oil TLC of which shows some product but very dirty. There are overall three fractions 1) pure product (1.8 g - main fraction in a vial), 2) black fraction with very dirty product as a solution in DCM in a 20 mL vial; 3) and more pure product washed off the cartridge in a plastic beaker.

Fractions 1 and 3 combined as TLC showed pure product for both; fraction 2 evaporated and stored just in case. Combined fractions 1 and 3 were combined and dried afforded 1.930 g of pure product (54% yield). ¹H-NMR (CDCl₃, 500 MHz): δ=7.67 (d, 2H, J = 2.4 Hz), 7.19 (d, 2H, J = 8.0 Hz), 6.77 (dd, 2H, J = 8.0 Hz, 2.4 Hz), 4.69 (s,

4H), 4.04 (s, 4H), 2.92 (m, 4H), 2.82 (m, 4H), 0.85 (s, 6H). ¹³C NMR (126 MHz, DMSO) δ 171.1, 157.8, 145.9, 130.7, 128.6, 113.5, 75.9, 75.7, 34.1, 30.2, 28.7, 22.4.



Synthesis of (Z)-2,2'-((2,2',3,3'-tetrahydro-[1,1'-biindenylidene]-6,6'-diyl)bis(oxy))diethanol⁵.

A solution of (Z)-2,2'-((2,2',3,3'-tetrahydro-[1,1'-biindenylidene]-6,6'-diyl)bis(oxy))diethanol (0.724 g, 2.054 mmol, 87 % yield) in dry THF (20 mL) was added dropwise to a stirred suspension of aluminum(III) lithium hydride (0.716 g, 18.86 mmol) in dry THF (100 mL).

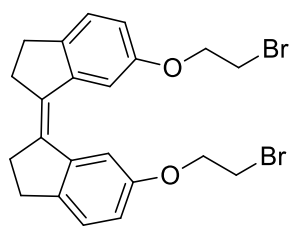
It was not a suspension of LiAlH₄ in THF: two tablets of LiAlH₄ of ~0.5 g each were added to THF, but they need time to dissolve. Left to stir at room temperature at vigorous stirring overnight.

TLC (EtOAc:Hex=1:1; sample quenched with water) showed no starting material (R_f=0.9) and one product (R_f=0.1)

10 mL of EtOAc were added to quench unreacted LiAlH₄; 5 mL of water; 1.5 mL of 15% NaOH; stir for 30 min; filter over celite and wash celite with EtOAc:MeOH=10:1 mixture (100 mL). Combined organic fractions were evaporated and purified on Combiflash (40 g regular silica column, 1st use, 0->100 % EtOAc in 5 CV; first a fraction of unknown impurity less polar than product came out, then product came out at 100% EtOAc in hex)

Combined fractions of product were evaporated to give white solid (1.3g) pure by TLC. Product had traces of EtOAc but it won't interfere in the next step. Yield: 86%.

¹H-NMR (CDCl₃, 500 MHz): δ= 7.68 (d, 2H, J = 2.4 Hz), 7.19 (d, 2H, J = 8.0 Hz), 6.77 (dd, 2H, J = 8.0 Hz, 2.4 Hz), 4.06 (t, 4H, J = 4.8 Hz), 3.93 (m, 4H), 2.93 (m, 4H), 2.82 (m, 4H), 2.65 (br, 2H). ¹³C NMR (126 MHz, DMSO) δ 161.7, 144.9, 130.6, 129.2, 113.6, 110.5, 69.7, 60.8, 34.1, 30.2.

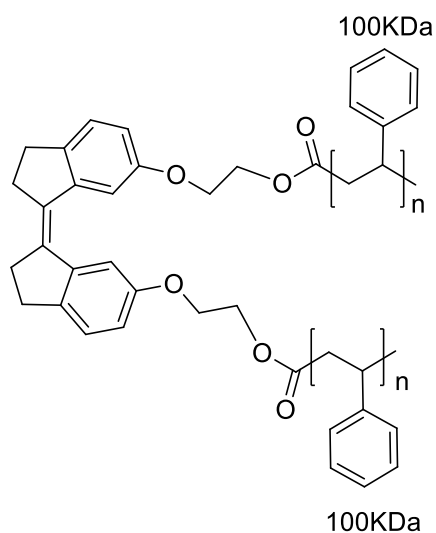


Synthesis of (Z)-6,6'-bis(2-bromoethoxy)-2,2',3,3'-tetrahydro-1,1'-biindenylidene⁵.

Perbromomethane (2.63 g, 7.94 mmol) was added to a dispersion of (Z)-2,2'-((2,2',3,3'-tetrahydro-[1,1'-biindenylidene]-6,6'-diyl)bis(oxy))diethanol (0.7 g, 1.986 mmol) in DCM with 10 drops of acetone. The mixture turned into a solution. triphenylphosphine (2.084 g, 7.94 mmol) was added and exothermic reaction occurred; the color changed to brownish. The mixture was left stirring for 6 hours.

TLC (EtOAc : Hex = 1 : 2) showed the product Rf=0.7; PPh3O (Rf = 0.2) and something on the start . Separated on CombiFlash (80g gold column; 1:1 = DCM:Hex). Yield: 60%.

¹H-NMR (CDCl₃, 500 MHz): δ=7.63 (d, 2H, J = 2.4 Hz), 7.20 (d, 2H, J = 8.0 Hz), 6.77 (dd, 2H, J = 8.0 Hz, 2.4 Hz), 4.27 (t, 4H, J = 6.0 Hz), 3.64 (t, 4H, J = 6.0 Hz), 2.93 (m, 4H), 2.82 (m, 4H). ¹³C NMR (126 MHz, DMSO) δ 161.9, 144.7, 145.33, 130.6, 128.3, 113.5, 110.4, 68.6, 34.1, 30.2, 29.2.



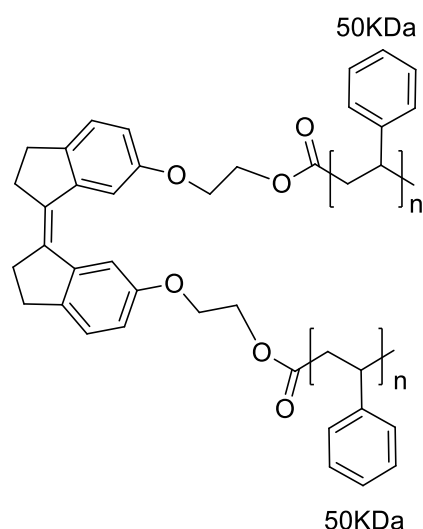
Polymer: (Z)-((2,2',3,3'-tetrahydro-[1,1'-biindenylidene]-6,6'-diyl)bis(oxy)) bis(ethane-2,1-diyl) bis(3-phenylbutanoate).

A stock solution of SS5 was made using 25mg (0.052 mmol) of SS-Probe in 2 ml of dry DMF (26 mM). In a 2 mL vial in the glovebox mixed Polystyrene monocarboxy terminated (0.15 g, 1.500 μmol), (Z)-6,6'-bis(2-bromoethoxy)-2,2',3,3'-tetrahydro-

1,1'-biindenylidene (0.026 ml, 0.682 μmol) and potassium carbonate (0.471 mg, 3.41 μmol) in DMF (so that the total volume of the reaction mixture is 200 μL). Took the vial out of the glovebox and left to stir overnight at room temperature. The reaction mixture was diluted in THF (to reach a $\sim 1\text{mg/mL}$ concentration), 1.5ml were taken from the solution, passed through a 45 μm syringe filter and analyzed by SEC.

Afterwards THF was evaporated and the sample dissolved in 1.5mL of EtOAc, concentration of 100mg/mL, for prepGPC (3 injections of 0.5 mL each). Only some vials contained the pure product, therefore another separation was necessary, running again through prepGPC the combined vials containing a mixture.

Combined vials (100% pure) afforded 20mg of product ready for sonication.



Polymer: (Z)-((2,2',3,3'-tetrahydro-[1,1'-biindenylidene]-6,6'-diyl)bis(oxy))bis(ethane-2,1-diyl) bis(3-phenylbutanoate).

A stock solution of SS5 was made using 25mg (0.052 mmol) of SS-Probe in 2 ml of dry DMF (26 mM). In a 2 mL vial in the glovebox mixed Polystyrene monocarboxy terminated (0.15 g, 3.00 μmol), (Z)-6,6'-bis(2-bromoethoxy)-2,2',3,3'-tetrahydro-1,1'-biindenylidene (0.052 ml, 1.364 μmol) and potassium carbonate (0.942 mg, 6.82 μmol) in DMF (so that the total volume of the reaction mixture is 200 μL). Took the vial out of the glovebox and left to stir overnight at room temperature. The reaction mixture was diluted in THF (to reach a $\sim 1\text{mg/mL}$ concentration), 1.5ml were taken from the solution, passed through a 45 μm syringe filter and analyzed by SEC.

Afterwards THF was evaporated and the sample dissolved in 1.5mL of EtOAc, concentration of 100mg/mL, for prepGPC (3 injections of 0.5 mL each). Only some vials contained the pure product, therefore another separation was necessary, running again through prepGPC the combined vials containing a mixture.

Combined vials (100% pure) afforded 15mg of product ready for sonication.

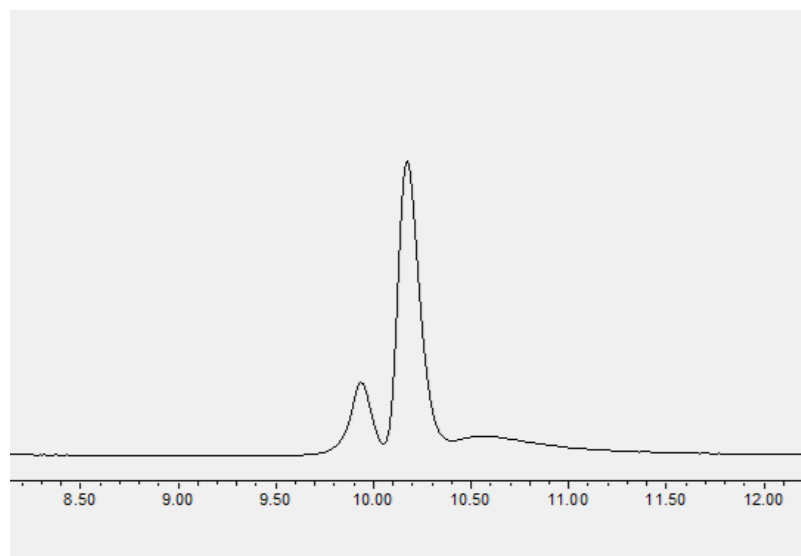


Figure 17: SEC of reaction mixture. The first peak contains the desired product, the second peak is unreacted starting polystyrene.

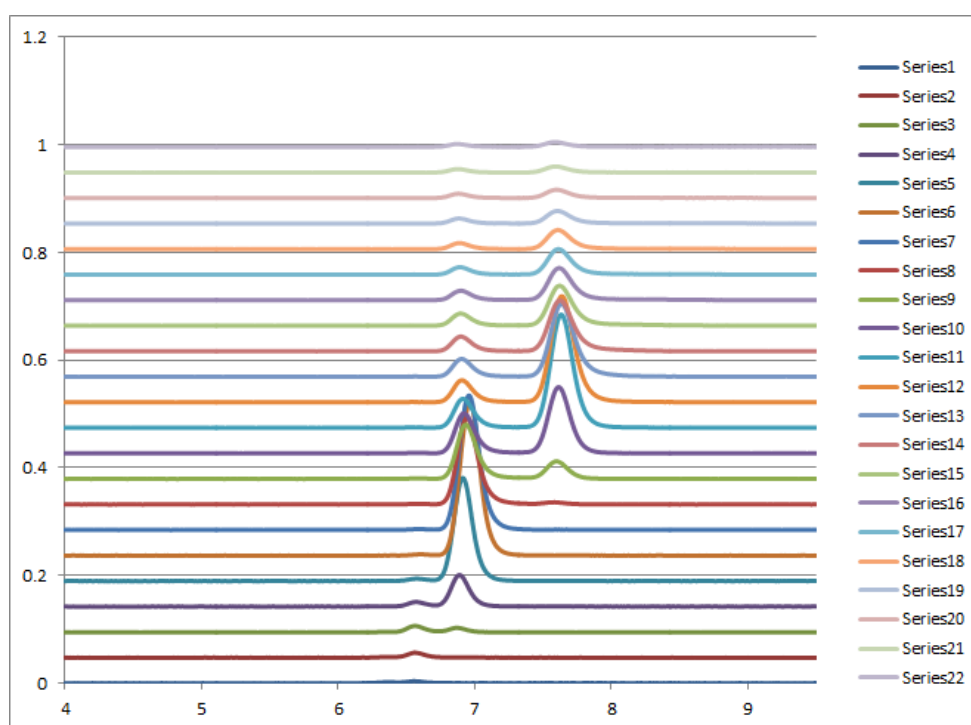
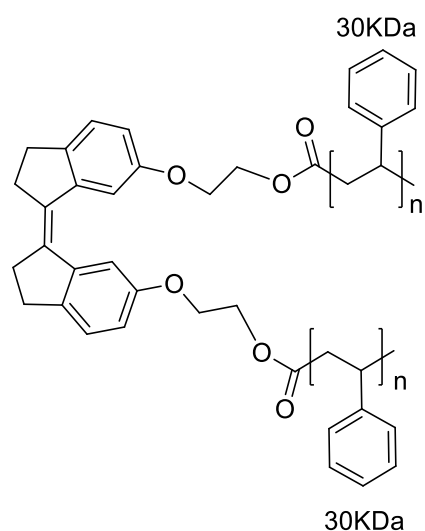


Figure 28: Chromatograms of each vial (labelled as "Series") contents after the first separation with prep GPC. Vials 5-8 contain the isolated product, vials 9-15 will be combined and will undergo another prep GPC separation.

'vial'	3	3	4	5	5	6	6	7	7	8	9
'peak rettime'	6.369967	6.553288	6.558287	6.56162	6.869931	6.57162	6.888263	6.57162	6.911595	6.963258	6.956592
'peak intensity @260 nm'	0.001831	0.003536	0.009154	0.011719	0.008178	0.008426	0.05849	0.004301	0.191253	0.28437	0.249393
Amount Desired Peak					0.411006		0.874075		0.978006		
'overlaps on left?'	0	1	0	0	1	0	1	0	0	0	0
'overlaps on right?'	1	0	0	1	0	1	0	0	0	0	0
'Mp (Da)'	110200	93900	93500	93300	71400	92500	70300	92500	68900	65900	66300
'DMp'	3200	2700	2700	2700	2100	2700	2100	2700	2000	1900	1900
'SS molec. per chain at peak max'	0.937085	0.901071	0.590065	0.309599	0.552857	0.620623	0.750374	0.55276	0.735538	0.711301	0.727873
'error'	0.045313	0.02657	0.017222	0.009131	0.01656	0.018359	0.022464	0.016684	0.02141	0.020568	0.020918
'E/Z ratio at peak max'	0.442686	1	1	1	1	1	1	1	1	1	1
'error'	0.017112	0.00922	0.005987	0.008042	0.008007	0.006785	0.002777	0.01085	0.003041	0.003108	0.003037
vial	5	6	6	7	7	8	8	9	9	10	11
peak rettime	6.348302	6.351635	6.664946	6.359968	6.676612	6.368301	6.691611	6.373301	6.708276	6.724942	6.728275
peak intensity @260 nm	0.002986	0.006926	0.002154	0.009631	0.019271	0.009332	0.082732	0.00608	0.188525	0.257796	0.234458
Amount Desired Peak					0.666767		0.898637		0.968758		
overlaps on left?	0	0	0	0	1	0	1	0	0	0	0
overlaps on right?	0	0	0	1	0	1	0	0	0	0	0
'Mp (Da)'	112300	112000	85300	111200	84400	110400	83300	109900	82200	81000	80700
'DMp'	3300	3300	2500	3200	2500	3200	2400	3200	2400	2400	2400
'SS molec. per chain at peak max'	0	0	0	0.624287	0.91772	0.962598	0.928833	0	0.891398	0.882273	0.885642
'error'	0	0	0	0.088131	0.027248	0.028215	0.026818	0	0.026088	0.026204	0.026401
'E/Z ratio at peak max'	0	0	0	0.977982	1	0.999999	1	0	1	1	1
'error'	0	0	0	0.135163	0.002886	0.006158	0.002647	0	0.002844	0.002896	0.002892
vial	3	4	4	5	5	6	6	7	7	8	9
peak rettime	6.338303	6.354969	6.656613	6.361635	6.674945	6.364968	6.689944	6.363301	6.709943	6.723275	6.723275
peak intensity @260 nm	0.003325	0.007336	0.00245	0.009804	0.022209	0.008628	0.091215	0.005619	0.20483	0.25492	0.221233
Amount Desired Peak					0.693747		0.913587		0.973299		
overlaps on left?	0	0	0	0	1	0	1	0	0	0	0
overlaps on right?	0	0	0	1	0	1	0	0	0	0	0
'Mp (Da)'	113300	111700	85900	111000	84600	110700	83500	110900	82000	81100	81100
'DMp'	3300	3300	2500	3200	2500	3200	2400	3200	2400	2400	2400
'SS molec. per chain at peak max'	0	0	0	0.631984	0.90287	0.750259	0.890983	0	0.87789	0.879549	0.882717
'error'	0	0	0	0.018383	0.02674	0.021909	0.025674	0	0.02576	0.026095	0.026188
'E/Z ratio at peak max'	0	0	0	0.999999	1	0.999999	1	0	1	1	1
'error'	0	0	0	0.005478	0.002777	0.005852	0.002893	0	0.002955	0.002973	0.002964
vial		4	4	5	5	6	6	7	7	8	
peak rettime		6.3549685	6.6566133	6.3599682	6.6766119	6.3599682	6.6916108	6.3633013	6.7082763	6.713276	
peak intensity @260 nm		0.0072835	0.0044683	0.0080734	0.0343639	0.0062517	0.1160579	0.0040131	0.1939417	0.197651	
Amount Desired Peak					0.8097563		0.9488864		0.9797273		
overlaps on left?		0	0	0	1	0	0	0	0	0	0
overlaps on right?		0	0	1	0	0	0	0	0	0	0
'Mp (Da)'		111700	85900	111200	84400	111200	83300	110900	82200	81800	
'DMp'		3300	2500	3200	2500	3200	2400	3200	2400	2400	
'SS molec. per chain at peak max'		0.00	1.05	0.71	0.90	0.00	0.89	0.00	0.89	0.88	
'error'		0	0.0308292	0.0207478	0.0267351	0	0.0257414	0	0.0259459	0.02601	
'E/Z ratio at peak max'		0	0.9999988	0.9999992	0.9999999	0	1	0	1	1	
'error'		0	0.0043468	0.0063716	0.0029495	0	0.0029257	0	0.0029568	0.00298	

Figure 29: Output from the Matlab script which shows a complete analysis of all the vials eluted after prepGPC. The vials highlighted in green are the ones containing the pure isolated desired product. Due to the high amount of reaction mixture, each separation required more than one injection (the maximum amount tolerated by the instrument is 0.5ml injection with a 100mg/ml maximum concentration).



Polymer: (Z)-((2,2',3,3'-tetrahydro-[1,1'-biindenylidene]-6,6'-diyl)bis(oxy))bis(ethane-2,1-diyl) bis(3-phenylbutanoate).

A stock solution of SS5 was made using 25mg (0.052 mmol) of SS-Probe in 2 ml of dry DMF (26 mM). In a 2 mL vial in the glovebox mixed Polystyrene monocarboxy terminated (0.15 g, 5.00 μmol), (Z)-6,6'-bis(2-bromoethoxy)-2,2',3,3'-tetrahydro-1,1'-biindenylidene (0.087 ml, 2.273 μmol) and potassium carbonate (1.571 mg, 0.011 mmol) in DMF (so that the total volume of the reaction mixture is 200 μL). Took the vial out of the glovebox and left to stir overnight at room temperature. The reaction mixture was diluted in THF (to reach a $\sim 1\text{mg/mL}$ concentration), 1.5ml were taken from the solution, passed through a 45 μm syringe filter and analyzed by SEC. Afterwards THF was evaporated and the sample dissolved in 1.5mL of EtOAc, concentration of 100mg/mL, for prepGPC (3 injections of 0.5 mL each). Only some vials contained the pure product, therefore another separation was necessary, running again through prepGPC the combined vials containing a mixture. Combined vials (100% pure) afforded 29mg of product ready for sonication.

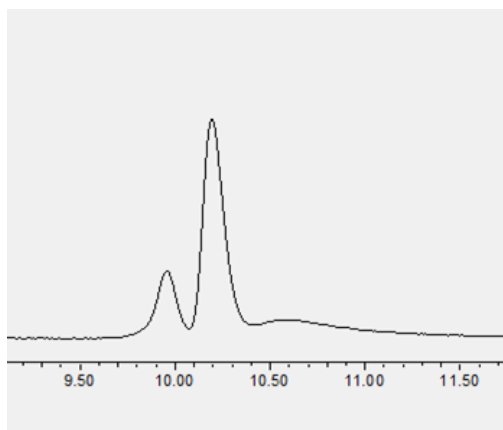


Figure 30: SEC of reaction mixture. The first peak contains the desired product, the second peak is unreacted starting polystyrene.

vial	5	6	6	7	7	8	9	10
peak retime	6.816602	6.823268	7.141578	6.821601	7.161577	7.184908	7.206573	7.209907
peak intensity @260 nm	0.002336	0.004326	0.014743	0.0047	0.092997	0.263942	0.377669	0.380664
IA								
Amount desired peak			0.773136		0.951893			
overlaps on left?	0	0	0	0	0	0	0	0
overlaps on right?	0	0	0	0	0	0	0	0
Mp (Da)	74800	74400	56400	74500	55400	54300	53300	53100
DMP	2200	2200	1600	2200	1600	1600	1600	1500
SS molec. per chain at peak max	0	1.134055	1.067399	1.337735	1.027639	1.021577	1.016324	1.015921
error	0	0.10651	0.030346	0.039742	0.029757	0.030182	0.030589	0.028784
E/Z ratio at peak max	0	0.973573	1	0.999999	1	1	1	1
error	0	0.086786	0.002621	0.004563	0.002934	0.003025	0.003057	0.003062

1st injection

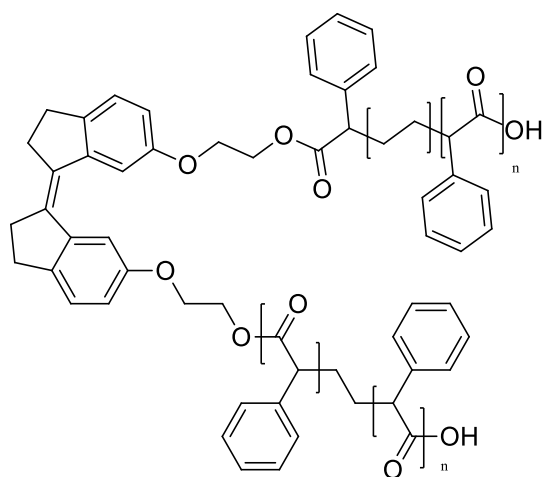
vial	4	5	5	6	6	7	8	9
peak retime	6.784937	6.818268	7.126579	6.833267	7.153244	7.176576	7.199907	7.206573
peak intensity @260 nm	0.001418	0.003491	0.005028	0.004678	0.055818	0.214973	0.362304	0.385632
Amount desired peak			0.590223		0.922671			
overlaps on left?	0	0	0	0	1	0	0	0
overlaps on right?	0	0	0	1	0	0	0	0
Mp (Da)	76900	74700	57200	73800	55800	54700	53600	53300
DMP	2200	2200	1700	2200	1600	1600	1600	1600
SS molec. per chain at peak max	0	1.443856	1.169765	1.041212	1.014658	1.024933	1.019081	1.019356
error	0	0.043015	0.034887	0.031371	0.029172	0.030061	0.030501	0.030681
E/Z ratio at peak max	0	0.999999	0.999999	0.999999	1	1	1	1
error	0	0.006301	0.003476	0.006154	0.002946	0.003016	0.003059	0.003073

2nd injection

vial	4	4	5	5	6	6	7	8
peak retime	6.799936	7.109914	6.808269	7.136579	6.814935	7.15991	7.181575	7.193241
peak intensity @260 nm	0.003278	0.00404	0.004624	0.041002	0.004276	0.171476	0.341962	0.392369
Amount desired compound		0.55203		0.898661		0.975671		
overlaps on left?	0	0	0	1	0	0	0	0
overlaps on right?	0	0	1	0	0	0	0	0
Mp (Da)	75900	58000	75400	56700	74900	55500	54500	53900
DMP	2200	1700	2200	1700	2200	1600	1600	1600
SS molec. per chain at peak r	1.239399	1.059857	1.061346	1.024869	1.117198	1.037436	1.030425	1.029739
error	0.036262	0.031198	0.031221	0.030808	0.033081	0.02999	0.030335	0.030651
E/Z ratio at peak max	0.999999	0.999999	0.999999	1	0.994016	1	1	1
error	0.005598	0.003808	0.005264	0.00304	0.005271	0.002998	0.003064	0.003077

3rd injection

Figure 31: Output from the Matlab script which shows a complete analysis of all the vials eluted after prepGPC. The vials highlighted in green are the ones containing the pure isolated desired product. Due to the high amount of reaction mixture, each separation required more than one injection (the maximum amount tolerated by the instrument is 0.5ml injection with a 100mg/ml maximum concentration).



Control polymer. A stock solution of SS5 was made using 25mg (0.052 mmol) of SS-Probe in 2 ml of dry DMF (26 mM). In a 2 mL vial in the glovebox mixed COOH-PSt-COOH, 25 kDa (390 mg, 0.016 mmol), 0.06ml of SS stock solution and potassium carbonate (3.23 mg, 0.023 mmol) in DMF. Took the vial out of the glovebox and left to stir overnight at room temperature.

The reaction mixture was diluted in THF (to reach a ~1mg/mL concentration), 1.5ml were taken from the solution, passed through a 45um syringe filter and analyzed by SEC. Afterwards THF was evaporated and the sample dissolved in 1.5mL of EtOAc, concentration of 100mg/mL, for prepGPC (3 injections of 0.5 mL each).

1st prepGPC analysis shows that there is no pure material available, but it's still mixed with other subproducts, therefore another separation was required.

References

- ¹ Vijayalakshmi, S. P.; Madras, G. *Polym. Degrad. Stab.* **2005**, 90, 116-122.
- ² Vijayalakshmi, S. P.; Madras, G. *Polym. Degrad. Stab.* **2004**, 84.2, 341-344.
- ³ Boulatov, R.; Kucharski, T. J. *J. Mater. Chem.* **2011**, 21, 8237.
- ⁴ Yang, Q. Z.; Huang, Z.; Kucharski, T. J.; Khvostichenko, D.; Chen, J.; Boulatov, R. *Nat. Nanotechnol.* **2009**, 4, 302.
- ⁵ Akbulatov, S.; Tian, Y.; Kapustin, E.; Boulatov, R. *Angew. Chem., Intl. Ed.* **2013**, 52, 6992.
- ⁶ Tian, Y.; Kucharski, T.J.; Yang, Q.Z.; Boulatov, R. *Nat Commun.*, **2013**, 4, 2538
- ⁷ Xu, J. F.; Chen, Y. Z.; Wu, D.; Wu, L. Z.; Tung, C. H.; Yang, Q. Z. *Angew. Chem., Intl. Ed.* **2013**, 52(37), 9738-9742.
- ⁸ McMurry, E.J.; Fleming, M.P. *J. Am. Chem. Soc.*, **1974**, 96 (14): 4708–4709.
- ⁹ Akbulatov, S.; Tian, Y.; Kapustin, E.; Boulatov, R. *Angew. Chem. Intl. Ed.* **2013**, 52, 6992
- ¹⁰ Waldeck, D. H. *Chem. Rev.* **1991**, 91, 415-436.
- ¹¹ Hiemenz C.P.; Lodge P.T. *Polym. Chem.* **2007**, 336, 338–339.

CHAPTER IV. Synthesis of topologically complex polymers with an H-shape

Abstract

Polymer architecture and the corresponding topologies are important considerations during the ultrasonic degradation of polymers. So far, only linear polymers have been sonicated in this project. Structurally more complex polymers, such as four-arm star and H-shaped mechanophore-containing polymers will be synthesised and sonicated in order to determine the effect that polymer topology has on the rate of chain scission and mechanophore activation, and the location of fragmentation. Suitable molecules for such challenge were polymers linked to an Anthracene-Maleimide core generated by Diels Alder reaction, displaying an “H” shape.

Introduction

Although synthesis of H-polymers has been reported in the literature, an investigation about the distribution of forces along such a complex polymer structure under load has not been carried out yet. The first H-shaped polymer was synthesized from styrene by Roovers and Toporowski¹ using anionic polymerization. Two molecules of poly(styryllithium) were reacted with one molecule of methyltrichlorosilane, and the resulting moiety was then condensed with difunctional poly(styryllithium). Since then, many studies have been conducted on H-polymers, aiming to understand their dynamics, rheology, and neutron-scattering properties² up to the design of self-healing materials³.

In order to follow the chain scission along the polymer chains, the presence of a “molecular probe” is essential. This is a moiety which is activated by force and its change under load is easy to follow. Boydston and co-workers revisited the mechanochemical chain scission of star-shaped polymers under sonication using a fluorogenic “turn-on” mechanophore. They synthesized moieties with polymers linked to the core by an anthracene-maleimide Diels–Alder adduct. Upon cycloreversion by mechanical force, it produces an anthracene moiety which displays

strong UV–Vis and photoluminescence signals. This mechanophore was also synthesized and studied by Bielawski and co-workers⁴. In comparison with the project described in Chapter III, the goal of this section is more challenging. In fact, we predict that several different species will be generated during the sonication of “H” shaped polymers compared to their linear analogues, and more complex kinetic schemes will be developed to allow analysis of the data obtained from sonication. The generalised scheme (**Figure 32**) shows how the ultrasonic degradation of three- and four-arm star polymers differs from that of linear polymers. Scission is generally accepted to occur through arm loss, after which individual arms degrade as in the linear case. In each case, the rate of degradation for the star polymer was found to correspond to the spanning molecular weight (M_{span})⁵, or roughly the molecular weight of two arms. This can result in the rather odd effect of the rate of degradation increasing with sonication time, as numerous polymer chains with molecular weight roughly equal to the spanning molecular weight of the parent star polymer being produced by scission⁶.

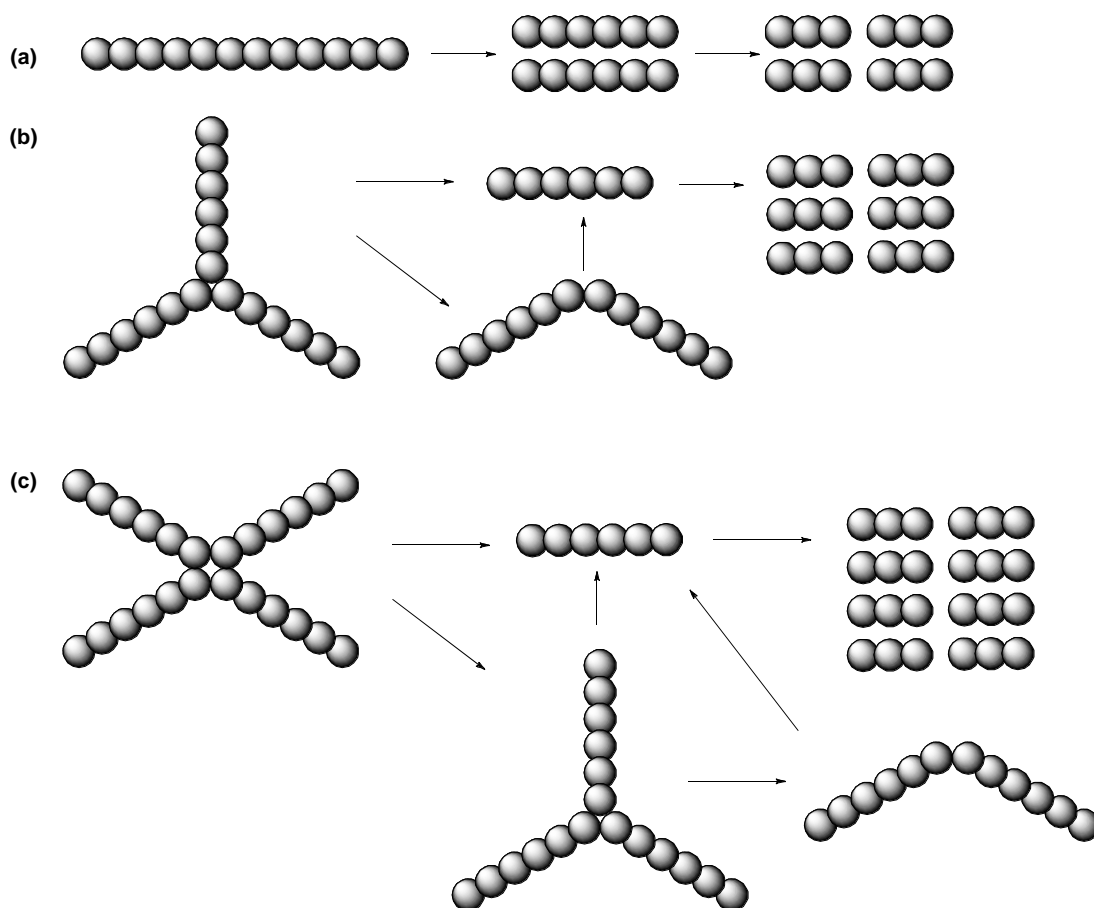


Figure 32: A simplified representation of how (a) linear, (b) three-arm star, and (c) four-arm star polymers undergo chain scission under ultrasonic irradiation. Purely midchain scission/arm loss is assumed for ease of illustration. Adapted from Peterson and Boydston paper. Rate constants for each step are not shown, but are assumed to be directly proportional to the spanning length, M_{span} .

The mechanically induced effect (**Figure 33(a)**) is a reverse Diels-Alder reaction, which produces anthracene and maleimide, the former of which is a chromophore (extinction coefficients in EtOAc are given in **Figure 33(b)**). Therefore, it is possible to calculate the extent to which this reaction has occurred in polymers of different molar masses. It is important to note that in contrast to the reaction of stiff stilbene under mechanical force, which is non-scissile, the mechanophore fragments will give two daughter chains – *i.e.* this is a scissile reaction.

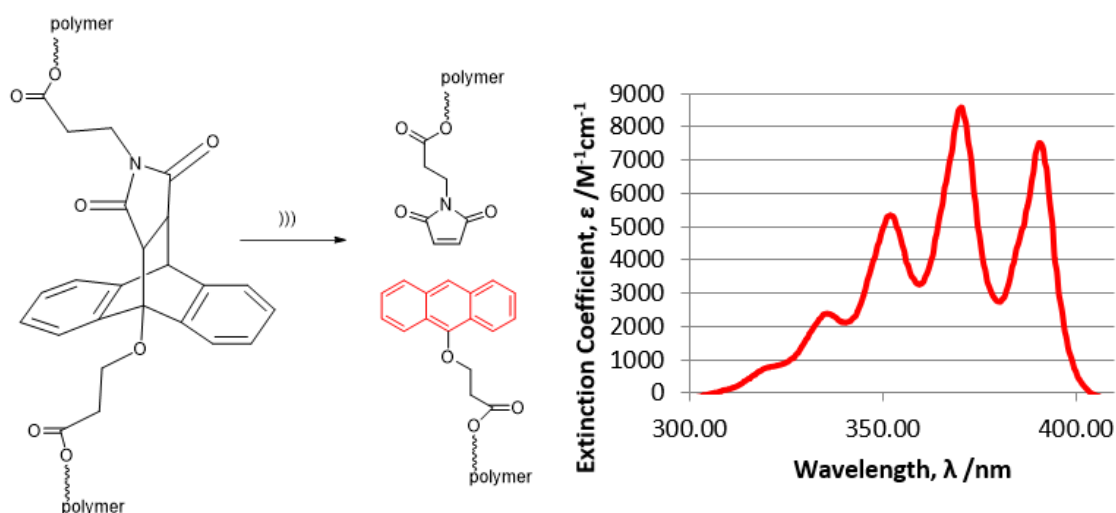
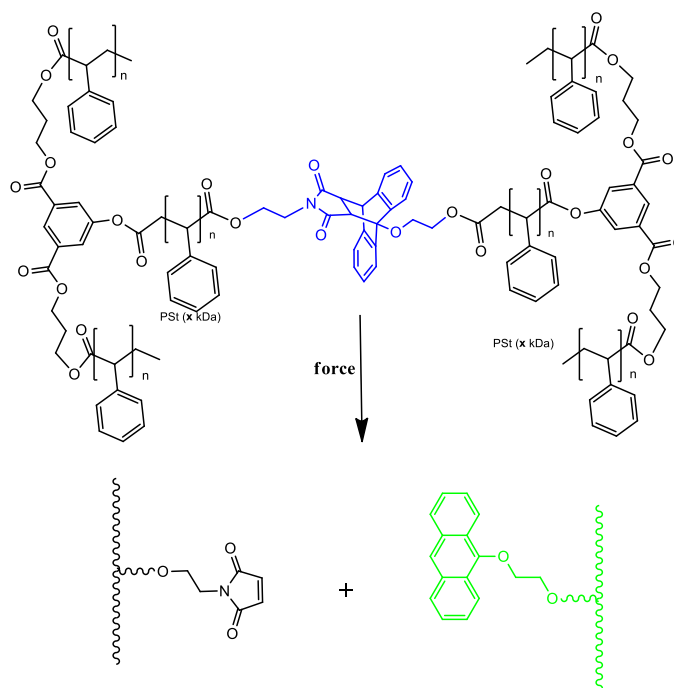


Figure 33: (a) The reverse Diels-Alder reaction which occurs in the mechanophore upon stretching with the chromophore produced, anthracene (Ant) highlighted, and (b) the extinction coefficients of the chromophore species above 300 nm wavelength recorded in anhydrous THF.

An anthracene-maleimide Diels–Alder adduct (AntrMal) attached to polymer chains displays strong UV–Vis and photoluminescence signals when subjected to ultrasonic irradiation due to formation of an anthracene molecule (**Scheme 11**). So, it’s possible to quantify the anthracene produced using its photoluminescence intensity at 411nm and therefore define the chain’s scission rate.



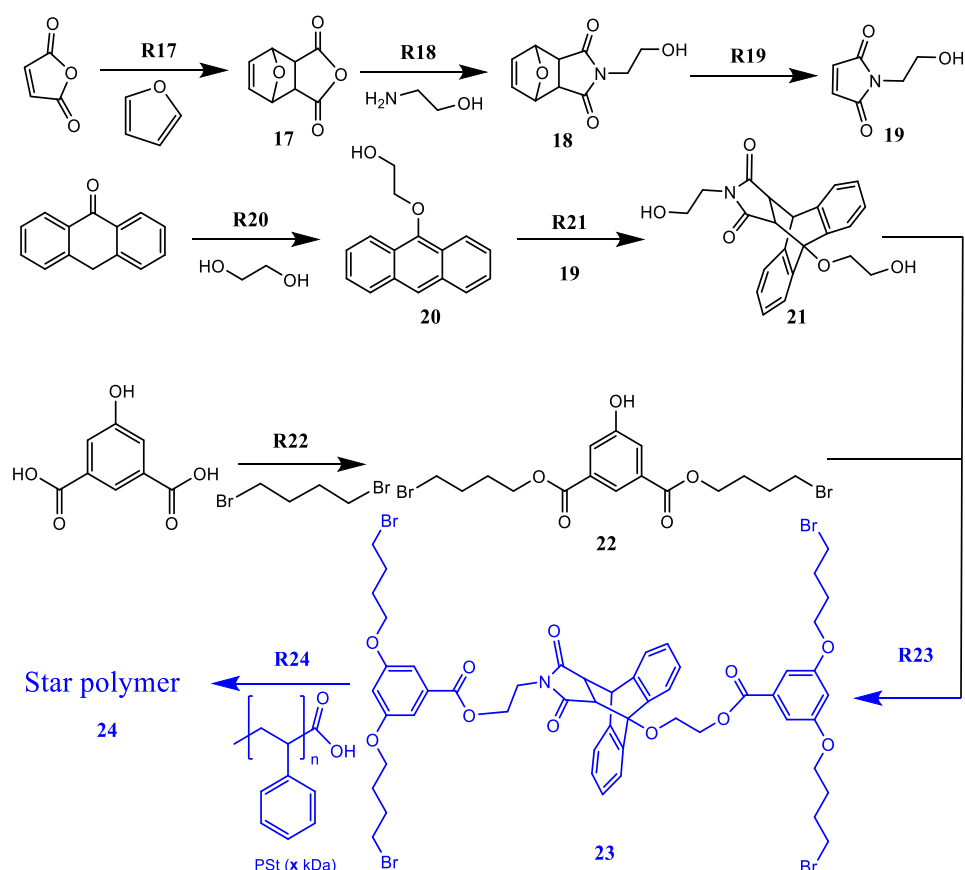
Scheme 11 H-polymer containing AntrMal as a mechanophore (in blue) undergoes a cycloreversion reaction on the core that produces an anthracene molecule (green) which displays a strong UV signal at 411 nm.

AntrMal structure is ideal to be included in “star” and “H” shaped polymers⁷. Despite topological complex polymers having been studied in the last 50 years⁸, there are no previous records of this AntrMal core attached to polystyrene chains in such a unique H-shaped moiety we designed (**Scheme 11**). So, this investigation is necessary given the lack of knowledge about the response of such multi-arm polymers under force (*i.e.* do the polymers arms arrange to prevent force accumulation on the core? Do they undergo chain scission at different times?).

Result and discussion

Molecular design

A molecule of anthracenone was initially functionalized with ethylene glycol with an alkylation of the anthracenone’s anion using sulfuric acid as a catalyst and removing the water by-product. Commercial anthracen-9-ylmethanol could be used but it can present some issues for further functionalization in the next steps due to the lack of reactivity of neopentyl carbon.



Scheme 12 Synthetic scheme to prepare an AntrMal molecule core suitable for a Star polymer design. In blue reactions and molecules just planned, not done yet.

The other molecule necessary to undergo the Diels Alder reaction was prepared starting from commercial furan and furan-2,5-dione. To create a linker on top of this molecule (and allow the structure of a H-polymer) a nucleophilic acyl substitution was performed between the acid anhydride and a commercial hydroxylamine. Afterwards, the product was heated and a retro-diels Alder reaction afforded the compound 19, ready for R21⁹.

Synthesis of a linker which connected the AntrMal core to further four polystyrene chains was challenging due to the last deprotection step, which compromised the Br groups. The connection of a linker to the AntrMal core is necessary to create a “Star” polymer shape. In case of a “H” polymer shape, the AntrMal core will be connected first to two polystyrene chains dicarboxy terminated, to allow the connection of this linker not directly onto the ANtrMal core but on the polystyrene chains, to have a much longer X axis (difference between the designs is shown in the Figure below).

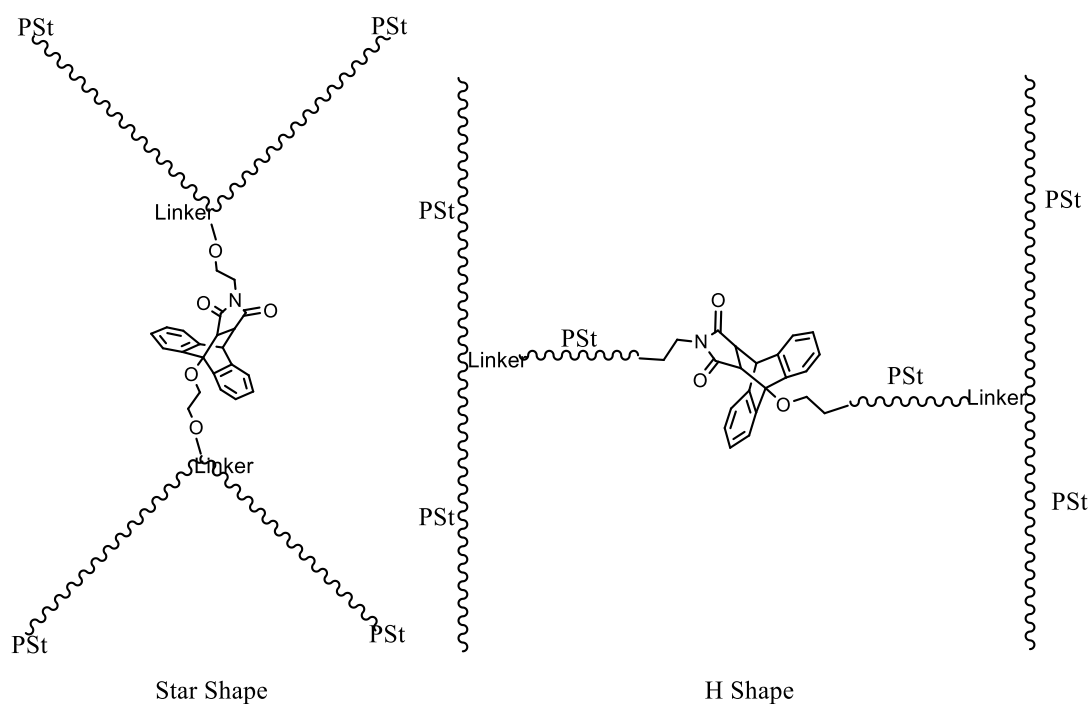
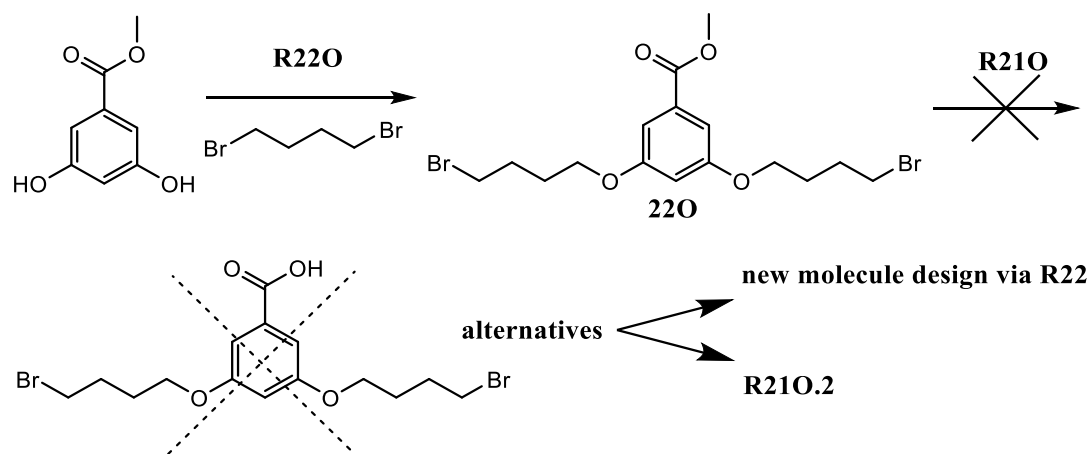


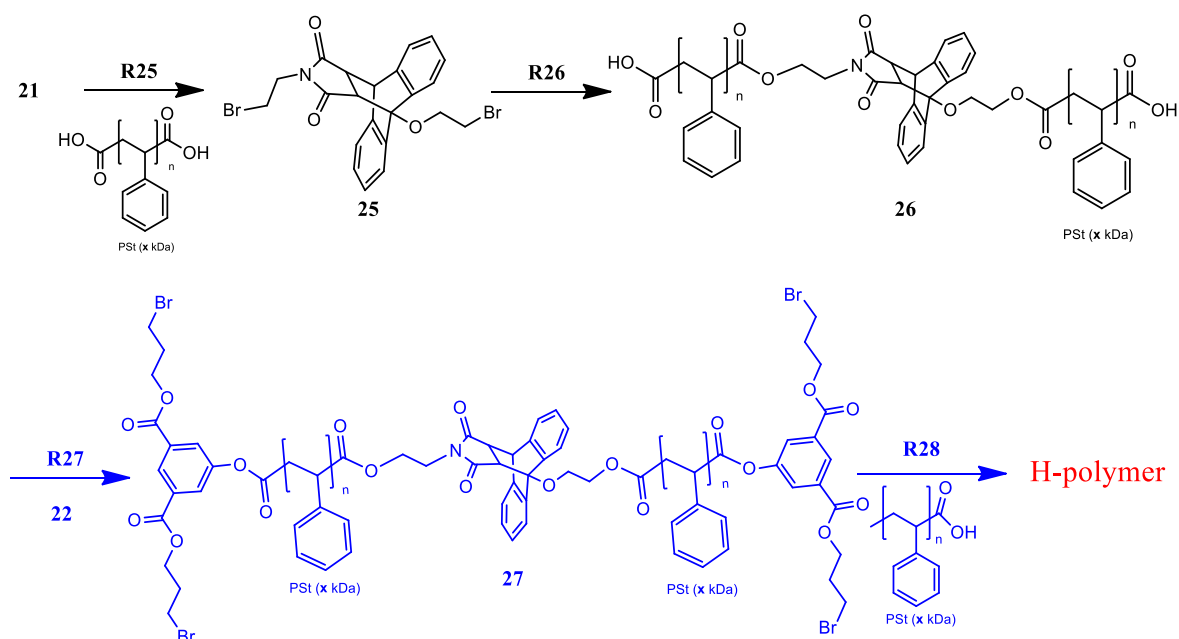
Figure 14: Difference between the Star and H polymer molecules.

The original plan (Scheme 7) was therefore replaced by two alternative routes.



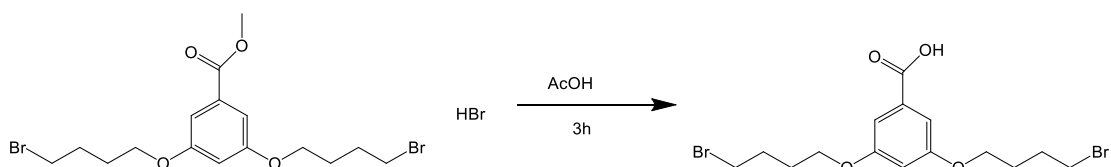
Scheme 13 Original synthesis of a linker suitable to connect AntrMal core to four polystyrene chains. **R210** didn't produce the desired molecule, therefore two alternative pathways were pursued.

Both NaOH and HCl in high concentrated solution were used (**R210**) to remove the methyl ester and obtain the free acid. The de-protection was achieved in both cases, but Br atoms were also displaced by OH or Cl atoms. To fix this issue, the hydrolysis could be performed on **220** using HBr or a different molecule (**22**) can be used with the same function, as shown in **Scheme 13**.



Scheme 14 Synthetic scheme to prepare an AntrMal molecule core suitable for an H polymer design. In blue, reactions and molecules just planned, not done yet.

Thanks to my group's colleague, it was possible to find a successful reaction to achieve the target molecule via the reaction R210.2 (see Scheme below).



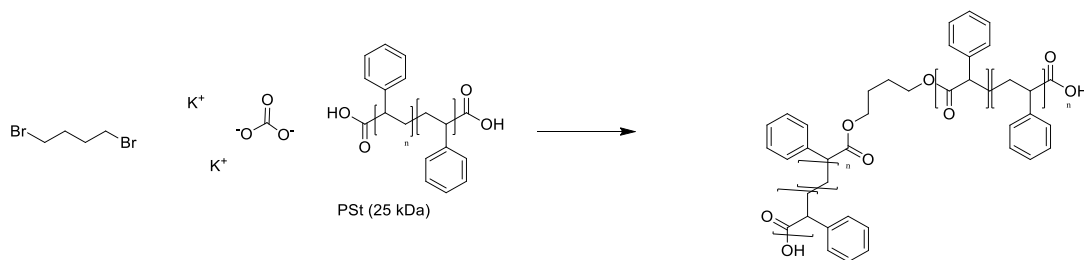
Scheme 15: Revised hydrolysis reaction to create the linker between the AntrMal core and the polystyrene chains.

In this case, the hydrolysis of the methyl protective group was run in a buffer of HBr to prevent the alteration of the terminal Br groups on the starting material.

Connecting the core to polystyrene chains

To test the reaction between a polystyrene with two terminal carboxylic acid, I initially used a commercial molecule. The pattern of separation after the first prepGPC run was compared to the pattern generated after separation using polystyrene and AntrMal core. The consistency between them confirmed the

successful procedure and the reaction was scaled up to obtain enough material for sonication.



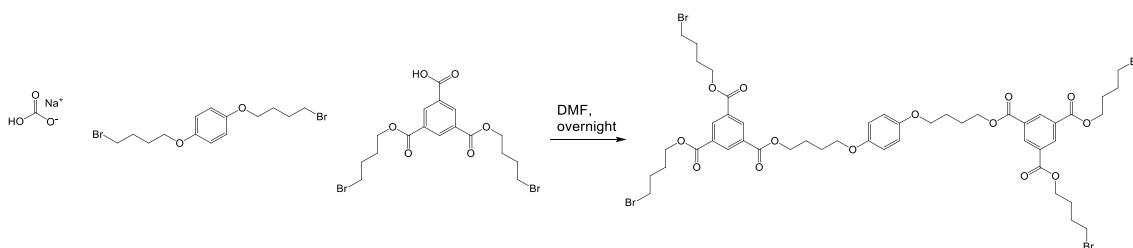
Scheme 16: Test performed to check the products separation pattern with prepGPC

To separate the required amount of AntrMal core connected with the two polystyrene dicarboxy terminated chains, it was necessary to perform preparative GPC twice (with six injections per separation). As shown in the Figure below, the average Mp of the polymer was 58KDa.

vial	9	9	9	10	10	11	11	12	12	12	13	13	13	14			
peak rettime	6.423297	6.698277	7.084916	6.704943	7.113247	6.691611	7.12158	6.689944	7.114913	7.739868	6.688278	7.109914	7.778199	7.104914			
peak intensity @260 nm	0.001959	0.024964	0.078932	0.014242	0.174032	0.009468	0.1593	0.006561	0.097806	0.012781	0.004098	0.0612	0.12268	0.041392			
overlaps on left?	0	0	1	0	1	0	1	0	1	1	1	0	1	0			
overlaps on right?	0	1	0	1	0	1	0	1	1	0	0	1	0	0			
Mp (Da)	105200	82900	59300	82400	57800	83300	57400	83500	57700	32600	83600	58000	31400	58300			
DMp	3100	2400	1700	2400	1700	2400	1700	2400	1700	900	2400	1700	900	1700			
SS molec. per chain at peak	0	0	0.182568	0	0.111258	0	0.112468	0	0.141524	0.757303	0	0.156125	0.142177	0.116812			
error	0	0	0.005412	0	0.003402	0	0.00346	0	0.004318	0.02155	0	0.004736	0.004192	0.007257			
E/Z ratio at peak max	0	0	1	0	1	0	1	0	1	1	0	1	1	0.887702			
error	0	0	0.01066	0	0.011832	0	0.011757	0	0.011228	0.009648	0	0.011049	0.009781	0.048693			
			Goal product														
			starting material														
	14	15	15	16	16	17	17	18	18	19	19	20	20	21	21	22	22
7.826529	7.108247	7.853193	7.114913	7.848194	7.101581	7.836528	7.11158	7.829862	7.096581	7.828195	7.098248	7.828195	7.089915	7.828195	7.099915	7.824862	
0.388761	0.02919	0.4537	0.019564	0.357308	0.010922	0.24699	0.006131	0.176248	0.004232	0.132574	0.003137	0.091119	0.002402	0.054808	0.001861	0.033587	
0	0	0	0	0	0	0	0	0	0	0	0	0	0	0	0	0	
0	0	0	0	0	0	0	0	0	0	0	0	0	0	0	0	1	
30000	58100	29200	57700	29300	58400	29700	57900	29900	58700	29900	58600	29900	59000	29900	58500	30000	
900	1700	800	1700	900	1700	900	1700	900	1700	900	1700	900	1700	900	1700	900	
0.061656	0	0.052423	0	0.058408	0	0.074122	0	0.092465	0	0.104134	0	0.123393	0	0.151766	0	0.169114	
0.00191	0	0.001496	0	0.00185	0	0.002311	0	0.002861	0	0.00322	0	0.003817	0	0.004689	0	0.005209	
0.999999	0	0.999999	0	0.999999	0	0.999999	0	0.999955	0	0.999999	0	1	0	1	0	1	
0.010886	0	0.011295	0	0.010931	0	0.010336	0	0.010122	0	0.009997	0	0.01007	0	0.00986	0	0.009851	

Figure35: Set of vials isolated after a prepGPC run on the reaction mixture. In yellow are highlighted the vials containing the desired product while in green the ones containing only starting material.

To test the synthesis of Star-polymers, I first performed the reaction on similar molecules less valuable and readily available. The final step of this test is shown in the Scheme below, and the successful synthesis of the model compounds is supported by the assigned H-NMR shown in **Figure 36**.



Scheme 17: preliminary reaction run using another linker and core molecules.

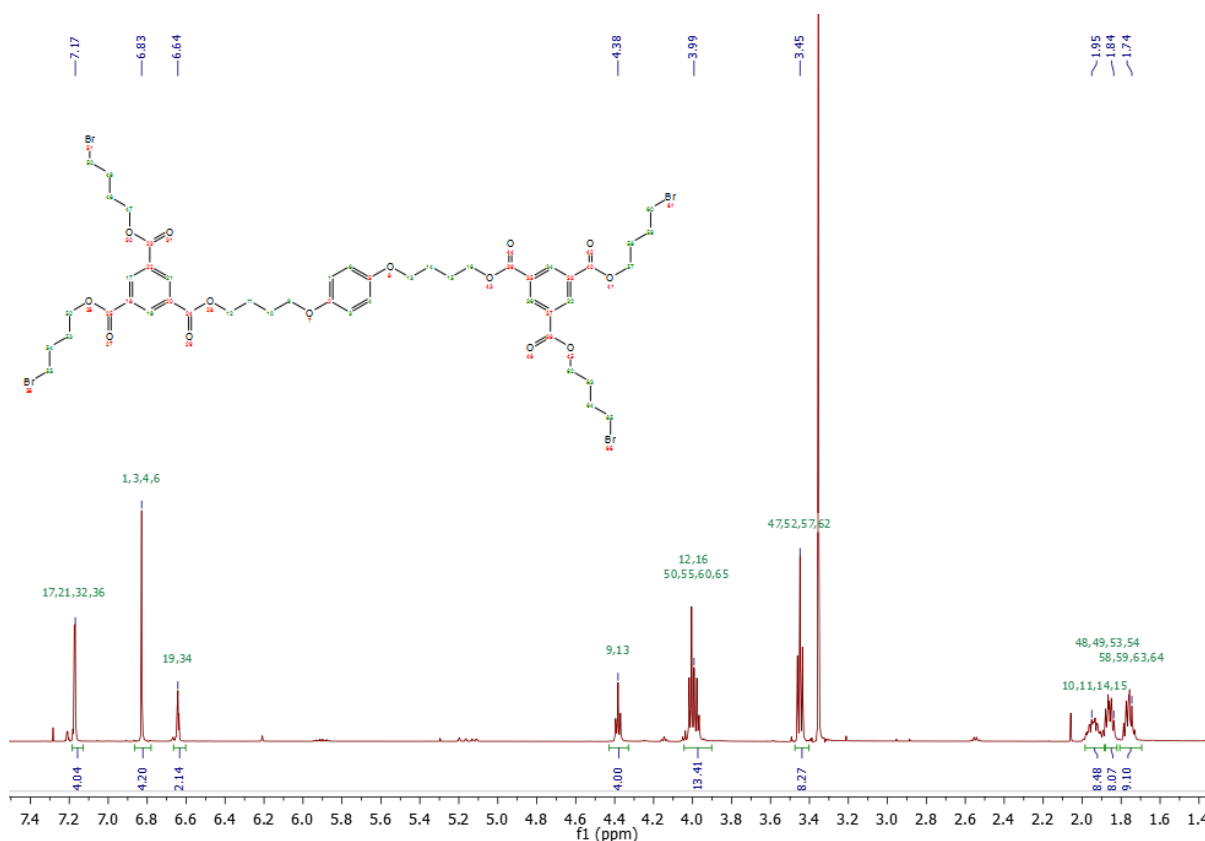


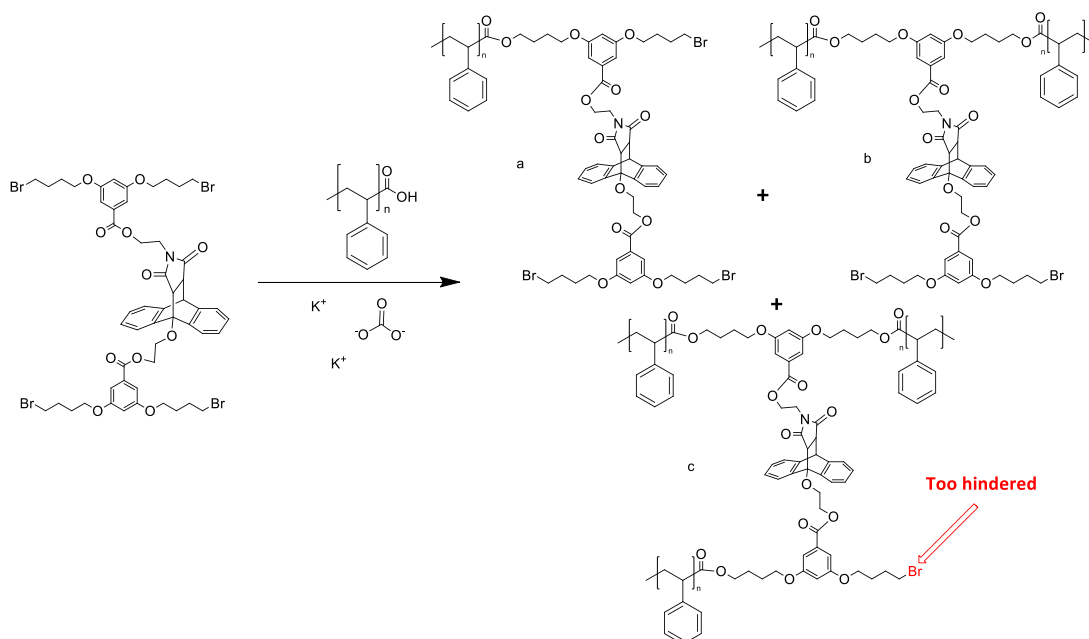
Figure 36: H-NMR of the isolated model compound prepared using commercial material before the synthesis of the H-shape core with the more valuable Diels-Alder adduct.

Conclusions and future work

In conclusion, I've successfully completed the synthesis of a mechanophore core (AntrMal) connected to two polystyrene chains. This will enable subsequent studies on the material which would lead to further understanding on how stresses are distributed on polymers with this or similar structure. Moreover, the synthesis and methods I used for this project would be helpful in future research when performing the same synthesis or when yielding similar moieties with a mechanophore in the centre connected to polymers. The pattern of side products generated during the

polystyrene attachment to the Anthracene-Maleimide DA adduct and their retention times during the isolation of the goal product during prepGPC are useful when synthesizing the same products faster in future work.

Despite the synthesis of the H-polymer requiring an extra step compared to the Star-polymer synthetic route as shown in the previous Schemes, the mechanophore is the same for both polymers. Furthermore, the reaction to connect the polystyrene chains to the core uses the same procedure. Therefore, the two synthesis can be run in parallel in order to have a further control and give insight on the outcome and issues of such synthesis. While I was working to the connection and subsequent isolation of the AntrMal core to the two polystyrene chains, my colleague was attempting the synthesis of a Star-shape polymer. The same mechanophore was used for that synthesis but the "four arms of the star " (polystyrene chains) could be connected to the core just after creating a dual reactive site on both end of the AntrMal (attaching two molecules **22**). After several synthetic attempts run under different conditions, prepGPC always showed the formation of AntrMal core connected to a maximum of three polystyrene chains (in the side products were present also moieties with only two or even one polystyrene chain connected to the mechanophore), but never linked to the aimed four chains in order to create the arms of the star (shown in **Scheme 1**).



Scheme 1: Last step to obtain a "Star"-shape polymer. The products obtained were a) mono-substituted, b) di-substituted and c) tri-substituted starting material. Despite several attempts, a "full Star" with four polystyrene connected was never yielded. We assumed that the connection of three polystyrene chains, the last Br atom is too hindered and not easily accessible.

This trend was caused by the generation of a bulky environment due to the presence of a large excess of polymer compared to the small reactive mechanophore (the minimum ratio was 4:1 and several different ratios were tried to achieve the final product). Therefore, at some point the mechanophore was too hindered by the presence of three polymer chains connected to it and the attachment of the last fourth chain was not possible.

Due to this issue encountered on the Star-shape polymer synthesis and with the possibility of a similar scenario manifesting with the H-shape polymer, further work is required to allow four polystyrene chains to react within a very small environment. This is a challenging goal due to the nature of polymer chains which keep twisting and coiling in solution, their terminal -COOH molecule is not readily available to react with the Br groups on the mechanophore. A new design of **22** with more spacing between the Br sites could be a solution to allow the connection of four polystyrene chains.

The aim of future work is therefore to finish the synthesis of both H and Star shaped polymers. This will create a topologically complex moiety which, during sonication,

could experience force in several directions. Once cycloreversion is triggered and anthracene is generated by AntrMal, it would be possible to quantify how much and how fast the force propagates through the polymer chains to the core. Hence, a model for the chains-scission pattern could be made, considering the size of polymer's fragment attached to the anthracene molecules. Understanding how such a complex polystyrene-based model behaves, could be a key factor in synthesis of elastomers, compatibilizers for polymer blends, and oil additives.

Experimental Section

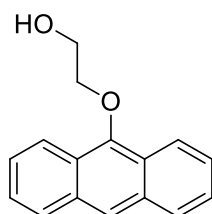
All reactions were performed under argon atmosphere using standard Schlenk techniques unless otherwise noted. All reagents were purchased from Sigma-Aldrich, Fisher Scientific or Fluorochem. DCM was purified using a solvent purification system. Flash chromatography was performed on Silicycle F60 (230-400 mesh) silica gel. Medium pressure liquid chromatography (MPLC) was performed on a Teledyne ISCO CombiFlash RF 200.

Mass spectra were run by operators using Micromass LCT Mass Spectrometer, using Ionization mode: ES^+ , Sample inlet: Syringe Pump, Sample run in MeOH, Sample Cone Voltage: 60 Volts. HPLC and GPC analyses were performed on a Shimadzu Prominence system with LC-20AT solvent delivery unit with integrated FCV-10AL VP quaternary gradient mixer, DGU-20A5 degasser, SPD-M20A photodiode array detector, CBM-20A system controller, SIL-20AHT autosampler with Rheodyne 7725i manual injector, CTO-20A column oven. J.T. Baker Silica Gel column (250 × 4.6 mm, particle size: 5 μm diameter) column was used for analytical HPLC ; Waters Prep Nova-Pak HR Silica column (19 x 300 mm, particle size: 6 μm diameter) was used for semi-preparatory HPLC; a set of three Agilent columns (PLgel 300 × 7.5 mm, 5 μm , 500 Å; PLgel 300 × 7.5 mm, 5 μm , 1,000 Å and PLgel 300 × 7.5 mm, 5 μm , 10,000Å) with a guard (PLgel 50 × 7.5 mm, 10 μm) was used for analytical GPC; a set of two Agilent columns (PLgel 300 × 25 mm, 10 μm , 1,000 Å and PLgel 300 × 25 mm, 10 μm , 10,000Å) with a guard (PLgel 25 × 25 mm, 10 μm) was used for preparatory GPC. Flow rate of THF for analytical GPC: 1 mL/min; for preparatory GPC: 5mL/min. Column heater temperature: 30 oC. SEC analyses were done on a Waters Acquity UPLC system with Acquity UPLC binary solvent manager, Acquity UPLC sample manager, Acquity UPLC column heater, Acquity UPLC PDA detector. A set of two Waters Acquity APC columns (APC XT 450, 150 × 4.6 mm) were used for SEC. Flow rate of THF: 0.6 mL/min. Column heater temperature: 30 oC. All polymers solutions were filtered through PTFE syringe filters (pore size: 0.45 μm) prior GPC/SEC analysis. The GPC and SEC columns were calibrated using narrow polystyrene standards obtained from Sigma-Aldrich and Scientific Polymers Inc.

Ultrasound experiments were performed on a Vibra-Cell VCX 750 liquid processor from Sonics and Materials with an aluminum coupler for two solid probes (part # 630-0562) and two solid probes (tip diameter: 1/2" (13 mm); Length: 53/8" (136 mm); part #630-0219) with stainless steel collars. Three-neck Suslick cells were made by a School of Physical Sciences Workshop (University of Liverpool). The distance between the horn tip and the bottom of the Suslick cell was 10 mm.

High-resolution mass spectrometry (HRMS) was performed on a Micromass LCT TOF Mass Spectrometer at the University of Liverpool Mass Spectrometry Laboratory.

^1H and ^{13}C NMR spectra were referenced to the residual solvent peak ($\text{CDCl}_3\delta=7.26$ (^1H) and 77.16 (^{13}C)) were collected on a Bruker 500MHz spectrometer. NMR spectra were analyzed using Mestrenova software.

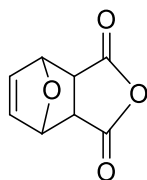


Synthesis of 2-(anthracen-9-yloxy)ethanol¹⁰. Anthracen-9(10H)-one (7 g, 36.0 mmol), ethane-1,2-diol (40.2 ml, 721 mmol) and sulfuric acid (1.921 ml, 36.0 mmol) were added to benzene (100 mL) in a round bottomed flask (0.5 L). Dean-Stark trap. Reflux (115 deg C in the bath).

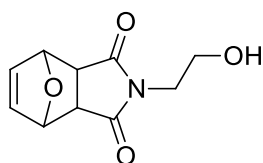
Solvent was evaporated; the residue was treated with water (500 mL) and precipitated yellow solid was collected by filtration and washed with water 500 mL.

Purified this material on CombiFlash: dissolved material in 100 mL of DCM, added 13 g of SiO_2 and evaporated.

80g gold SiO_2 column, second use; solid load; 0->30% EtOAc in DCM, 2nd fraction is my product. Yield: 51%. ^1H NMR (500 MHz, Chloroform-d) δ 8.36 (d, 2H), 8.27 (s, 1H), 8.02 (d, 2H), 7.54 – 7.46 (m, 4H), 4.36 (t, 1H), 4.21 (t, J = 4.4 Hz, 1H). ^{13}C NMR (126 MHz, CDCl_3) δ 150.44, 132.39, 128.51, 125.54, 125.42, 124.57, 122.54, 122.09, 76.52, 62.59.



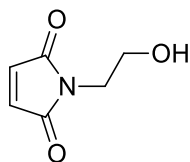
Synthesis of 3a,4,7,7a-tetrahydro-4,7-epoxyisobenzofuran-1,3-dione⁵. Maleic anhydride (19g), toluene(50ml) and furan (13.2g) were added to a dried round bottom flask, equipped with amagnetic stir bar. The solution was heated under reflux for 24 hours, and then allowed to cool toambient temperature. The product precipitated out of solution, and was washed with diethyl ether. The resulting white powder (20.8g) was used without further purification. Yield: 64%. ¹H NMR (500 MHz, Chloroform-d) δ 6.60 (br s, J = 0.9 Hz, 2H), 5.48 (br s, J = 0.8 Hz, 2H), 3.20 (br s, 2H). ¹³C NMR (126 MHz, CDCl₃) δ 169.87, 136.99, 82.22, 48.72.



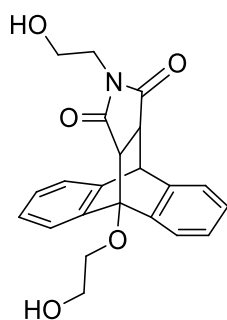
Synthesis of 2-(2-hydroxyethyl)-3a,4,7,7a-tetrahydro-1H-4,7-epoxyisindole-1,3(2H)-dione⁵. 3a,4,7,7a-tetrahydro-4,7-epoxyisobenzofuran-1,3-dione (18.9 g, 114 mmol) was added to a dried round bottom flask, equipped with a magnetic stirred bar, and methanol (0.24 M). The solution was purged with nitrogen for 10 minutes, after which 2-aminoethanol (6.88 ml, 114 mmol) and Et₃N (15.86 ml, 114 mmol) were added. The temperature steadily increased to 70 C for 15h. The flask was cooled to ambient temperature and the product precipitated from solution.

TLC showed a single spot with R_f = 0.4 Eluent conditions 1:2 Hexane:EtOAc

The resultant crop of white crystals (17.7g) were washed with isopropyl alcohol and used without further purification. Yield: 67%. ¹H NMR (500 MHz, Chloroform-d) δ 6.55 (br s, 2H), 5.31 (br s, 2H), 3.80 (t, J = 4.9 Hz, 2H), 3.73 (t, J = 5.0 Hz, 2H), 2.92 (br s, 2H). ¹³C NMR (126 MHz, CDCl₃) δ 176.78, 136.52, 80.99, 60.36, 47.50, 41.80.



Synthesis of 1-(2-hydroxyethyl)-1H-pyrrole-2,5-dione¹¹. A dried round bottom flask, fitted with a refluxcondenser and magnetic stirrer, was charged with toluene and 2-(2-hydroxyethyl)-3a,4,7,7a-tetrahydro-1H-4,7-epoxyisoindole-1,3(2H)-dione (17.7 g, 85 mmol). The reaction was refluxed for 24 hours. The resulting solution was filtered whilst hot, and the product (11.1g) crystallised upon cooling. Yield: 93%. ¹H NMR (500 MHz, Chloroform-d) δ 6.76 (s, 2H), 3.81 (t, J = 3.8 Hz, 2H), 3.75 (t, J = 3.8 Hz, 2H), 2.13 (b,1H). ¹³C NMR (126 MHz, CDCl₃) δ 171.13, 134.24, 60.88, 40.68.



Synthesis of (9R,10R,15R)-9-(2-hydroxyethoxy)-13-(2-hydroxyethyl)-10,11-dihydro-9H-9,10-[3,4]epipyrroloanthracene-12,14(13H,15H)-dione⁵.

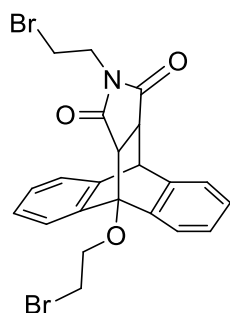
The reagents were mixed in toluene to form dispersion. Upon heating (110 C) it turned into a solution.

In a 100 mL round bottomed flask everything mixed and heated at 110 C overnight under nitrogen. The flask is putted for few hours in the fridge and product crashed out as a sticky yellow material.

TLC of reaction mix (Hex:EtOAc 2:1) shows 3 spot with Rf=0.7 0.3 and 0.1(product)

MPLC was used to separated the species with 80g reg silica column,the eluent system was a gradient of Hex:EtOAc from 0% to 100%.After chromatography the solvent was evaporated affording 5.6g of yellow powder. Yield: 81%. ¹H NMR (500 MHz, DMSO-d₆) δ 7.77 (d, J = 7.3 Hz, 1H), 7.50 (d, J = 7.2 Hz, 1H), 7.45 (d, J = 7.3 Hz, 1H), 7.26 – 7.15 (m, 4H), 7.13 (t, J = 7.3 Hz, 1H), 5.08 (t, J = 5.4 Hz, 1H), 4.71 (d, J = 3.3 Hz, 1H), 4.61 (t, J = 5.9 Hz, 1H), 4.44 (dt, J = 8.5, 4.0 Hz, 1H), 4.14 (dt, J = 8.4, 4.1 Hz, 1H), 4.04 – 3.97 (m, 1H), 3.91 (dt, J = 11.7, 4.5 Hz, 1H), 3.76 (d, J = 8.5 Hz, 1H), 3.40 (dd, J = 8.5,

3.4 Hz, 1H), 3.00 (t, J = 7.5 Hz, 2H), 2.55 (q, J = 7.0, 6.6 Hz, 2H). ¹³C NMR (126 MHz, DMSO) δ 176.51, 174.58, 142.42, 141.27, 141.05, 137.66, 126.86, 126.82, 126.72, 126.45, 124.72, 124.66, 122.21, 121.86, 80.92, 67.76, 61.01, 56.84, 47.60, 45.67, 43.92.



Synthesis of (9R,10R,15R)-9-(2-bromoethoxy)-13-(2-bromoethyl)-10,11-dihydro-9H-9,10-[3,4]epipyrroloanthracene-12,14(13H,15H)-dione. Perbromomethane

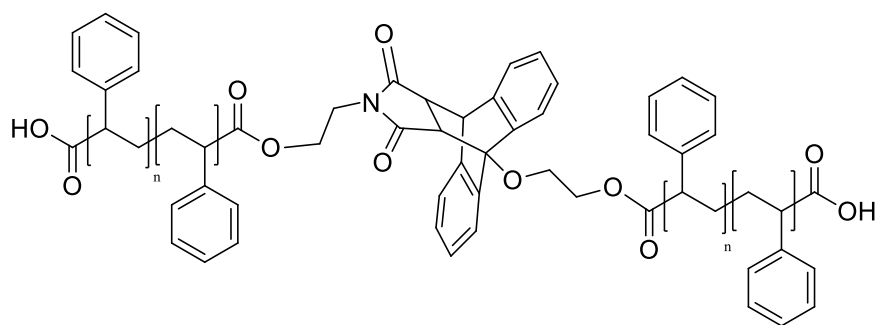
(2.360 g, 7.12 mmol) was added to a dispersion of (9R,10R,15R)-9-(2-hydroxyethoxy)-13-(2-hydroxyethyl)-10,11-dihydro-9H-9,10-[3,4]epipyrroloanthracene-12,14(13H,15H)-dione (1 g, 2.64 mmol) in DCM. The mixture turned into a solution. triphenylphosphine (1.797 g, 6.85 mmol) was added and exothermic reaction occurred; the color changed to brownish

The mixture was left overnight.

TLC (EtOAc : Hex = 1 : 2) showed the product R_f=0.7; some mixture (R_f = 0.9; disappears in time on air); PPh₃O (R_f = 0.2) and something on the start

MPLC was used to separated the species with 12g gold column; the eluent system was 30% EtOAc in Hex. The product (second fraction) was eluted after ~6CV.

¹H NMR (500 MHz, DMSO) δ 7.60, 7.52, 7.46, 7.24, 7.15, 4.77, 4.44, 4.10, 3.88, 3.46, 3.36, 3.33, 2.67, 2.51. ¹³C NMR (126 MHz, DMSO) δ 176.07, 174.24, 142.12, 141.16, 137.53, 126.64, 124.84, 121.69, 81.26, 65.76, 47.63, 45.73, 43.78, 32.89, 26.81. HRMS [ESI] calculated for (C₂₂H₁₉Br₂NO₃ +): 503.9810; found: 503.9825.



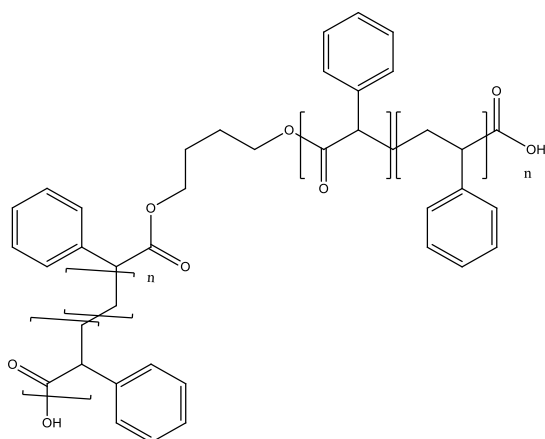
Synthesis of poly-6-(2-(9-(2-((5-carboxy-2,5-diphenylpentanoyl)oxy)ethoxy)-12,14-dioxo-11,12,14,15-tetrahydro-9H-9,10-[3,4]epipyrroloanthracen-13(10H)-yl)ethoxy)-6-oxo-2,5-diphenylhexanoic acid.

A stock solution was prepared using 25mg (0.049 mmol) of H-polymer-239 in 2 ml of dry DMF (24.5 mM).

In a 2 mL vial in the glovebox mixed Polystyrene dicarboxy, 25 kDa (400 mg, 0.016 mmol), 0.06ml of stock solution and potassium carbonate (3.32 mg, 0.024 mmol) in DMF. Took the vial out of the glovebox and left to stir overnight at room temperature. The reaction mixture was diluted in THF (to reach a ~1mg/mL concentration), 1.5ml were taken from the solution, passed through a 45um syringe filter and analyzed by SEC (see SEC spreadsheet file).

Afterwards THF was evaporated and the sample dissolved in 4mL of EtOAc, concentration of 100mg/mL, for prepGPC (8 injections of 0.5 mL each).

Comparison with the control moiety (H-polymer-250) shows the same MW pattern achieved, suggesting that the reaction is done and vials 10-12 (the ones with highest intensity) were combined and separated again to isolate the product with the right MW (~58KDa), 35mg.

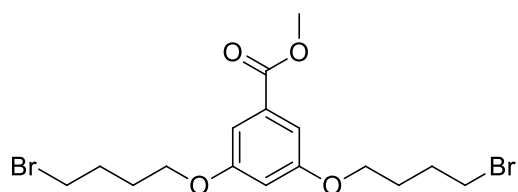


Synthesis of model polymer. A solution of using 10 μL 1,4-dibromobutane in 10ml of DMF (8.37mM).

In a 2 mL vial in the glovebox mixed Polystyrene dicarboxy 25KDa (0.268 g, 8.37 μmol), 1,4-dibromobutane (100 μL , 0.837 μmol) and K_2CO_3 (1.735 mg, 0.013 mmol) in DMF. Took the vial out of the glovebox and left to stir overnight at room temperature.

DMF was evaporated and the reaction mixture diluted in 3mL of EtOAc, concentration of 100mg/mL, for prepGPC.

Afterwards THF was evaporated and the sample dissolved in 3mL of EtOAc, concentration of 100mg/mL, for prepGPC (6 injections of 0.5 mL each).



Synthesis of methyl 3,5-bis(4-bromobutoxy)benzoate. A mixture of methyl 3,5-dihydroxybenzoate (6.535 g, 38.9 mmol), 1,4-dibromobutane (46.4 ml, 389 mmol), potassium carbonate (16.11 g, 117 mmol) and tetrabutylammonium bromide (1.253 g, 3.89 mmol) was stirred in DMF at room temperature under N_2 atmosphere.

TLC: $r_f = 0.6$ (my compound) Eluent conditions - 1:2 EtOAc, Hexane

This crude product was purified by flash column chromatography on silica gel, on a 80g column with eluent gradient of EtOAc :Hex affording 4 fractions. My desire fraction is the 2nd (11.4g). Yield: 66%. ^1H NMR (500 MHz, Chloroform- d) δ 7.18 (d, J =

2.3 Hz, 2H), 6.64 (s, 1H), 4.04 (t, J = 6.0 Hz, 4H), 3.92 (s, 3H), 3.51 (t, J = 6.6 Hz, 4H), 2.12 – 2.06 (m, 4H), 2.01 – 1.94 (m, 4H). ¹³C NMR (126 MHz, CDCl₃) δ 166.78, 159.88, 131.99, 107.74, 106.56, 67.18, 52.25, 33.35, 29.42, 27.79. HRMS [ESI] calculated for (C₁₆H₂₂Br₂O₄⁺): 434.9902; found: 434.9926.

References

- ¹ Roovers, J.; Toporowski, P. M.; *Macromolecules* **1981**, *14*, 1174.
- ² McLeish, T.C.B., Allgaier, J., Bick, D.K., Bishko, G., Biswas, P., Blackwell, R., Blottiere, B., Clarke, N., Gibbs, B., Groves, D.J. and Hakiki, A., *Macromolecules*, **1999**, *32*(20), pp 6734-6758.
- ³ Zheng, W., Chen, L.J., Yang, G., Sun, B., Wang, X., Jiang, B., Yin, G.Q., Zhang, L., Li, X., Liu, M. and Chen, G., *J. Am. Chem. Soc.* **2016**, *138*(14), pp 4927-4937.
- ⁴ Konda SSM, Brantley JN, Varghese BT, Wiggins KM, Bielawski CW, Makarov DE., *J. Am. Chem. Soc.*, **2013**, *135*:12722–12729
- ⁵ Church, D. C.; Peterson, G. I.; Boydston, A. J. *ACS Macro Lett.* **2014**,*3*, 648–651.
- ⁶ Striegel, A.M. *J. Biochem. Biophys. Methods* **2003**,*56*, 117.
- ⁷ Peterson, G. I.; Boydston, A. J. *Macromol. Theory Simul.* **2014**,*23*,555–563
- ⁸ Liu, Ying-Ling, Tsai-Wei Chuo. *Polym. Chem.* **2013**, *4.7*, 2194-2205.
- ⁹ Syrett, J. A.; Mantovani, G.; Barton, W. R. S.; Price, D.;Haddleton, D. M. *Polym. Chem.* **2010**,*1*, 102
- ¹⁰ Pirkle,W.H.; Finn,J.M. *J. Org.Chem.***1983**,*48*,2779
- ¹¹ Heath, W. H.; Palmieri, F.; Adams, J. R.; Long, B. K.; Chute, J.;Holcombe, T. W.; Zieren, S.; Truitt, M. J.; White, J. L.; Willson, C. G. *Macromolecules* **2008**,*41*, 719–726

CHAPTER V. General Conclusions and Perspectives

Polymer mechanochemistry occurs whenever chemical reactivity is affected by an external mechanical force. Therefore, as might be expected, polymers play a crucial role in many technologically relevant processes. Because the most common way this shows is deleterious in nature, *i.e.* a net loss of load-bearing bonds occurs, polymer mechanochemistry is thought to limit the suitability of polymers in several processing methods. These include, but are not limited to the behaviour of tires, polymer membranes, and polymer melt processing¹. A systematic study of mechanochemistry in the above-mentioned processes therefore presents a unique opportunity in that it would have a significant technological and potentially economic impact. Despite this, polymer mechanochemistry need not be destructive. Mechanophores - groups which can be embedded within polymer backbones to undergo chemistry more complex than homolysis of a single bond upon experiencing enough external force, have been designed with practical uses in mind.

In these projects I synthesised moieties with different peculiarity: a macrocycle which works as a molecular gate, with two mechanophores controlling the force required to undergo failure of the polymer structure where it could be inserted. The key molecule chosen for such synthesis was dihalocyclopropane. Manipulation of molecular reactivity and control of reaction selectivity remains the major challenge to the broad field of today's chemistry research. With dihalocyclopropane moiety likely being the most promising reactive site studied in polymer mechanochemistry, the principle aim is to understand the complex patterns of chemical response of these moieties in the presence of transient or long-lasting externally-imposed constraints, as is seen from the recent flourish of experimental investigations. Exploiting the behavior of this structure could improve the understanding of the mechanochemical principle which regulates the complex patterns of chemical response of a reactive moiety to the long-lasting external mechanical force. In the presence of a long-lasting mechanical constraint, the thermally various complex ring opening reaction pathways of reactive group would be reduced to a unique simple one complying with the constraint. The principle derived from the mechanochemistry of dihalocyclopropanes could be exploited to guide the rational design of mechanochemical reactive polymeric materials.

The species synthesized in Chapter II (shown in **Figure 39**) are monomers which could be polymerized in a single linear chain, one with mechanochemical heteroallostery properties (macrocycle with a DCC and a cyclobutane highlighted in red) the other one with homoallostery properties (macrocycle with two DCC). If force will be applied to such linear polymer chains until they break, the fragmentation pattern obtained could help the understanding of some polymer mechanochemistry principles. The final macrocycles isolated show NMR spectra and MS analysis consistent with the prediction (see **Experimental section**, Chapter II). However, the issues encountered in the polymerization of both macrocycles arose the theory of potentially not clean structures but a mixture of enantiomers instead. Despite several attempts, it was impossible to synthesize a linear polymer chain made by repeating units of either M1 or M2. Overall, the design and synthesis achieved in this project, can enable other scientists to perform synthesis of a variety of similar molecules containing mechanophores.

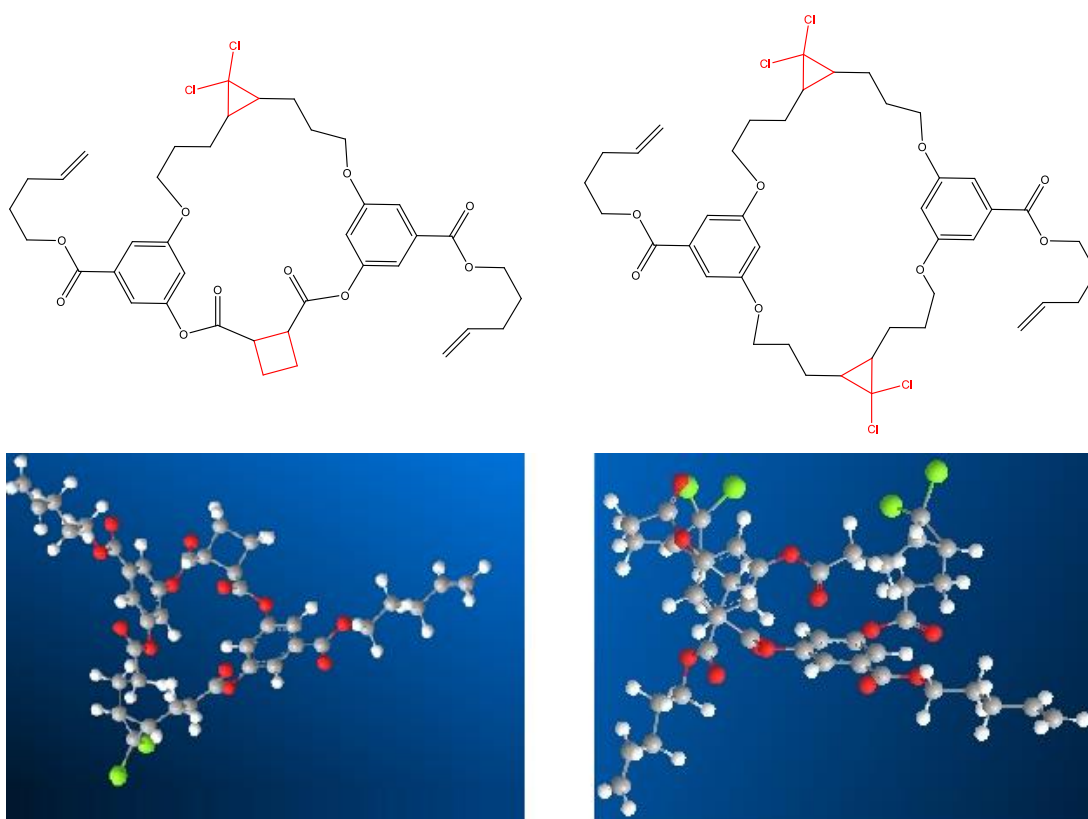


Figure 39: Macrocycles containing dihalocyclopropane and cyclobutane (with their 3D structure predictions).

Mechanochemical fragmentation of polymer chains is thought to be an important contributor to the growth and propagation of cracks² leading to macroscopic failure of polymeric materials under mechanical load and in polymer solutions subject to elongational flows¹. These mechanochemical chain fragmentations are always highly localized, i.e., they occur by dissociation of one or two covalent bonds within a few Å of each other. A stretched polymer chain has never been observed to fragment at multiple spatially separated sites because as soon as the chain breaks at one site, the resulting fragments rapidly adopt strain-free conformations and thus become mechanochemically inert³. By synthesizing a Stiff-Stilbene core connected to two polystyrene chains, it could be possible to study the fragmentation pattern of such polymer chains connected to a strained core, with an analysis of the areas which experience the highest amount of force, where the polymer chain breaks (near the core, in the middle) and how many times it breaks when subjected to ultrasonic waves. The outcome of such measurements can be used for determination of loading rates in complex hydrodynamic flows, e.g. sonication, where the lack of understanding of polymer dynamics and distribution of force/loading rates experienced by polymers limits quantitative interpretation of mechanochemical phenomena¹.

In order to investigate the fragmentation pattern on a polymer under load, I was able to synthesize and isolate three different moieties containing Stiff-Stilbene connected with two polystyrene chains (shown in **Figure 40**), with an overall MW of ~ 60KDa, 100KDa and 200KDa. The total MW of the final product was dependent on the size of the commercial polystyrene chains connected to the Stiff-Stilbene mechanophore. The project I described and achieved in Chapter III not only show an ideal candidate for investigating how force is distributed on a polymer under force, it also provides a guideline for the synthesis and isolation of polystyrenes connected to a mechanophore. The main difference of the goal achieved in this chapter compared to the previous one, it's the complexity of the polymer prepared. While in Chapter II the synthesis was focus on a monomer which will be polymerize into a single linear chain (with several repeating mechanophore units inside the chain), in this case the final compound contained a single mechanophore connected to two polymer chains.

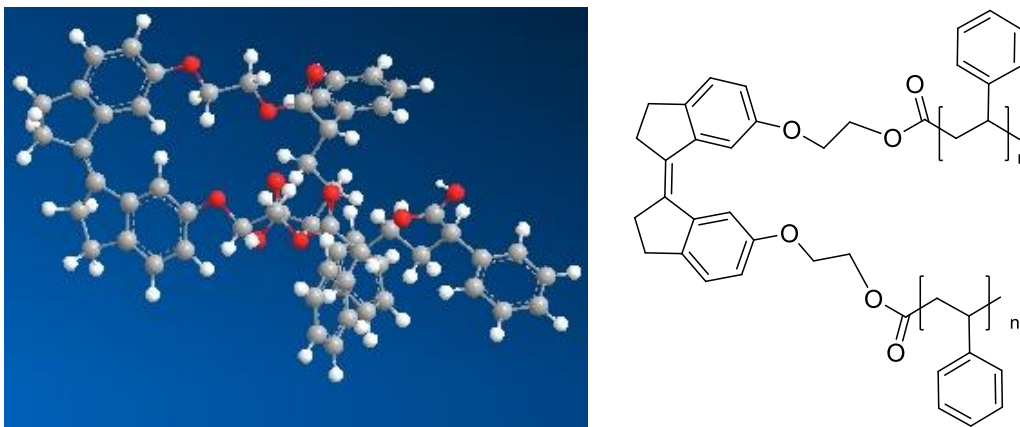


Figure 40: Stiff-Stilbene connected to two polystyrene chains (with its 3D structure prediction).

The main feature of mechanochemistry which underlies all the aspects, both destructive and productive, is coupling over multiple length scales, from below the nanoscale, within which chemical reactions occur, to the macroscale. Such coupling complicates understanding and analysis of mechanochemical phenomena, but also provides opportunities to routinely induce anisotropic strain within macromolecules which is not possible in small molecules. The synthesis of the core of a “H” polymer would lead to the discovery and improvement of self-healing material with unique characteristics useful in industry, research and development. Understanding the effect of force on polymers is vital to improve technologies and manufacturing. Such polymers hold promise for production of so-called stress-responsive materials, which could either prevent catastrophic failure through self-strengthening, or highlight regions of the material which are most likely to fail, respectively.

In order to address the current issues in current materials, I was able to synthesize the central core of the H-shaped polymer designed in Chapter IV (the structure highlighted in red in **Figure 41** on the right). While for the synthesis performed in Chapter III it was used a commercial mono-carboxy terminated polystyrene, in this case a di-carboxy terminated polystyrene was needed to allow further functionalization of the core. The structure of this moiety is a good model (but simpler) similar to the polymers widely used in industry.

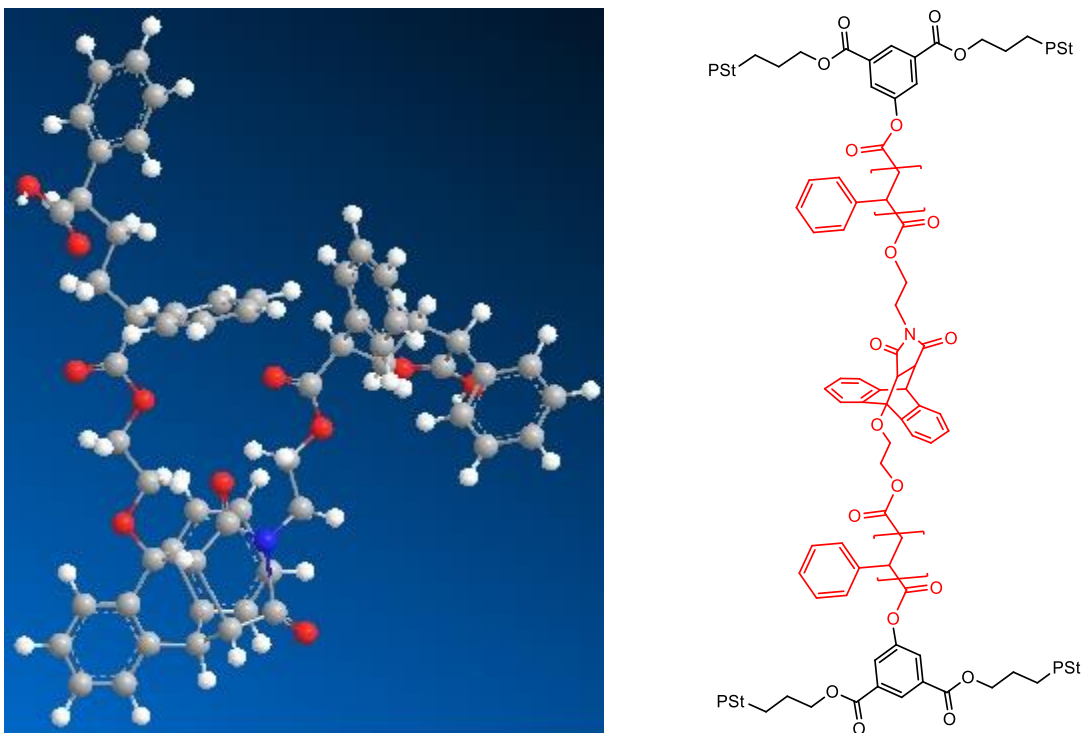


Figure 41: On the right, Antr-Mal Diels Alder adduct connected to two polystyrene chains (highlighted in red). on the left, the 3D structure prediction.

In conclusion, I provided three different examples of synthesis of molecules containing mechanophores throughout my thesis. The design and synthesis accomplished can be used to perform physical measurement and test to improve materials used in the industry on daily basis. Moreover, all three projects are linked given that they each demonstrate the importance of using the correct mechanophore to understand the behaviour of macroscopic polymer chains. The design of a single polymer chain with DCC and with allosteric properties helps with the interpretation of its fragmentation pattern under load induced by an AFM. On the other hand, a more rigid moiety (*i.e.* Stiff-Stilbene) was chosen in order to investigate the distribution of stresses on a polymer formed by two chains. Finally, the geometry of AntrMal was ideal to accommodate four chains polymer moiety.

References

- ¹ Akbulatov, S. and R. Boulatov, *Chemphyschem*, **2017**, 18(11), 1422-1450.
- ² Persson, B. N. J., Albohr, O., Heinrich, G. & Ueba, H. *J. Phys.: Condens. Matter*, **2005** 17, 1071-1142.
- ³ Peterson, G. I.; Larsen, M. B.; Boydston, A.J. *Macromolecules* **2012**, 45, 7317-7328